

Report Number CCEER-91-4

**A Study of Protective Overlays for Highway
Bridge Decks in Nevada, with Emphasis on
Polyester-Styrene Polymer Concrete**

D. N. O'Connor and M. "Saiid" Saiidi

Prepared for

Nevada Department of Transportation
Structural Design Division
Carson City, Nevada

Center for Civil Engineering Earthquake Research
Department of Civil Engineering
University of Nevada
Reno, Nevada 89557

October 1991

Abstract

A major problem facing state and federal highway departments is the deterioration of bridge decks due to the corrosion of reinforcing steel. Polyester-styrene polymer concrete overlays provide durable and wear-resistant surfaces for portland cement concrete bridge decks, and can be formulated to provide low water and chloride permeabilities. In order to study the effects of the composite action between the portland cement concrete deck and the polymer concrete overlay, a knowledge of the material properties of the chosen polymer must be obtained, and the compatibility of the material with portland cement concrete must be determined.

This report provides an introduction to the materials under consideration and a comparison of the engineering properties of portland cement concrete and polyester-styrene polymer concrete. Properties considered include compressive strength, modulus of elasticity, tensile strength, flexural strength, thermal expansion characteristics, rate of compressive strength gain, high temperature strength degradation, shrinkage, and creep.

The bond between the polymer concrete overlay and the portland cement concrete deck results in a composite section with distinct areas of different physical properties. Because the polyester-styrene concrete and the portland cement concrete exhibit different coefficients of thermal expansion and moduli of elasticity, composite action under temperature change raises a concern.

Two finite element models were used to determine the compatibility between the concrete bridge deck and the polyester-styrene overlay. Allowable stresses due to temperature were determined using the ACI ultimate strength method and both AASHTO service load and ultimate strength methods. Results of the analysis are presented, and an attempt to explain any excessive stresses is made.

Acknowledgements

This research was conducted under a grant from the Nevada Department of Transportation. The opinions expressed in this paper belong solely to the authors, and do not represent the official position of either the University of Nevada or the Nevada Department of Transportation.

The authors would like to express their appreciation to Floyd Marcucci and Bill Crawford of the Nevada Department of Transportation, Structural Design Division, and to Henry Jerzak of the California Department of Transportation, Division of New Technology, Materials and Research, for their valuable assistance.

Contents

Abstract.....	iii
Acknowledgements	v
Contents	vii
List of Tables	xi
List of Figures.....	xiii
Chapter 1 Introduction.....	1
1.1 Background.....	1
1.2 Object and Scope	2
1.3 Organization of the Report.....	3
Chapter 2 Bridge Deck Reinforcing Steel Corrosion and Methods of Protection	5
2.1 The Galvanic Corrosion Process in Bridge Decks	5
2.1.1 Conditions Required for Corrosion.....	5
2.1.2 Active Corrosion Process.....	6
2.1.3 Secondary Effects: Concrete Cracking and Spalling	7
2.2 Protection Against Reinforcing Steel Corrosion.....	8
2.3 Cathodic Protection Systems.....	10
2.4 Epoxy-Coated Reinforcing Steel.....	10
2.5 Impenetrable Membranes with Asphalt Concrete Overlays	11
2.6 Latex-Modified Concrete Overlays	11
2.7 Low-Slump Dense Concrete Overlays.....	13
2.8 Polymer Impregnated Concrete.....	14
2.9 Polymer Concrete Overlays.....	15
2.9.1 Epoxy Binder	17

2.9.2 Methyl Methacrylate Binder.....	17
2.9.3 High Molecular Weight Methacrylate Binder.....	17
2.9.4 Polyester-Styrene Binder.....	18
Chapter 3 Protection of Bridge Decks in Nevada	23
3.1 Introduction.....	23
3.2 Protection Methods Used in Nevada.....	26
Chapter 4 Comparison of the Engineering Properties of Polyester-Styrene Polymer Concrete and Portland Cement Concrete	47
4.1 Introduction.....	47
4.2 What are Polymers?.....	47
4.3 Hydration, Polymerization, and Binder Mechanisms	48
4.4 Typical Mix Designs	49
4.4.1 Portland Cement Concrete.....	49
4.4.2 Polymer Concrete	49
4.4.3 Polymer Concretes from Previous Research.....	50
4.5 Principle Properties	52
4.5.1 Compressive Strength	52
4.5.2 Modulus of Elasticity.....	52
4.5.3 Splitting Tensile Strength.....	54
4.5.4 Modulus of Rupture	56
4.6 Other Properties	57
4.6.1 Thermal Expansion Characteristics	57
4.6.2 Rate of Strength Gain.....	58
4.6.3 Sensitivity of Strength to Temperature.....	58
4.6.4 Shrinkage.....	59

4.6.5 Creep.....	60
4.7 Summary.....	62
Chapter 5 Thermal Compatibility between Portland Cement Concrete and Polyester-Styrene Polymer Concrete.....	73
5.1 Introduction.....	73
5.2 Temperature Loads on Highway Bridges.....	73
5.3 Concrete Properties.....	75
5.4 Thermal Compatibility Modeling.....	76
5.4.1 Description of Models.....	76
5.4.2 Generalized ACI Ultimate Strength Method.....	78
5.4.2.1 Compression in Portland Cement Concrete.....	78
5.4.2.2 Tension in Portland Cement Concrete.....	80
5.4.2.3 Compression in Polyester-Styrene Polymer Concrete.....	80
5.4.2.4 Tension in Polyester-Styrene Polymer Concrete.....	81
5.4.2.5 Interface Shear.....	83
5.4.3 AASHTO Design Loads.....	83
5.4.4 AASHTO Service Load Method.....	85
5.4.4.1 Compression in Portland Cement Concrete.....	85
5.4.4.2 Compression in Polyester-Styrene Polymer Concrete.....	86
5.4.4.3 Tension in Polyester-Styrene Polymer Concrete.....	87
5.4.4.4 Interface Shear.....	88
5.4.5 AASHTO Ultimate Strength Method.....	88
5.4.5.1 Compression in Portland Cement Concrete.....	89

5.4.5.2	Compression in Polyester-Styrene Polymer Concrete	93
5.4.5.3	Tension in Polyester-Styrene Polymer Concrete	95
5.4.5.4	Interface Shear	96
5.5	Results.....	97
5.6	Summary.....	99
Chapter 6	Summary and Conclusions.....	131
6.1	Summary.....	131
6.2	Conclusions.....	133
References	135
Appendix A	Symbols and Abbreviations.....	139
Appendix B	Glossary of Polymer Concrete Terms.....	143
Glossary References	148
Appendix C	List of CCEER Publications.....	149

List of Tables

3-1	Database of Nevada Bridges with Protection Systems.....	28
4-1	Comparison of Empirical Formulae to Measured Values for Polyester-Styrene Polymer Concretes.....	63
5-1	Engineering Properties of Materials used in the Finite Element Models.....	102
5-2	Finite Element Analysis Results for Model 1: All Supports Fixed; 35°F Temperature Increase with 25°F Thermal Gradient Across Deck.....	103
5-3	Finite Element Analysis Results for Model 1: All Supports Fixed; 35°F Isothermal Temperature Increase.....	104
5-4	Finite Element Analysis Results for Model 1: All Supports Fixed; 45°F Temperature Decrease with 15°F Thermal Gradient Across Deck.....	105
5-5	Finite Element Analysis Results for Model 1: All Supports Fixed; 45°F Isothermal Temperature Decrease.....	106
5-6	Finite Element Analysis Results for Model 1: Left support Fixed, Rollers at Center and Right Supports; 35°F Temperature Increase with 25°F Thermal Gradient Across Deck.....	107
5-7	Finite Element Analysis Results for Model 1: Left support Fixed, Rollers at Center and Right Supports; 35°F Isothermal Temperature Increase.....	108
5-8	Finite Element Analysis Results for Model 1: Left support Fixed, Rollers at Center and Right Supports; 45°F Temperature Decrease with 15°F Thermal Gradient Across Deck.....	109
5-9	Finite Element Analysis Results for Model 1: Left support Fixed, Rollers at Center and Right Supports; 45°F Isothermal Temperature Decrease.....	110
5-10	Finite Element Analysis Results for Model 1: Cantilever Beam—Left Support Fixed, Center and Right Supports Free; 35°F Temperature Increase with 25°F Thermal Gradient Across Deck.....	111
5-11	Finite Element Analysis Results for Model 1: Cantilever Beam—Left Support Fixed, Center and Right Supports Free; 35°F Isothermal Temperature Increase.....	112

5-12	Finite Element Analysis Results for Model 1: Cantilever Beam—Left Support Fixed, Center and Right Supports Free; 45°F Temperature Decrease with 15°F Thermal Gradient Across Deck	113
5-13	Finite Element Analysis Results for Model 1: Cantilever Beam—Left Support Fixed, Center and Right Supports Free; 45°F Isothermal Temperature Decrease	114
5-14	Finite Element Analysis Results for Model 2: All Supports Fixed; 35°F Temperature Increase with 25°F Thermal Gradient Across Deck	115
5-15	Finite Element Analysis Results for Model 2: All Supports Fixed; 45°F Isothermal Temperature Decrease	116
5-16	Finite Element Analysis Results for Model 2: Left support Fixed, Rollers at Center and Right Supports; 35°F Temperature Increase with 25°F Thermal Gradient Across Deck	117
5-17	Finite Element Analysis Results for Model 2: Left support Fixed, Rollers at Center and Right Supports; 45°F Isothermal Temperature Decrease	118
5-18	Finite Element Analysis Results for Model 2: Cantilever Beam—Left Support Fixed, Center and Right Supports Free; 35°F Temperature Increase with 25°F Thermal Gradient Across Deck	119
5-19	Finite Element Analysis Results for Model 2: Cantilever Beam—Left Support Fixed, Center and Right Supports Free; 45°F Isothermal Temperature Decrease	120
5-20	Comparison of Finite Element Analysis Results and Calculated Allowable Stresses for Model 1	121
5-21	Comparison of Finite Element Analysis Results and Calculated Allowable Stresses for Model 2	122

List of Figures

2-1	Infiltration of Deicing Salt, Water, and Oxygen into Bridge Deck Concrete	20
2-2	Differential Chloride Concentration in Contaminated Bridge Deck Concrete	20
2-3	Electrical Current Flow in Contaminated Bridge Deck.....	21
2-4	Cracking in Bridge Deck caused by Corrosion Products	21
4-1	Stress-Strain Curves for Polyester-Styrene Polymer Concrete and Portland Cement Concrete	64
4-2	Comparison of Empirical Relationships between Compressive Strength and Modulus of Elasticity for Polyester-Styrene Concrete	66
4-3	Comparison of Empirical Relationships between Compressive Strength and Splitting Tensile Strength for Polyester-Styrene Concrete	67
4-4	Early Strength Gain of Polyester-Styrene Polymer Concrete and Portland Cement Concrete	68
4-5	Early Strength Gain of Polyester-Styrene Polymer Concrete and Portland Cement Concrete (logarithmic scale)	69
4-6	Sensitivity of Polyester-Styrene Concrete Compressive Strength to Temperature	70
4-7	Restrained Shrinkage Stress of two Polyester-Styrene Concretes	71
4-8	Standard Creep Coefficient Variation for Portland Cement Concrete with Duration of Loading.....	72
4-9	Compressive Creep of Polyester-Styrene Concretes and Portland Cement Concretes Loaded at Stress/Strength Ratio of 17 Percent	73
5-1	Actual Temperature Gradient through Slab Bridge Deck and Simplified Parabolic Gradient used in the Analysis.....	123
5-2	Deck Section of Humboldt River Bridge used for the Second Finite Element Model	124
5-3	Multiple Span Model used to Minimize End Effects	125
5-4	End Restraint Conditions used in the Finite Element Models	126

5-5	Finite Element Mesh for Model 1	127
5-6	Finite Element Mesh for Model 2	128
5-7	Strength Interaction Diagram for Model 1	129
5-8	Strength Interaction Diagram for Model 2	130

Chapter 1

Introduction

1.1 Background

A major problem facing state and federal Departments of Transportation is the rapid deterioration of highway bridge decks due to the corrosion of reinforcing steel.¹ Deterioration of the bridge deck degrades the riding quality of the deck and, depending on its location and magnitude, can reduce the bridge's load carrying capacity. High repair and replacement costs and inconvenience to the travelling public make protection of bridges against early failure a necessity.

The widespread use of road deicing salts to keep bridges free of snow and ice in the winter has been identified as one of the major causes of bridge deck deterioration.² The infiltration of chloride ions, water and oxygen into the deck result in corrosion of the steel reinforcement. This corrosion leads to a reduction in cross-sectional area of the reinforcement and results in cracking and spalling of the concrete surface. The cracking of concrete, in turn, increases the chloride, water and oxygen access to the steel, further increasing the corrosion rate.

Because of the inherent alkalinity (pH between 12 and 13) of portland cement concrete, reinforcing steel will not corrode in uncontaminated concrete; however, in the presence of chlorides, water and oxygen, this high pH environment begins to neutralize, and rusting of the steel occurs.² The corrosion products occupy a larger volume than the steel they replace, causing internal tensile stresses to develop in the concrete. When these internal stresses are larger than the tensile strength of the concrete, delamination and surface spalling result.

The characteristics of concrete that indirectly affect the corrosion phenomenon are permeability, which governs the access that water, chlorides, and oxygen have to the steel; electrical resistivity, which determines the magnitude of corrosion current that can

flow at a given potential; and the alkalinity of the concrete, which provides a passivating environment for the steel.³

There are two major categories of techniques used to retard the corrosion process: mechanical methods, which physically prevent the access of oxygen, chlorides and water to the steel; and electrochemical methods, which use an applied electrical current to alter the electrical characteristics of the reinforcement to make the steel less susceptible to corrosion. The mechanical category includes the use of epoxy-coated reinforcing steel to isolate the steel from the aggressive environment; sealers, membranes and overlays to prevent ingress of water and chlorides into the concrete; and silica fume admixtures and improvements in concrete mix designs and placement procedures to produce less permeable concrete with higher electrical resistivity.³

Nevada has used a variety of mechanical protection methods with varying success. Methods used include impermeable membranes with asphalt concrete overlays, epoxy-coated rebar, latex-modified concrete (LMC) overlays, low-slump dense concrete (LSDC) overlays and, most recently, polyester-styrene polymer concrete (PC) overlays.

1.2 Object and Scope

This research program was originally intended to aid in determining the optimum bridge deck protection method for the harsh northern Nevada climate.

The original object was changed when the decision was made by the Nevada Department of Transportation (NDOT) to exclusively use polymer concrete for bridge deck overlays. The decision to abandon the previously preferred low-slump dense concrete overlay in favor of polymer concrete was based on cracking problems in low-slump overlays and on successful use of polymer concrete overlays in California. Thus, the focus of this research project was revised to determine what makes polymer concrete successful as a protective overlay material.

The bond between the polymer concrete overlay and the portland cement concrete substrate is generally stronger than the strength of the portland cement concrete itself.⁴ The overlay and the deck form a composite section with distinct areas of different physical properties. In order to study the effects of the composite action and the behavioral differences between portland cement concrete and polymer concrete, a knowledge of the material properties of polyester-styrene polymer concrete was obtained from available literature.

Because of the different properties of polyester-styrene concrete and conventional portland cement concrete, thermal performance and compatibility can be critical. A finite element analysis was conducted to determine the effects of the composite action under temperature changes between the overlay and the bridge deck substrate.

1.3 Organization of the Report

Chapter 2 of this report presents an introduction into the physical process of reinforcing steel corrosion and provides an overview of several methods used to protect bridge decks against deterioration.

A database of bridges in Nevada which have protective systems installed is presented in Chapter 3. This database served as a means of determining which of the various protection systems are being used in Nevada, and will serve as a reference for the comparison of performance in the future. A brief discussion concerning problems encountered with protection methods used in Nevada is also included.

Chapter 4 contains a review of previous research conducted on the properties of polyester-styrene polymer concrete. These properties are compared to the properties of conventional portland cement concrete in an effort to highlight the physical differences between the two materials.

Because of the differences between polyester-styrene polymer concrete and portland cement concrete, thermal compatibility between the bridge deck and the overlay

was questioned. Chapter 5 presents two finite element models which were studied to ensure satisfactory thermal performance.

Chapter 6 presents a summary of the project's findings and outlines suggestions for future research.

The first two appendices provide a list of symbols and abbreviations used in this report and a glossary of terms related to polymer concrete. Appendix C contains a listing of other Center for Civil Engineering Earthquake Research reports published by the University of Nevada Department of Civil Engineering.

Chapter 2

Bridge Deck Reinforcing Steel Corrosion and Methods of Protection

2.1 The Galvanic Corrosion Process in Bridge Decks

Corrosion is the natural process of a metal releasing energy to reform the ores from which it was manufactured.⁵ As a metal ore is smelted and refined to make commercial products, such as steel, energy must be added. However, the tendency of the metal is to revert to its unprocessed natural state, usually a metallic oxide. Corrosion is a process with two primary aspects: a physical change in the metal occurs and an electric current is generated.

A corroding metal releases electrical energy, which must be conserved in nature. To achieve this, some other metal receives the energy, allowing the second metal to remain stable and maintain its manufactured form. The metal releasing energy is the anode and the metal receiving the energy is the cathode. An electrical connection between the two metals must exist for current to flow; this connection may be any direct conductive mechanical connection, such as wire ties, metallic supports, welding, and other physical contact.

2.1.1 Conditions Required for Corrosion

For galvanic (electrolytic) corrosion to occur, four items must be present. There must be two metals existing at different energy levels, an electrical connection between the two metals, and an electrolytic solution to conduct ionic current flow between the anode and cathode. When these conditions are present, a galvanic cell is created and corrosion begins.⁵

Galvanic corrosion can also occur between two regions of the same metal, for instance, a single length of reinforcing steel.⁵ When steel reinforcement is shaped and bent, energy is imparted into the steel. The working process heats the steel and increases

the energy level in the heated region. A single piece of reinforcing steel may have several areas with different energy levels; these areas are ideal for creating galvanic cells.

The energy levels of reinforcing steel can also be influenced by chemical variations in the concrete.⁵ Active ions may be present in the concrete due to admixtures or chemical contamination. Differences in oxygen concentration also promote galvanic cell formation. Indeed, oxygen and moisture must be present in the electrolyte for galvanic corrosion to proceed.

2.1.2 Active Corrosion Process

Steel embedded in alkaline concrete does not naturally corrode.⁵ In the normally high-pH concrete environment, a thin oxide layer forms on the surface of the reinforcing steel. This oxide, known as Gamma Ferric Oxide ($\gamma\text{-Fe}_2\text{O}_3$), or black iron oxide, isolates the steel from the environment and prevents corrosion for as long as the layer remains intact. Protected within the concrete, the oxide layer is seldom disturbed and the integrity of the concrete-steel combination is maintained.

When chloride ions are present in the concrete, a complex chemical reaction occurs which destroys the $\gamma\text{-Fe}_2\text{O}_3$ oxide layer by converting it to red iron oxide, or rust, $\text{Fe}(\text{OH})_2$.⁵ The chloride ions act as a catalyst and are not consumed in the reaction, thus they remain in solution to continue the degradation of the protective oxide layer. Once the oxide layer is removed, the reinforcing steel is subject to galvanic corrosion. Chlorides can be introduced into the bridge deck in admixtures and mixing water; however, the major source of chloride ions in bridge decks is road deicing salts, used to keep the structure free of snow and ice during the winter months.^{2,5} The chloride concentration required to destroy the passive oxide film can be as low as 1 pound per cubic yard.⁵

Because chloride ions are not uniformly distributed within the concrete, differential-concentration galvanic cells are formed in bridge decks. Portions of the

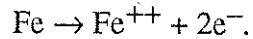
reinforcing steel remain passive while chlorides degrade the oxide layer at other locations. Energy differences result from the active and passive nature of the steel. The concrete acts as the electrolyte and the electrical connection is provided by ties, chair supports, and other steel reinforcing bars.

Oxygen, in addition to chloride ions, is required for reinforcing steel to corrode. Steel in chloride-free concrete with a large oxygen concentration will not corrode and steel in concrete with chloride concentrations above the threshold limit but with no oxygen present will have a greatly reduced corrosion rate. The chlorides act as an initiator by breaking down the protective oxide layer, while the oxygen allows the corrosion process to proceed.⁵ The chloride induced corrosion process is illustrated in Figures 2-1 through 2-4.

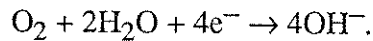
In addition to the reaction of chlorides with the protective oxide layer, the passivation of steel embedded in concrete can also be destroyed by a reduction of pH.⁵ When the pH decreases into the 11 to 12 range, reinforcing steel can corrode given an adequate supply of moisture and oxygen. A decrease in alkalinity can be caused by concrete absorption of carbon dioxide from the atmosphere or the infiltration of acid rain. When carbon dioxide, CO_2 , is absorbed into the concrete, calcium carbonate is formed from the calcium hydroxide in the cement. The reaction converts the hydroxyl ions, OH^- , to water, lowering the pH. This process is known as carbonation, and can decrease pH to about 9. If carbonation occurs in the concrete adjacent to the reinforcing steel, galvanic corrosion is initiated.⁵

2.1.3 Secondary Effects: Concrete Cracking and Spalling

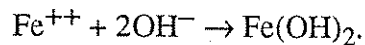
Several electrochemical reactions occur during the galvanic corrosion process to change steel into rust.⁵ At the top mat of steel, the anode, iron atoms are stripped of electrons to become positively-charged ions:



The electrons flow as an electric current to the cathode where, in the presence of water and oxygen, they combine to form negatively-charged hydroxyl ions:



These hydroxyl ions form part of the ionic current that flows through the electrolytic concrete toward the anode, where they react with the positively-charged iron ions to form iron oxide corrosion products:



These corrosion products occupy many times the volume of the steel that was consumed. The increased volume causes a bursting force in the concrete surrounding the corroded steel reinforcement. When the bursting force exceeds the tensile strength of the concrete, cracking will result.⁵ Figure 2-4 illustrates this process.

As the corrosion process continues, more cracks will develop. Cracks which reach the surface can provide a low-resistance path for chlorides, water, and oxygen, thus increasing the rate of corrosion. When cracks intersect, spalling and delamination of the concrete surface can result, further exposing the reinforcing steel to chlorides, water, and oxygen.

2.2 Protection Against Reinforcing Steel Corrosion

If the chloride contaminated area is small, the most effective means of preventing corrosion to bridge deck reinforcing steel is the physical removal of contaminated concrete and replacement with uncontaminated patching materials. Some care must be taken with this method, however, to ensure that all contaminated concrete is removed. Problems have occurred where highly-contaminated concrete has been replaced, but

lesser-contaminated concrete has not. The replacement concrete, being free of chlorides, can set up a difference of potential with the concrete that was not replaced, resulting in accelerated corrosion of reinforcement surrounding the patched area.⁶

If the contaminated deck area is large and removal of contaminated concrete is uneconomical, and for protection of new bridge decks, there are two broad classes of protection available: electrochemical methods and mechanical methods.

The most common electrochemical method is cathodic protection. A cathodic protection system uses electrical energy to counteract the corrosion process. The electrical continuity of the reinforcing steel is used to distribute the electrical current and to prevent galvanic corrosion of isolated segments of reinforcement.⁵

The three most common mechanical methods of bridge deck protection include the use of epoxy-coated reinforcing steel, waterproofing deck sealants, and protective overlays. The use of epoxy coated reinforcing steel has been extensively studied and found to be a reliable and economical method of protection against chlorides.^{1,3,7} Waterproofing deck sealants such as linseed oil have seen use in the past, but are no longer the protection method of choice, mainly because they require frequent re-application to maintain their effectiveness. One type of modern concrete sealing technique is polymer-impregnated concrete (PIC). In polymer impregnation treatment, a monomer is injected into the concrete deck and polymerized in place, forming an impermeable layer in the concrete.

Protective overlays are being used by many state Departments of Transportation.¹ This method employs a thin overlay on the bridge deck to prevent the ingress of water, chlorides, and oxygen. A number of overlay systems have been developed: waterproof membranes with asphalt concrete overlays; low slump dense concrete (LSDC) overlays; latex-modified concrete (LMC) overlays; and polymer concrete (PC) overlays made with acrylics, epoxies, or polyesters.

2.3 Cathodic Protection Systems

A cathodic protection system uses electrical energy to counteract the corrosion process.⁵ The cathodic protection system uses replaceable anodes placed near the surface of the deck, either in sawn grooves or as flat "pancakes" with an electrically-conductive deck overlay. The impressed electrical current counteracts the potential created by chloride ions, and causes the top steel reinforcing mat to behave as a cathode instead of an anode. Because cathodes remain unchanged in the galvanic corrosion process, the reinforcing steel is protected.

Cathodic protection systems have the benefit that contaminated, but sound, concrete does not have to be removed. However, cathodic protection systems can be expensive and labor intensive, and must be located near a source of electrical power.

2.4 Epoxy-Coated Reinforcing Steel

The use of epoxy-coated reinforcing steel will prevent its corrosion. Research has estimated that, at the same chloride concentration in the concrete, annual steel corrosion will average 12 times less for epoxy coated top mat steel than for plain steel.¹ Maximum protection is afforded by the use of epoxy-coated reinforcement for the bottom mat as well as the top mat. The amount of top mat steel consumed by corrosion is reduced 46 times by epoxy-coating both the top and bottom steel mats.¹ One of the most important factors governing the performance of epoxy-coated bars is the quality control during coating.³ Damage to the epoxy coating during the coating process or during subsequent handling can reduce or negate the protection provided by the coating. Once the chloride concentration in the concrete reaches the threshold level, accelerated corrosion may occur at epoxy-coating damage sites. The resulting pitting can also lead to premature fatigue failure of the bar.¹

Epoxy-coated reinforcing steel cannot be used to retrofit an existing bridge deck; its use is limited to new construction, deck replacement, and large patches. It is the policy of the Nevada Department of Transportation to use epoxy-coated steel in new construction for all reinforcement within the top 12 inches of the structure.⁸

2.5 Impenetrable Membranes with Asphalt Concrete Overlays

This protective strategy uses an impermeable waterproofing membrane applied to the bridge deck followed by application of a 2- to 3-inch thick asphalt concrete overlay to protect the membrane and serve as a wearing course. Membranes are typically factory preformed sheeting or applied-in-place liquids. While the claimed life of membrane systems can be as great as 50 years, the actual life of the system is generally 10 to 15 years, and is governed by deterioration of the asphalt overlay.¹

In addition to design features, membrane effectiveness depends greatly on construction quality. Particular care in sealing the membrane at curbs and drains, where ponding can be severe, is important. Damage to the membrane under the asphalt paver has also been reported.¹

Several states, including Nevada, have experienced debonding and stripping of the asphalt concrete overlay.^{1,8} One major factor is infiltration of water through cracks and fissures in the overlay and accumulation of water above the membrane. When this water is subjected to repeated combinations of freezing and thawing and hydraulic pressures under traffic, the asphalt layer tends to separate from the membrane. Blistering under the membrane during construction will result in a poor bond with the bridge deck and subsequent early failure of the protection system.¹

2.6 Latex-Modified Concrete Overlays

Latex-modified concrete (LMC) overlays, typically 1.5 to 2 inches thick, have been used successfully in several states. Research has found that a 1-inch thick layer of

latex-modified concrete provides the same protection against chloride intrusion as 3 inches of concrete made with a water/cement ratio of 0.50.¹ The addition of an acrylic latex, typically styrene-butadiene rubber (SBR),⁹ to a conventional portland cement concrete creates a non-permeable concrete. The latex is introduced to the concrete in an emulsion which replaces a portion of the mixing water. Upon placement, the latex rapidly begins to cure and forms a continuous impermeable film within the concrete.¹⁰

Latex-modified concrete overlays must be applied to a clean, sound surface. The bridge deck must first be scarified to remove unsound concrete from the surface. Next, the surface is sand blasted to remove laitance from the concrete and rust from any exposed reinforcing steel. Finally, the surface is blown clean with compressed air. Prior to placement of the latex-modified concrete overlay, the deck is wetted, to prevent excessive absorption and early drying of the latex emulsion. This step is normally performed within the 24 hours preceding placement.¹¹

The concrete can be mixed and placed using any conventional equipment, but the use of continuous mixers and self-propelled roller finishers is the more common approach.¹¹ Ahead of concrete placement a latex slurry is broomed into the deck surface to enhance the bond between the latex-modified concrete and the bridge deck. Care must be exercised to avoid applying the slurry too far ahead of the concrete placement operation, to ensure that the slurry does not prematurely set.

The freshly placed latex-modified concrete surface must be finished as rapidly as possible before the latex film begins to form. Brooming or tining done after film formation will tear the surface and destroy the integrity of the latex film. Immediately after the finishing operation, wet burlap covered with polyethylene film must be applied to keep the top surface moist for approximately 24 hours. After this initial moist cure, the overlay is allowed to cure in air. Latex-modified concrete cures at about the same rate as conventional concrete.¹¹

A properly applied latex-modified concrete overlay may be expected to perform for a minimum of 20 years.¹⁰ Minor overlay debonding has occurred, but is usually related to improper construction techniques.¹ Latex-modified concrete is especially susceptible to plastic shrinkage cracking if curing is not begun immediately after placement. Severe flexural cracking in the overlay of some installations has also been reported.¹ Any cracking that develops should be sealed as soon as possible, as the cracks destroy the integrity of the overlay, allowing water, oxygen and chlorides access to the bridge deck substrate.

2.7 Low-Slump Dense Concrete Overlays

Low-slump dense concrete (LSDC) overlays are usually applied in thicknesses of 2 to 3 inches. Low-slump dense concrete typically has a maximum water/cement ratio of 0.34, a maximum slump of 1 inch, and an air content of 6.0 ± 1.0 percent.¹² To achieve the desired air content, low-slump dense concrete often requires up to 10 times the normal air entraining admixture dosage.¹ A 1-inch thick layer of low-slump dense concrete generally provides the same protection against chlorides as 2 inches of concrete made with a 0.50 water/cement ratio.¹

As with latex-modified concrete overlays, low-slump dense concrete must be applied to a clean, sound surface. The bridge deck must be scarified to remove unsound concrete, sand blasted to clean laitance from the concrete and rust from any exposed reinforcing steel, and blown clean with compressed air. Unlike latex-modified concrete, which requires the deck to be wetted, low-slump dense concrete overlays must be placed on a dry substrate.¹³ The use of a mortar slurry ahead of concrete placement enhances the bond between the overlay and the deck.

There have been a few cases of overlay debonding caused by improper construction practices and inefficient substrate texturing.¹ When constructed properly, the bond between the low-slump, dense concrete overlay and the bridge deck should be

durable; however, the bond can be affected by thermal cycling, repeated loading, and wetting and drying.¹ Due to the low water/cement ratio, low-slump dense concrete is especially susceptible to plastic shrinkage cracking if not properly cured. Cracks should be immediately sealed to prevent chloride and water ingress.

2.8 Polymer Impregnated Concrete

A method of protection that is especially suited for new decks is polymer impregnated concrete (PIC). The deck surface is impregnated to a depth of not less than 1 inch with a liquid monomer which is subsequently polymerized in place.¹⁴ After polymerization has occurred, the resulting material consists of two interpenetrating networks: the original network of hydrated cement concrete and an essentially continuous network of polymer that fills most of the voids in the concrete.¹⁵ This method effectively seals the deck from chloride, water and oxygen intrusion. The most common polymer system used for impregnating concrete is methyl methacrylate (MMA), often with trimethylolpropane trimethacrylate (TMPTMA) added as a cross-linking agent.¹⁵

Before the concrete can be impregnated, the deck surface must be clean and free of asphalt, rubber, and oil. The bridge deck is then dried to a depth greater than the desired depth of impregnation using gas fired or electric-infrared heaters. Drying is required to rid the concrete voids of water, which impedes or blocks the diffusion of the monomer and limits the amount that may be absorbed into the concrete.¹⁴ Because of the extreme volatility of methyl methacrylate, the deck must be allowed to cool before application of the monomer.

The methyl methacrylate monomer is initiated, usually with benzoyl peroxide (BPO) or methyl ethyl ketone peroxide (MEKP), prior to application. The bridge deck is covered with a ¼- to ½-inch layer of dry sand and then saturated with the liquid monomer system.¹⁴ The monomer diffuses into the deck under gravity and capillary action. Generally, two or three applications of the monomer are required during the

impregnation cycle. This process is usually performed at night, since solar radiation may cause premature polymerization.

Polymerization of the monomer in the concrete can be achieved by either the thermal-catalytic method or the promoted-catalytic method.¹⁵ In the thermal-catalytic method, polymerization is accomplished by applying sufficient heat to the concrete to raise its temperature to between 165°F to 185°F.¹⁴ Electric ovens, hot water, or steam can be used as the heat source. The primary advantage of thermal-catalytic polymerization is that the polymerization rates are very rapid, thus processing time is short.¹⁵

To allow polymerization to occur at room temperature, without the application of heat, the promoted-catalytic method can be used. A promoter is added to the monomer system prior to application. This promoter accelerates the decomposition of the initiator, which, in turn, causes polymerization. Difficulties in obtaining predictable polymerization rates and in matching the onset of polymerization with the monomer saturation time are two disadvantages of this method.¹⁵

Polymer impregnated concrete has been shown to have improved tensile, flexural, and compressive strengths. Abrasion resistance, permeability, and resistance to freezing and thawing are also greatly improved.¹⁵ Increases in strength in partially impregnated concrete are not as great as the increases in full-depth impregnation; therefore, it should generally not be assumed that partial impregnation significantly increases the strength of a member.

2.9 Polymer Concrete Overlays

Polymer concrete (PC) is a composite material of mineral aggregates bound in a polymer binder matrix. Polymer concrete overlays provide durable and wear-resistant surfaces for portland cement concrete bridge decks, and can be formulated to provide low water and chloride permeabilities.¹⁶ Polymer concrete properties include rapid curing at

ambient temperature, high strength, good adhesion to concrete surfaces, long-term freezing and thawing durability, low permeability to water and chlorides, and good chemical resistance.¹⁶ Polymer concrete overlays may be placed in thicknesses from $\frac{3}{8}$ inch to 1 inch, reducing the dead load and clearance problems of other overlay systems.⁴

Polymer concrete overlays must be applied to a clean, dry, physically sound substrate. Surface preparations include scarifying to increase surface roughness and remove unsound concrete and sand blasting to remove laitance and clean exposed aggregate and reinforcing steel.¹⁷

Prior to mixing and placement of the polymer concrete overlay, a prime coat of the polymer binder or other polymer is applied to the deck surface. The primer penetrates microcracks in the concrete substrate to seal them and yield a sound, strong surface for overlay bonding.⁴ The primer also prevents the polymer concrete binder from being absorbed into the portland cement concrete deck and thus removed from the overlay.

Polymer concrete is mixed in a portable concrete mixer or in a continuous mixing machine. If a concrete mixer is used, the resin system components are thoroughly blended to ensure proper mixing before the fine and coarse aggregate portions are added. The mixed concrete is placed on the deck surface and then spread and compacted, usually using a vibrating screed.¹⁵ Some overlays require a final broadcasting of blasting sand, prior to resin gelling, to provide a skid-resistant surface. The surface can be further finished by tining after the polymer concrete has first started to gel or by sawing grooves after the overlay has hardened.

Polymer concrete can be made with any suitable polymer binder. The most commonly used binders, in order of decreasing cost and increasing popularity, are epoxy resins, high molecular weight methacrylates and methyl methacrylate acrylic resins, and

polyester-styrene resin systems. Binder costs vary from about \$3.50 per pound for epoxy resins to about \$1.10 per pound for polyesters.¹⁸

2.9.1 Epoxy Binder

Epoxy resins are usually formulated in two-component systems which are mixed 1:1 or 2:1. Epoxy resins are generally slow setting and continue to gain strength for weeks; however, resins can be formulated to support traffic within two or three hours. Epoxy has a high viscosity and a putty-like concrete consistency, is impermeable to water and chlorides, has good resistance to abrasion, has relatively low initial shrinkage, has good adhesion characteristics, and has excellent chemical resistance.⁴

2.9.2 Methyl Methacrylate Binder

Methyl methacrylate (MMA) bonds very well to a dry portland cement concrete surface. The methyl methacrylate initiator/promoter system consists of an organic peroxide, such as benzoyl peroxide (BPO) or methyl ethyl ketone peroxide (MEKP), and a metal drier, usually cobalt naphthenate. The amount of initiator and promoter can be varied to provide 30 to 60 minutes of working time before gelling occurs. Methyl methacrylate concrete is impermeable to water and has excellent abrasion resistance. The material is, however, extremely volatile, and should not be used when high temperatures or winds are present, as excessive evaporation could result.⁴

2.9.3 High Molecular Weight Methacrylate Binder

High molecular weight methacrylate (HMWM) was developed specifically to address the volatility problems of methyl methacrylate.⁴ High molecular weight methacrylates can be directly substituted for methyl methacrylate, and used in concrete as explained previously.

2.9.4 Polyester-Styrene Binder

Polyester resins are among the most versatile and readily available polymers. The most common polyester resin system used for polymer concrete is an unsaturated isophthalic polyester dissolved in a styrene monomer, with methyl ethyl ketone peroxide (MEKP) and cobalt naphthenate used as the initiator/promoter system. During polymerization, the styrene cross-links with the main polyester chains to form a three-dimensional network.¹⁹

The polyester-styrene resin is usually supplied with the promoter already added in an amount necessary for room-temperature curing. The amount of initiator added can be varied to provide a working time of 30 to 60 minutes. Often a silane coupling agent is also included, to enhance the bond strength between the inorganic aggregate and the organic polymer.

Polyester is formed through an esterification process in which an organic acid and an alcohol are combined to yield an ester and water.¹⁹ An ester is the organic equivalent of the inorganic salt obtained from the chemical reaction between an inorganic acid and base. Like the inorganic reaction, the esterification process is reversible; a re-introduction of water under favorable conditions will convert the polyester into its original constituents.¹⁹ For this reason, moisture in aggregates must be kept below one-half of the aggregate's absorption capacity.⁴

Although alkali-resistant polyesters are available at additional cost, typical polyester-styrene resin is sensitive to the high-pH environment of portland cement concrete.⁴ This sensitivity can, in time, result in a loss of bond between the overlay and the bridge deck; therefore, a prime coat is required. High molecular weight methacrylate is often used as a primer for polyester-styrene overlays.

Polyester-styrene resin also exhibits high shrinkage during curing that can result in debonding or cracking.¹⁷ To minimize shrinkage effects, a high aggregate content in polyester-styrene polymer concrete is essential.

The physical properties which make polyester-styrene polymer concrete a suitable choice for overlays are described in Chapter 4.

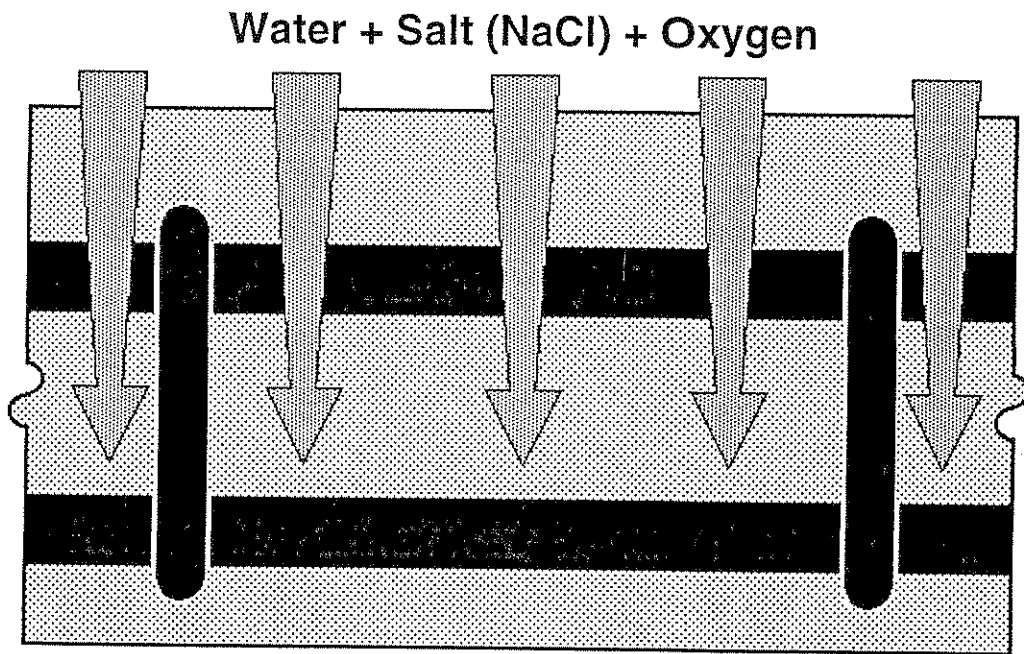


Figure 2-1. Infiltration of Deicing Salt (chloride ions), Water, and Oxygen into Bridge Deck Concrete (After Ref. 5).

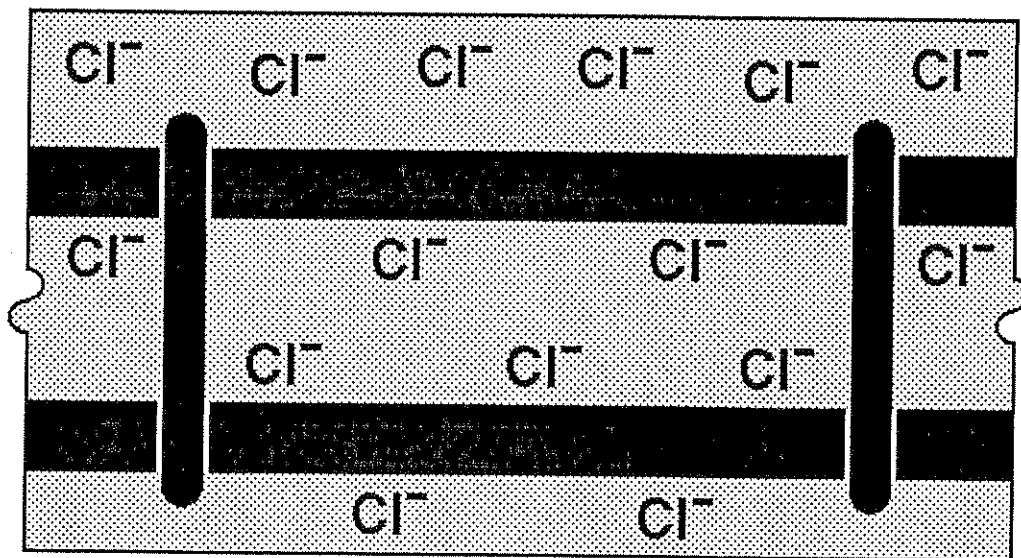


Figure 2-2. Differential Chloride Concentration in Contaminated Bridge Deck Concrete (After Ref. 5).

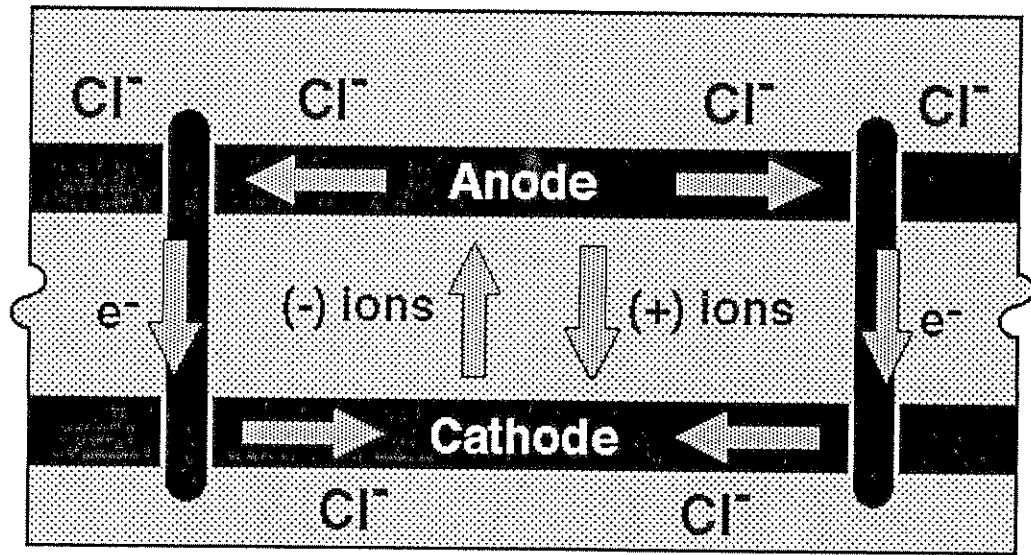


Figure 2-3. Electrical Current Flow in Contaminated Bridge Deck (After Ref. 5).

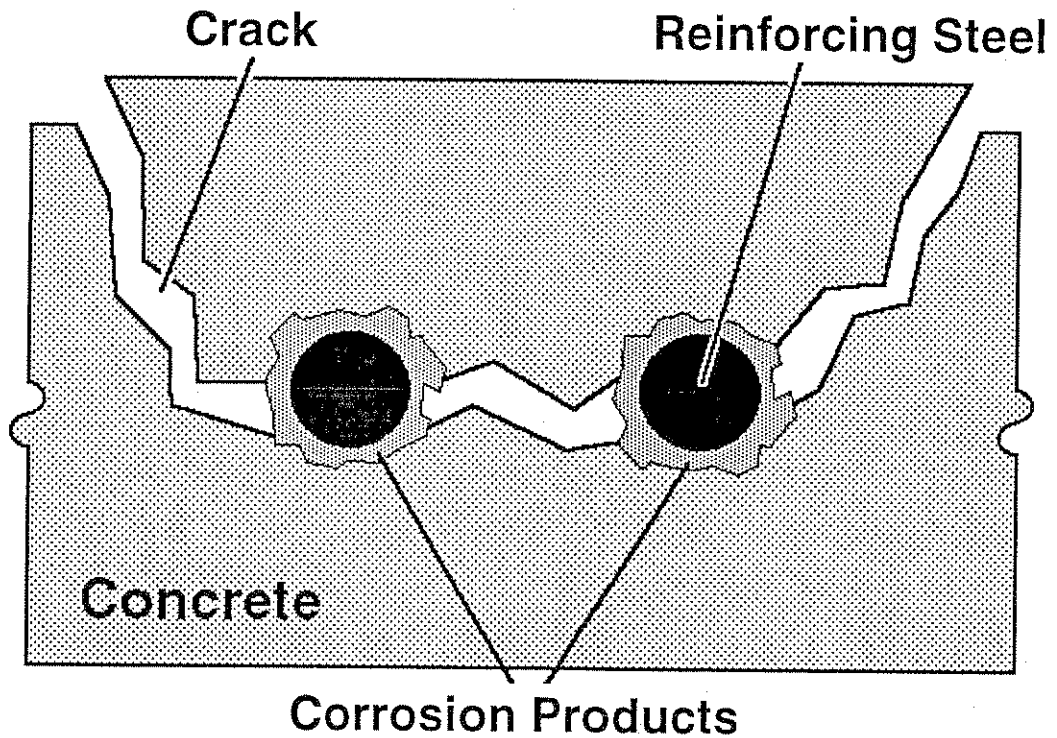


Figure 2-4. Cracking in Bridge Deck caused by Corrosion Products (After Ref. 5).

Chapter 3

Protection of Bridge Decks in Nevada

3.1 Introduction

An early goal of this research project was to identify a bridge deck protection strategy which would provide adequate reinforcing steel protection at a reasonable cost. As an aid to identifying the various types of protective systems which have been used in Nevada in the past, a database of protected bridges was compiled. In addition to identifying the various protection systems, the database was designed with a view toward tracking the long-term effectiveness of installed systems.

For ease of use and updating, the protective system database was designed as a two-dimensional worksheet, or flat-file database, using Microsoft® Excel for Windows²⁰ on an IBM®-compatible computer. This format provides two benefits: expensive relational database management software is not required, and the database can be readily used with Lotus® 1-2-3 spreadsheet software.

Information for the database was gathered from Nevada Department of Transportation (NDOT) contract records and plans, structural inspection records, and the National Bridge Inventory²¹ (NBI) records. For each bridge with a protective system, the following information was recorded:

- Bridge type and number, and direction if more than one structure has the same number, e.g., eastbound and westbound on divided highways. The bridge type and number is the primary identification method for structures in Nevada. Bridge structures are divided into five main categories: bridges over waterways (B), culvert structures with a span greater than 20 feet (C), railroad/highway grade separations (G), other road/highway grade separations (H), and interchanges on controlled-access highways (I). Culvert structures were not included in the database.

- Route classification and number. Federal-aid routes are classified as Interstate highways (FAI); primary highways (FAP), such as U.S. highways; secondary highways (FAS), such as important state routes and business loops; and urban highways (FAU), such as expressways and major arterials. The route classification and number is used to locate the structure and to identify the type of facility carried by the structure. Private, city, and county bridges not under the direct responsibility of the Nevada Department of Transportation were not included in this study.
- Milepost location by county. In Nevada, highway mileposts are designated by county, with milepost locations beginning at zero at the west or south county line. All bridges in Nevada have a specific milepost location. The county codes used in the database are:

CC	Carson City,
CH	Churchill County,
CL	Clark County (Las Vegas),
DO	Douglas County,
EL	Elko County,
ES	Esmeralda County,
EU	Eureka County,
HU	Humboldt County,
LA	Lander County,
LI	Lincoln County,
LY	Lyon County,
MN	Mineral County,
NY	Nye County,
PE	Pershing County,

ST Storey County,
WA Washoe County (Reno), and
WP White Pine County.

- Structure name and descriptive location, as listed in the Nevada Department of Transportation's bridge index.²²
- Type of structure, e.g., concrete deck slab, concrete box girder, steel plate girder, etc., obtained from the bridge construction plans, and the year the structure was built, NBI item 27. This data provides information for tracking past and future performance of various deck protection strategies. Certain protection systems may undergo different detrimental effects on different types of structures, e.g., excessive cracking of overlays on long-span prestressed structures.
- Average daily traffic across the bridge and the year the average daily traffic was determined, NBI items 29 and 30, respectively. These items provide an estimate of the amount of traffic a bridge carries. A bridge with higher traffic can expect its protective system to deteriorate faster, requiring increased maintenance.
- Number of traffic lanes on the bridge, NBI item 28. This item is important in determining the average lane traffic. Lanes with a high traffic volume can expect to exhibit faster wearing surface deterioration and, subsequently, increased maintenance expenses.
- Design load of the structure, NBI item 31. The design load is listed as the AASHTO loading used in the structure's design, e.g., H-15, HS-20, modified HS-20, etc., and is useful in determining the bridge's overload capacity.
- Angle of bridge deck skew in degrees, NBI item 34. This information was included to aid in tracking deterioration of protective overlays near the acute angle corners of skewed bridge decks. A "99" value indicates a curved bridge or other bridge with changing or multiple skew angles.

- Number of spans in the structure, sum of NBI items 45 and 46, and the overall structure length and the length of the longest span, NBI items 49 and 48, respectively. This information may be of use in tracking deterioration of protective systems due to excessive deflections, moment cracking, or thermal stresses and strains.
- Roadway width from curb to curb and overall width of the structure, NBI items 51 and 52, respectively. This data was included to aid in tracking protective system deterioration caused by transverse flexure in wide structures.
- Current protection system and previous system, if applicable. This information is needed to identify the types of protection systems employed in the state of Nevada, and to track the performance of installed systems. Information for protective systems includes the type of protective system, e.g., waterproofing, low-slump dense concrete overlay, etc.; the bid cost and pay unit for the protection system; and the contract number and year in which the protective system was installed.

A complete listing of the database is presented in Table 3-1.

3.2 Protection Methods Used in Nevada

Nevada lies in the rain-shadow of the Sierra Nevada mountain range and is a desert region; however, several north-south ranges which accumulate snow in the winter lie within the state. Major highways traversing these mountains are kept clear in the winter using snow-removal equipment and road deicing salts mixed with sand. Several bridge deck protection strategies have been used in Nevada, including impermeable membranes with asphalt concrete overlays, latex-modified concrete overlays, and low-slump dense concrete overlays, each with only marginal success.⁸

Impermeable membrane systems with asphalt overlays were the earliest form of overlay protection, replacing linseed oil sealers as the preferred method of protection.

When applied properly, these systems performed adequately; however, the relatively short life-span of the asphalt concrete overlay combined with several instances of overlay stripping, due to freezing and thawing action, made seeking alternatives desirable.⁸

The first alternative to be tried was the latex-modified concrete overlay. Several systems were installed, but few were successful. Two notable debonding failures are the Winnemucca Viaduct (H-869E/W) and the Winnemucca Boulevard-East Interchange (I-874E/W) on Interstate 80. These systems were placed in 1981 and have debonded to such an extent that they had to be completely removed from the structures within the first 10 years. Almost all problems with latex-modified concrete overlays have been due to incorrect concrete formulation and/or placement.⁸ The low humidity, high daytime temperatures, and windy conditions common in Nevada serve to make placement of latex-modified concrete difficult.

The problems associated with latex-modified concrete overlays led to the use of low-slump dense concrete overlays beginning in the early 1980s. While there have been some problems with localized debonding, chiefly as a result of improper surface preparation,⁸ most low-slump overlays have performed satisfactorily. Unfortunately, many low-slump overlays are now beginning to show signs of excessive cracking due to transverse flexure in the bridge deck. Some pattern cracking has also been noted in the acute-angle corners of skewed bridge decks.

Based on successful use in California, the protective system of choice in Nevada today is the polyester-styrene polymer concrete overlay. Polyester-styrene overlays have been placed on sixteen bridges in Nevada over the last two years, and several more are planned for the near future.⁸

Table 3-1. Database of Nevada Bridges with Protection Systems.

BRIDGE NUMBER	ROUTE	MILEPOST	STRUCTURE NAME AND DESCRIPTIVE LOCATION	STRUCTURE TYPE	YEAR BUILT
B- 16	FAS 427	WA 4.04	TRUCKEE RIVER-WADSWORTH	PRESTRESSED GIRDER	1926
G- 19	FAS 343	LY 3.02	FERNLEY OVERPASS	STEEL GIRDER	1928
G- 52	FAS 230	EL 0.84	S.P.T.CO. OVERPASS-DEETH	STEEL GIRDER	1924
G- 53	FAS 230	EL 1.05	U.P.R.R. OVERPASS-DEETH	STEEL GIRDER	1935
G- 208	FAS 168	CL 2.91	WEST WALKER RIVER	CONCRETE BOX GIRDER	1988
B- 223	FAP 095	HU 0.25	HUMBOLDT RIVER, MELARKEY ST.	STEEL GIRDER	1986
G- 224	FAP 095	HU 0.40	WINNEMUCCA U.P.R.R. OVERPASS	STEEL GIRDER	1936
G- 229	FAP 093	EL 74.37	S.P.T.CO. OVERPASS NEAR WELLS	STEEL & CONCRETE GIRDER	1934
B- 238	FAP 95A	LY 57.21	TRUCKEE CANAL	STEEL GIRDER	1930
B- 288	FAS 116	CH 1.62	"S" CANAL	CONCRETE BOX GIRDER	1936
B- 406	FAS 230	EL 1.25	MARY'S RIVER-DEETH	PRESTRESSED, PRECAST GIRDER	1940
B- 407	FAS 230	EL 1.48	HUMBOLDT RIVER-DEETH	PRESTRESSED, PRECAST GIRDER	1940
I- 681	FAI 080	WA 36.84	THISBE INTERCHANGE	CONCRETE BOX GIRDER	1958
I- 682 E	FAI 080	PE 49.60	HUMBOLDT HOUSE INTERCHANGE	CONCRETE DECK SLAB	1961
I- 682 W	FAI 080	PE 49.60	HUMBOLDT HOUSE INTERCHANGE	CONCRETE DECK SLAB	1961
I- 683 N	FAP 395	WA 33.70	STEAD INTERCHANGE	CONCRETE DECK SLAB	1960
I- 683 S	FAP 395	WA 33.70	STEAD INTERCHANGE	CONCRETE DECK SLAB	1960
G- 686	FAP 050	WP 65.61	KEYSTONE NNRR O/P NEAR JCT. US 6	STEEL GIRDER	1958
I- 699 E	FAI 080	PE 40.52	RYE PATCH INTERCHANGE	CONCRETE DECK SLAB	1961
I- 699 W	FAI 080	PE 40.52	RYE PATCH INTERCHANGE	CONCRETE DECK SLAB	1961
I- 700 E	FAI 080	WA 43.86	WEST WADSWORTH INTERCHANGE	CONCRETE DECK SLAB	1963
I- 700 W	FAI 080	WA 43.86	WEST WADSWORTH INTERCHANGE	CONCRETE DECK SLAB	1963
B- 716 E	FAI 080	WA 44.67	TRUCKEE R.-SOUTH WADSWORTH	PRESTRESSED, PRECAST GIRDER	1961
B- 716 W	FAI 080	WA 44.67	TRUCKEE R.-SOUTH WADSWORTH	PRESTRESSED, PRECAST GIRDER	1961
I- 717 E	FAI 080	LY 1.13	WEST MAIN ST. INTERCHANGE	PRESTRESSED, PRECAST GIRDER	1963
I- 717 W	FAI 080	LY 1.13	WEST MAIN ST. INTERCHANGE	PRESTRESSED, PRECAST GIRDER	1963
I- 740 E	FAI 080	LY 3.66	EAST MAIN ST. INTERCHANGE	CONCRETE DECK SLAB	1963
I- 740 W	FAI 080	LY 3.66	EAST MAIN ST. INTERCHANGE	CONCRETE DECK SLAB	1963

Table 3-1 (Continued). Database of Nevada Bridges with Protection Systems.

BRIDGE NUMBER	ADT	ADT YEAR	LANES ON BRIDGE	DESIGN LOAD	SKEW ANGLE	NO OF SPANS	STRUCT LENGTH	MAX. SPAN LENGTH	WIDTH CURB-CURB	WIDTH OUT-OUT
B- 16	1,370	1987	2	HS-15	0	6	268	51	40.0	43.0
G- 19	7,435	1987	2	H-15	30	4	154	38	30.0	34.5
G- 52	70	1986	2	MOD HS-20	15	4	135	33	32.0	34.5
G- 53	70	1986	2	MOD HS-20	6	3	129	50	32.2	34.7
G- 208	815	1988	2	MOD HS-20	26	3	195	96	40.0	43.0
B- 223	5,080	87	2	MOD HS-20	0	3	275	107	44.0	56.0
G- 224	5,080	1987	2	H-15	11	1	195	73	34.0	41.0
G- 229	1,130	1986	2	HS-20	0	2	155	42	32.0	36.0
B- 238	4,440	1987	2	HS-15	0	3	79	56	32.0	37.0
B- 288	1,020	1987	2	HS-20	0	1	42	40	30.0	31.5
B- 406	70	1986	2	MOD HS-20	0	3	79	27	32.0	34.5
B- 407	70	1986	2	MOD HS-20	0	3	92	30	32.0	34.5
I- 681	11,335	1986	2	MOD HS-20	0	4	215	71	38.0	43.0
I- 682 E	2,610	1987	2	MOD HS-20	0	3	94	35	38.0	43.0
I- 682 W	2,610	1987	2	MOD HS-20	0	3	94	35	38.0	43.0
I- 683 N	5,420	1986	2	HS-20	13	3	123	47	38.0	43.0
I- 683 S	5,420	1986	2	HS-20	13	3	123	47	38.0	43.0
G- 686	1,275	1987	2	HS-20	0	4	351	92	40.0	46.0
I- 699 E	2,410	1987	2	MOD HS-20	0	3	94	35	38.0	43.0
I- 699 W	2,410	1987	2	MOD HS-20	0	3	94	35	38.0	43.0
I- 700 E	5,525	1987	2	MOD HS-20	31	3	134	52	38.0	43.0
I- 700 W	5,525	1987	2	MOD HS-20	30	3	135	52	38.0	43.0
B- 716 E	5,690	1987	2	MOD HS-20	30	4	313	78	38.0	43.0
B- 716 W	5,690	1987	2	MOD HS-20	30	4	313	78	38.0	43.0
I- 717 E	3,543	1987	2	MOD HS-20	10	4	229	60	38.0	43.0
I- 717 W	3,543	1987	2	MOD HS-20	10	4	229	59	38.0	43.0
I- 740 E	1,750	1987	2	MOD HS-20	30	3	134	52	38.0	43.0
I- 740 W	1,750	1987	2	MOD HS-20	30	3	134	52	38.0	43.0

Table 3-1 (Continued). Database of Nevada Bridges with Protection Systems.

BRIDGE NUMBER	CURRENT PROTECTION SYSTEM				PREVIOUS PROTECTION SYSTEM			
	PROTECTIVE SYSTEM	BID COST	PAY UNIT	DATE INSTALLED*	PROTECTIVE SYSTEM	BID COST	PAY UNIT	DATE INSTALLED*
B- 16	WATERPROOFING	\$0.80	SQ.FT.	1975 (1533)	(NONE)			
G- 19	WATERPROOFING	\$0.91	SQ.FT.	1982 (1971)	(NONE)			
G- 52	WATERPROOFING	\$0.90	SQ.FT.	1981 (1953)	(NONE)			
G- 53	WATERPROOFING	\$0.90	SQ.FT.	1981 (1953)	(NONE)			
G- 208	LSDC OVERLAY	\$100.00	CU.YD.	1988 (2268)	(NONE)			
B- 223	WATERPROOFING	\$1.00	SQ.FT.	1982 (1962)	(NONE)			
G- 224	WATERPROOFING	\$1.00	SQ.FT.	1982 (1962)	(NONE)			
G- 229	WATERPROOFING	\$0.65	SQ.FT.	1975 (1524)	(NONE)			
B- 238	WATERPROOFING	\$0.91	SQ.FT.	1982 (1131)	(NONE)			
B- 288	PAINT WATERPROOF	\$1.00	SQ.FT.	1986 (2170)	(NONE)			
B- 406	WATERPROOFING	\$0.90	SQ.FT.	1981 (1953)	(NONE)			
B- 407	WATERPROOFING	\$0.90	SQ.FT.	1981 (1953)	(NONE)			
I- 681	WATERPROOFING	\$1.00	SQ.FT.	1985 (2116)	(NONE)			
I- 682 E	WATERPROOFING	\$0.50	SQ.FT.	1978 (1681)	(NONE)			
I- 682 W	WATERPROOFING	\$0.50	SQ.FT.	1978 (1681)	(NONE)			
I- 683 N	WATERPROOFING	\$0.75	SQ.FT.	1981 (1903)	(NONE)			
I- 683 S	WATERPROOFING	\$0.75	SQ.FT.	1981 (1903)	(NONE)			
G- 686	WATERPROOFING	\$0.35	SQ.FT.	1974 (1494)	(NONE)			
I- 699 E	WATERPROOFING	\$0.50	SQ.FT.	1978 (1681)	(NONE)			
I- 699 W	WATERPROOFING	\$0.50	SQ.FT.	1978 (1681)	(NONE)			
I- 700 E	WATERPROOFING	\$0.50	SQ.FT.	1978 (1728)	(NONE)			
I- 700 W	WATERPROOFING	\$0.50	SQ.FT.	1978 (1728)	(NONE)			
B- 716 E	WATERPROOFING	\$0.50	SQ.FT.	1978 (1728)	(NONE)			
B- 716 W	WATERPROOFING	\$0.50	SQ.FT.	1978 (1728)	(NONE)			
I- 717 E	WATERPROOFING	\$0.50	SQ.FT.	1978 (1728)	(NONE)			
I- 717 W	WATERPROOFING	\$0.50	SQ.FT.	1978 (1728)	(NONE)			
I- 740 E	WATERPROOFING	\$0.50	SQ.FT.	1978 (1728)	(NONE)			
I- 740 W	WATERPROOFING	\$0.50	SQ.FT.	1978 (1728)	(NONE)			

*Number in parenthesis is Nevada Department of Transportation contract number.

Table 3-1 (Continued). Database of Nevada Bridges with Protection Systems.

BRIDGE NUMBER	ROUTE	MILEPOST	STRUCTURE NAME AND DESCRIPTIVE LOCATION	STRUCTURE TYPE	YEAR BUILT
I- 750	FAI 080	WA 22.55	LOCKWOOD INTERCHANGE	PRESTRESSED BOX GIRDER	1962
I- 753 E	FAI 080	WA 23.97	MUSTANG INTERCHANGE	PRESTRESSED GIRDER	1962
I- 753 W	FAI 080	WA 23.97	MUSTANG INTERCHANGE	PRESTRESSED GIRDER	1962
B- 764 E	FAI 080	WA 3.12	TRUCKEE RIVER S.W. OF VERDI	STEEL GIRDER	1963
B- 764 W	FAI 080	WA 3.12	TRUCKEE RIVER S.W. OF VERDI	STEEL GIRDER	1963
G- 765 E	FAI 080	WA 3.28	S.P.T.CO. OVERPASS WEST OF VERDI	STEEL GIRDER	1962
G- 765 W	FAI 080	WA 3.28	S.P.T.CO. OVERPASS WEST OF VERDI	STEEL GIRDER	1962
H- 767 E	FAI 080	WA 8.50	MAE ANNE GRADE SEPARATION	STEEL GIRDER	1962
H- 767 W	FAI 080	WA 8.50	MAE ANNE GRADE SEPARATION	CONCRETE BOX GIRDER	1966
I- 770	FAI 080	WA 4.89	HANSEN INTERCHANGE	CONCRETE BOX GIRDER	1966
G- 772 E	FAI 080	WA 5.45	TRUCKEE RIVER S.E. OF VERDI	CONCRETE BOX GIRDER	1964
G- 772 W	FAI 080	WA 5.45	TRUCKEE RIVER S.E. OF VERDI	CONCRETE BOX GIRDER	1964
I- 773 E	FAI 080	WA 5.69	EAST VERDI INTERCHANGE	STEEL GIRDER	1964
I- 773 W	FAI 080	WA 5.69	EAST VERDI INTERCHANGE	STEEL GIRDER	1964
I- 774 E	FAI 080	WA 7.08	MOGUL INTERCHANGE	STEEL GIRDER	1964
I- 774 W	FAI 080	WA 7.08	MOGUL INTERCHANGE	CONCRETE GIRDER	1964
I- 775 E	FAI 080	WA 7.75	LAWTON INTERCHANGE	CONCRETE GIRDER	1964
I- 775 W	FAI 080	WA 7.75	LAWTON INTERCHANGE	CONCRETE GIRDER	1964
I- 816 E	FAI 080	LY 22.09	U.S. 95 INTERCHANGE	CONCRETE DECK SLAB	1961
I- 816 W	FAI 080	LY 22.09	U.S. 95 INTERCHANGE	CONCRETE DECK SLAB	1961
I- 827 E	FAI 080	EL 32.91	OSINO INTERCHANGE	CONCRETE DECK SLAB	1964
I- 827 W	FAI 080	EL 32.91	OSINO INTERCHANGE	CONCRETE DECK SLAB	1964
I- 831 E	FAI 080	EL 36.95	DEVIL'S GATE-RYNDON INTERCHANGE	CONCRETE DECK SLAB	1964
I- 831 W	FAI 080	EL 36.95	DEVIL'S GATE-RYNDON INTERCHANGE	CONCRETE DECK SLAB	1964
I- 832 E	FAI 080	EL 39.18	ELBURZ INTERCHANGE	CONCRETE DECK SLAB	1964
I- 832 W	FAI 080	EL 39.18	ELBURZ INTERCHANGE	CONCRETE DECK SLAB	1964
B- 835 E	FAI 080	EL 40.09	NORTH FORK HUMBOLDT RIVER	CONCRETE DECK SLAB	1964
B- 835 W	FAI 080	EL 40.09	NORTH FORK HUMBOLDT RIVER	CONCRETE DECK SLAB	1962

Table 3-1 (Continued). Database of Nevada Bridges with Protection Systems.

BRIDGE NUMBER	ADT	ADT YEAR	LANES ON BRIDGE	DESIGN LOAD	SKEW ANGLE	NO OF SPANS	STRUCT LENGTH	MAX. SPAN LENGTH	WIDTH CURB-CURB	WIDTH OUT-OUT
I- 750	990	1987	2	HS-20	30	2	143	71	38.0	40.8
I- 753 E	6,403	1987	2	MOD HS-20	0	3	120	40	38.0	40.8
I- 753 W	6,402	1987	3	MOD HS-20	0	3	120	40	38.0	40.8
B- 764 E	9,540	1986	2	MOD HS-20	33	6	305	102	38.0	43.0
B- 764 W	9,540	1986	2	MOD HS-20	33	6	447	101	38.0	43.0
G- 765 E	9,540	1986	2	MOD HS-20	38	7	473	117	38.0	43.0
G- 765 W	9,540	1986	2	MOD HS-20	38	7	473	117	38.0	43.0
H- 767 E	10,985	1986	2	MOD HS-20	11	3	122	72	40.0	42.0
H- 767 W	10,985	1986	2	MOD HS-20	11	3	122	72	40.0	42.0
I- 770	2,320	1986	2	MOD HS-20	19	4	252	70	26.0	31.0
G- 772 E	10,263	1986	2	MOD HS-20	35	11	980	120	38.0	43.0
G- 772 W	10,263	1986	2	MOD HS-20	35	11	1070	120	38.0	43.0
I- 773 E	10,263	1986	2	MOD HS-20	36	3	161	51	38.0	43.0
I- 773 W	10,263	1986	2	MOD HS-20	36	3	157	50	38.0	43.0
I- 774 E	10,985	1986	2	MOD HS-20	0	3	128	50	38.0	43.0
I- 774 W	10,985	1986	2	MOD HS-20	0	3	128	50	38.0	43.0
I- 775 E	10,985	1986	2	MOD HS-20	45	3	152	60	38.0	43.0
I- 775 W	10,985	1986	2	MOD HS-20	45	3	152	60	38.0	43.0
I- 816 E	2,405	1987	2	MOD HS-20	31	3	123	47	38.0	43.0
I- 816 W	2,405	1987	2	MOD HS-20	31	3	123	47	44.0	49.0
I- 827 E	2,142	1986	2	MOD HS-20	0	3	94	35	38.0	43.0
I- 827 W	2,143	1986	2	MOD HS-20	0	3	94	35	38.0	43.0
I- 831 E	2,103	1986	2	MOD HS-20	0	3	94	35	38.0	43.0
I- 831 W	2,102	1986	2	MOD HS-20	0	3	94	35	38.0	43.0
I- 832 E	2,027	1986	2	MOD HS-20	0	3	94	35	38.0	43.0
I- 832 W	2,028	1986	2	MOD HS-20	0	3	94	35	38.0	43.0
B- 835 E	2,042	1986	2	MOD HS-20	0	3	114	43	38.0	43.0
B- 835 W	2,043	1986	2	MOD HS-20	0	3	114	43	38.0	43.0

Table 3-1 (Continued). Database of Nevada Bridges with Protection Systems.

BRIDGE NUMBER	CURRENT PROTECTION SYSTEM				PREVIOUS PROTECTION SYSTEM			
	PROTECTIVE SYSTEM	BID COST	PAY UNIT	DATE INSTALLED*	PROTECTIVE SYSTEM	BID COST	PAY UNIT	DATE INSTALLED*
I- 750	WATERPROOFING	\$3.00	SQ.FT.	1980 (1841)	(NONE)			
I- 753 E	PC OVERLAY (ASPHALT)	\$75.00	CU.FT.	1990 (2335)	WATERPROOFING	\$3.00	SQ.FT.	1980 (1841)
I- 753 W	PC OVERLAY (ASPHALT)	\$75.00	CU.FT.	1990 (2335)	WATERPROOFING	\$3.00	SQ.FT.	1980 (1841)
B- 764 E	LSDC OVERLAY	\$100.00	CU.YD.	1982 (1925)	WATERPROOFING	\$0.70	SQ.FT.	1977 (1591)
B- 764 W	LSDC OVERLAY	\$100.00	CU.YD.	1982 (1925)	WATERPROOFING	\$0.70	SQ.FT.	1977 (1591)
G- 765 E	LSDC OVERLAY	\$100.00	CU.YD.	1982 (1925)	WATERPROOFING	\$0.70	SQ.FT.	1976 (1591)
G- 765 W	LSDC OVERLAY	\$100.00	CU.YD.	1982 (1925)	WATERPROOFING	\$0.70	SQ.FT.	1976 (1591)
H- 767 E	LSDC OVERLAY	\$254.00	CU.YD.	1983 (1937)	(NONE)			
H- 767 W	LSDC OVERLAY	\$254.00	CU.YD.	1983 (1937)	(NONE)			
I- 770	WATERPROOFING	\$0.80	SQ.FT.	1982 (1937)	WATERPROOFING	\$0.70	SQ.FT.	1976 (1591)
G- 772 E	LSDC OVERLAY	\$254.00	CU.YD.	1983 (1937)	WATERPROOFING	\$0.70	SQ.FT.	1976 (1591)
G- 772 W	LSDC OVERLAY	\$254.00	CU.YD.	1984 (1937)	WATERPROOFING	\$0.70	SQ.FT.	1976 (1591)
I- 773 E	LSDC OVERLAY	\$254.00	CU.YD.	1983 (1937)	WATERPROOFING	\$0.70	SQ.FT.	1976 (1591)
I- 773 W	LSDC OVERLAY	\$254.00	CU.YD.	1984 (1937)	WATERPROOFING	\$0.70	SQ.FT.	1976 (1591)
I- 774 E	LSDC OVERLAY	\$254.00	CU.YD.	1983 (1937)	WATERPROOFING	\$0.70	SQ.FT.	1976 (1591)
I- 774 W	LSDC OVERLAY	\$254.00	CU.YD.	1983 (1937)	WATERPROOFING	\$0.70	SQ.FT.	1976 (1591)
I- 775 E	LSDC OVERLAY	\$254.00	CU.YD.	1983 (1937)	WATERPROOFING	\$0.70	SQ.FT.	1976 (1591)
I- 775 W	LSDC OVERLAY	\$254.00	CU.YD.	1983 (1937)	WATERPROOFING	\$0.70	SQ.FT.	1976 (1591)
I- 816 E	WATERPROOFING	\$2.00	SQ.FT.	1980 (1868)	(NONE)			
I- 816 W	WATERPROOFING	\$2.00	SQ.FT.	1980 (1868)	(NONE)			
I- 827 E	WATERPROOFING	\$0.77	SQ.FT.	1979 (1813)	(NONE)			
I- 827 W	WATERPROOFING	\$0.77	SQ.FT.	1979 (1813)	(NONE)			
I- 831 E	WATERPROOFING	\$0.77	SQ.FT.	1979 (1813)	(NONE)			
I- 831 W	WATERPROOFING	\$0.77	SQ.FT.	1979 (1813)	(NONE)			
I- 832 E	WATERPROOFING	\$0.77	SQ.FT.	1979 (1813)	(NONE)			
I- 832 W	WATERPROOFING	\$0.77	SQ.FT.	1979 (1813)	(NONE)			
B- 835 E	WATERPROOFING	\$0.77	SQ.FT.	1979 (1813)	(NONE)			
B- 835 W	WATERPROOFING	\$0.77	SQ.FT.	1979 (1813)	(NONE)			

*Number in parenthesis is Nevada Department of Transportation contract number.

Table 3-1 (Continued). Database of Nevada Bridges with Protection Systems.

BRIDGE NUMBER	ROUTE	MILEPOST	STRUCTURE NAME AND DESCRIPTIVE LOCATION	STRUCTURE TYPE	YEAR BUILT
I- 836 E	FAI 080	EL 43.70	HALLECK INTERCHANGE	CONCRETE DECK SLAB	1964
I- 836 W	FAI 080	EL 43.70	HALLECK INTERCHANGE	CONCRETE DECK SLAB	1964
G- 843 E	FAI 080	LY 1.26	S.P.T.CO. MODOC LINE OVERPASS	PRESTRESSED, PRECAST GIRDER	1963
G- 843 W	FAI 080	LY 1.26	S.P.T.CO. MODOC LINE OVERPASS	PRESTRESSED, PRECAST GIRDER	1963
H- 844 E	FAI 080	LY 2.68	FERNLEY GRADE SEPARATION	CONCRETE DECK SLAB	1963
H- 844 W	FAI 080	LY 2.68	FERNLEY GRADE SEPARATION	CONCRETE DECK SLAB	1963
I- 848 E	FAI 080	PE 4.60	TOULON INTERCHANGE	CONCRETE DECK SLAB	1965
I- 848 W	FAI 080	PE 4.60	TOULON INTERCHANGE	CONCRETE DECK SLAB	1965
H- 849 E	FAI 080	PE 13.22	PERTH GRADE SEPARATION	CONCRETE DECK SLAB	1971
H- 849 W	FAI 080	PE 13.22	PERTH GRADE SEPARATION	CONCRETE DECK SLAB	1971
H- 850 E	FAI 080	PE 15.63	BIG MEADOW GRADE SEPARATION	PRECAST BOX BEAM	1974
H- 850 W	FAI 080	PE 15.63	BIG MEADOW GRADE SEPARATION	PRECAST BOX BEAM	1974
B- 855 E	FAI 080	PE 18.59	HUMBOLDT RIVER NEAR LOVELOCK	STEEL GIRDER	1976
B- 855 W	FAI 080	PE 18.59	HUMBOLDT RIVER NEAR LOVELOCK	STEEL GIRDER	1976
I- 861 E	FAI 080	PE 69.64	COSGRAVE INTERCHANGE	CONCRETE DECK SLAB	1967
I- 861 W	FAI 080	PE 69.64	COSGRAVE INTERCHANGE	CONCRETE DECK SLAB	1967
G- 863 E	FAI 080	HU 3.40	ROSE CREEK, S.P.T.CO. OVERPASS	STEEL PLATE GIRDER	1970
G- 863 W	FAI 080	HU 3.40	ROSE CREEK, S.P.T.CO. OVERPASS	STEEL PLATE GIRDER	1970
H- 865 E	FAI 080	HU 8.60	AIRPORT GRADE SEPARATION	CONCRETE DECK SLAB	1970
H- 865 W	FAI 080	HU 8.60	AIRPORT GRADE SEPARATION	CONCRETE DECK SLAB	1970
H- 866 E	FAI 080	WA 16.48	SPARKS VIADUCT	CONCRETE BOX GIRDER	1966
H- 866 W	FAI 080	WA 16.48	SPARKS VIADUCT	CONCRETE BOX GIRDER	1966
H- 869 E	FAI 080	HU 14.27	WINNEMUCCA VIADUCT	PRESTRESSED BOX GIRDER	1977
H- 869 W	FAI 080	HU 14.27	WINNEMUCCA VIADUCT	PRESTRESSED BOX GIRDER	1977
I- 871 E	FAI 080	HU 14.96	WINNEMUCCA BLVD. EAST INTERCHANGE	PRESTRESSED BOX GIRDER	1977
I- 871 W	FAI 080	HU 14.96	WINNEMUCCA BLVD. EAST INTERCHANGE	PRESTRESSED BOX GIRDER	1977
I- 874 E	FAI 080	HU 23.68	BUTTON POINT INTERCHANGE	CONCRETE DECK SLAB	1965
I- 874 W	FAI 080	HU 23.68	BUTTON POINT INTERCHANGE	CONCRETE DECK SLAB	1965

Table 3-1 (Continued). Database of Nevada Bridges with Protection Systems.

BRIDGE NUMBER	ADT	ADT YEAR	LANES ON BRIDGE	DESIGN LOAD	SKIEW ANGLE	NO OF SPANS	STRUCT LENGTH	MAX. SPAN LENGTH	WIDTH CURB-CURB	WIDTH OUT-OUT
I- 836 E	1,992	1986	2	MOD HS-20	0	3	94	35	38.0	43.0
I- 836 W	1,993	1986	2	MOD HS-20	0	3	94	35	38.0	43.0
G- 843 E	3,818	1987	2	MOD HS-20	58	3	184	60	44.0	49.0
G- 843 W	3,818	1987	2	MOD HS-20	58	3	184	60	44.0	49.0
H- 844 E	3,818	1987	2	MOD HS-20	0	3	93	35	38.0	43.0
H- 844 W	3,818	1987	2	MOD HS-20	0	3	93	35	38.0	43.0
I- 848 E	3,045	1989	2	MOD HS-20	0	3	87	35	38.0	40.0
I- 848 W	3,045	1989	2	MOD HS-20	0	3	93	35	38.0	40.0
H- 849 E	3,105	1989	2	MOD HS-20	0	3	94	35	42.0	44.3
H- 849 W	3,105	1989	2	MOD HS-20	0	3	94	35	42.0	44.3
H- 850 E	3,105	1989	2	MOD HS-20	24	1	44	42	42.0	45.0
H- 850 W	3,105	1989	2	MOD HS-20	24	1	44	42	42.0	45.0
B- 855 E	3,090	1989	2	MOD HS-20	26	3	259	86	42.0	45.0
B- 855 W	3,090	1989	2	MOD HS-20	26	3	259	86	42.0	45.0
I- 861 E	3,000	1989	2	MOD HS-20	0	3	93	35	40.0	42.0
I- 861 W	3,000	1989	2	MOD HS-20	0	3	93	34	40.0	42.0
G- 863 E	2,778	1987	2	MOD HS-20	30	3	337	130	42.0	44.0
G- 863 W	2,778	1987	2	MOD HS-20	30	3	337	130	42.0	44.0
H- 865 E	2,298	1987	2	MOD HS-20	0	3	93	35	42.0	44.0
H- 865 W	2,298	1987	2	MOD HS-20	0	3	93	35	42.0	44.0
H- 866 E	28,150	1986	2	MOD HS-20	0	17	1040	65	44.4	48.0
H- 866 W	28,150	1986	2	MOD HS-20	0	17	1040	65	39.2	42.2
H- 869 E	1,970	1989	2	MOD HS-20	0	29	903	100	42.0	45.5
H- 869 W	1,970	1989	2	MOD HS-20	0	29	903	100	42.0	45.5
I- 871 E	2,625	1989	2	MOD HS-20	49	2	313	167	42.0	45.5
I- 871 W	2,625	1989	2	MOD HS-20	49	2	313	167	42.0	45.5
I- 874 E	2,970	1989	2	MOD HS-20	0	3	104	42	40.0	42.0
I- 874 W	2,970	1989	2	MOD HS-20	0	3	104	42	40.0	42.0

Table 3-1 (Continued). Database of Nevada Bridges with Protection Systems.

BRIDGE NUMBER	CURRENT PROTECTION SYSTEM				PREVIOUS PROTECTION SYSTEM			
	PROTECTIVE SYSTEM	BID COST	PAY UNIT	DATE INSTALLED*	PROTECTIVE SYSTEM	BID COST	PAY UNIT	DATE INSTALLED*
I- 836 E	WATERPROOFING	\$0.77	SQ.FT.	1979 (1813)	(NONE)			
I- 836 W	WATERPROOFING	\$0.77	SQ.FT.	1979 (1813)	(NONE)			
G- 843 E	WATERPROOFING	\$0.50	SQ.FT.	1978 (1728)	(NONE)			
G- 843 W	WATERPROOFING	\$0.50	SQ.FT.	1978 (1728)	(NONE)			
H- 844 E	WATERPROOFING	\$0.50	SQ.FT.	1978 (1728)	(NONE)			
H- 844 W	WATERPROOFING	\$0.50	SQ.FT.	1978 (1728)	(NONE)			
I- 848 E	PC OVERLAY (ASPHALT)	\$55.00	CU.FT.	1991 (2409)	WATERPROOFING	\$0.50	SQ.FT.	1978 (1681)
I- 848 W	PC OVERLAY (ASPHALT)	\$55.00	CU.FT.	1991 (2409)	WATERPROOFING	\$0.50	SQ.FT.	1978 (1681)
H- 849 E	PC OVERLAY (EXPOSED)	\$55.00	CU.FT.	1991 (2409)	WATERPROOFING	\$0.60	SQ.FT.	1974 (1483)
H- 849 W	PC OVERLAY (EXPOSED)	\$55.00	CU.FT.	1991 (2409)	WATERPROOFING	\$0.60	SQ.FT.	1974 (1483)
H- 850 E	PC OVERLAY (ASPHALT)	\$55.00	CU.FT.	1991 (2409)	WATERPROOFING	\$0.60	SQ.FT.	1974 (1483)
H- 850 W	PC OVERLAY (ASPHALT)	\$55.00	CU.FT.	1991 (2409)	WATERPROOFING	\$0.60	SQ.FT.	1974 (1483)
B- 855 E	LMC OVERLAY	NOT AVAILABLE		1972 (1600)	(NONE)			
B- 855 W	LMC OVERLAY	NOT AVAILABLE		1972 (1600)	(NONE)			
I- 861 E	PC OVERLAY (ASPHALT)	\$43.00	CU.FT.	1991 (2393)	WATERPROOFING	\$0.75	SQ.FT.	1979 (1819)
I- 861 W	PC OVERLAY (ASPHALT)	\$43.00	CU.FT.	1991 (2393)	WATERPROOFING	\$0.75	SQ.FT.	1979 (1819)
G- 863 E	WATERPROOFING	\$0.52	SQ.FT.	1978 (1681)	(NONE)			
G- 863 W	WATERPROOFING	\$0.52	SQ.FT.	1978 (1681)	(NONE)			
H- 865 E	WATERPROOFING	\$0.52	SQ.FT.	1978 (1681)	(NONE)			
H- 865 W	WATERPROOFING	\$0.52	SQ.FT.	1978 (1681)	(NONE)			
H- 866 E	WATERPROOFING	\$0.48	SQ.FT.	1973 (1476)	(NONE)			
H- 866 W	WATERPROOFING	\$0.48	SQ.FT.	1973 (1476)	(NONE)			
H- 869 E	(NONE)				LMC OVERLAY	\$19.30	SQ.YD.	1981 (1872)
H- 869 W	(NONE)				LMC OVERLAY	\$19.30	SQ.YD.	1981 (1872)
I- 871 E	(NONE)				LMC OVERLAY	\$19.30	SQ.YD.	1981 (1872)
I- 871 W	(NONE)				LMC OVERLAY	\$19.30	SQ.YD.	1981 (1872)
I- 874 E	PC OVERLAY (ASPHALT)	\$42.00	CU.FT.	1991 (2420)	WATERPROOFING	\$0.52	SQ.FT.	1977 (1681)
I- 874 W	PC OVERLAY (ASPHALT)	\$42.00	CU.FT.	1991 (2420)	WATERPROOFING	\$0.52	SQ.FT.	1977 (1681)

*Number in parenthesis is Nevada Department of Transportation contract number.

Table 3-1 (Continued). Database of Nevada Bridges with Protection Systems.

BRIDGE NUMBER	ROUTE	MILEPOST	STRUCTURE NAME AND DESCRIPTIVE LOCATION	STRUCTURE TYPE	YEAR BUILT
I- 878	FAI 080	LA 4.77	WEST BATTLE MTN. INTERCHANGE	CONCRETE BOX GIRDER	1976
I- 882	FAI 080	LA 8.13	EAST BATTLE MTN. INTERCHANGE	CONCRETE BOX GIRDER	1976
I- 892	FAI 080	EL 2.85	CENTRAL CARLIN INTERCHANGE	CONCRETE BOX GIRDER	1967
I- 896	FAI 080	EL 4.17	EAST CARLIN INTERCHANGE	PRESTRESSED BOX GIRDER	1967
I- 901	FAI 080	EL 23.27	ELKO DOWNTOWN INTERCHANGE	PRESTRESSED BOX GIRDER	1976
I- 908	FAI 080	EL 55.97	DEETH-STARR VALLEY INTERCHANGE	CONCRETE BOX GIRDER	1965
I- 909 E	FAI 080	EL 57.24	JARBRIDGE GRADE SEPARATION	CONCRETE DECK SLAB	1965
I- 909 W	FAI 080	EL 57.24	JARBRIDGE GRADE SEPARATION	CONCRETE DECK SLAB	1965
B- 911 E	FAI 080	EL 58.19	MARY'S RIVER	CONCRETE DECK SLAB	1965
B- 911 W	FAI 080	EL 58.19	MARY'S RIVER	CONCRETE DECK SLAB	1965
H- 912 E	FAI 080	EL 58.96	METROPOLIS GRADE SEPARATION	CONCRETE DECK SLAB	1965
H- 912 W	FAI 080	EL 58.96	METROPOLIS GRADE SEPARATION	CONCRETE DECK SLAB	1965
H- 914 E	FAI 080	EL 61.50	GREY'S CREEK GRADE SEPARATION	CONCRETE DECK SLAB	1965
H- 914 W	FAI 080	EL 61.50	GREY'S CREEK GRADE SEPARATION	CONCRETE DECK SLAB	1965
I- 915	FAI 080	EL 65.89	WELCOME INTERCHANGE	CONCRETE BOX GIRDER	1968
G- 919 E	FAI 080	EL 72.89	WELLS U.P.R.R. OVERPASS	STEEL GIRDER	1977
G- 919 W	FAI 080	EL 72.89	WELLS U.P.R.R. OVERPASS	STEEL GIRDER	1977
I- 920 E	FAI 080	EL 73.14	WEST WELLS INTERCHANGE	CONCRETE BOX GIRDER	1977
I- 920 W	FAI 080	EL 73.14	WEST WELLS INTERCHANGE	CONCRETE BOX GIRDER	1977
I- 921 E	FAI 080	EL 74.04	EAST WELLS INTERCHANGE	CONCRETE BOX GIRDER	1977
I- 921 W	FAI 080	EL 74.04	EAST WELLS INTERCHANGE	CONCRETE BOX GIRDER	1977
I- 923 E	FAI 080	EL 87.40	INDEPENDENCE INTERCHANGE	CONCRETE DECK SLAB	1965
I- 923 W	FAI 080	EL 87.40	INDEPENDENCE INTERCHANGE	CONCRETE DECK SLAB	1965
H- 993	FAI 080	WA 13.35	VIRGINIA GRADE SEPARATION	CONCRETE BOX GIRDER	1969
I- 1000	FAI 080	WA 14.81	RAMP 18 N-E	CONCRETE BOX GIRDER	1969
I- 1001	FAI 080	WA 14.83	RAMP 20 E-S	CONCRETE BOX GIRDER	1969
H- 1003	FAI 080	WA 15.54	KIETZKE GRADE SEPARATION	CONCRETE BOX GIRDER	1969
I- 1005 E	FAI 080	WA 16.09	ROCK BLVD. INTERCHANGE	CONCRETE BOX GIRDER	1968

Table 3-1 (Continued). Database of Nevada Bridges with Protection Systems.

BRIDGE NUMBER	ADT	ADT YEAR	LANES ON BRIDGE	DESIGN LOAD	SKEW ANGLE	NO OF SPANS	STRUCT LENGTH	MAX. SPAN LENGTH	WIDTH CURB-CURB	WIDTH OUT-OUT
I- 878	1,620	1987	3	MOD HS-20	24	2	320	160	48.0	55.5
I- 882	1,628	1987	3	MOD HS-20	62	2	320	160	48.0	55.5
I- 892	680	1987	2	MOD HS-20	0	2	224	110	46.0	53.0
I- 896	2,590	1987	2	MOD HS-20	0	2	276	137	36.0	39.5
I- 901	1,420	1986	2	MOD HS-20	19	2	297	152	72.0	81.5
I- 908	90	1986	2	MOD HS-20	0	5	270	66	29.0	31.0
I- 909 E	1,992	1986	2	MOD HS-20	8	3	94	35	40.0	42.0
I- 909 W	1,993	1986	2	MOD HS-20	8	3	94	35	40.0	42.0
B- 911 E	1,992	1986	2	MOD HS-20	0	3	93	35	40.0	42.0
B- 911 W	1,993	1986	2	MOD HS-20	0	3	93	35	40.0	42.0
H- 912 E	1,992	1986	2	MOD HS-20	24	3	94	35	40.0	42.0
H- 912 W	1,993	1986	2	MOD HS-20	24	3	94	35	40.0	42.0
H- 914 E	1,992	1986	2	MOD HS-20	0	3	93	35	40.0	42.0
H- 914 W	1,993	1986	2	MOD HS-20	0	3	93	35	40.0	42.0
I- 915	80	1987	2	MOD HS-20	0	4	240	92	29.0	31.0
G- 919 E	2,012	1986	2	MOD HS-20	10	3	162	63	54.5	58.0
G- 919 W	2,012	1986	2	MOD HS-20	10	3	162	63	61.8	65.3
I- 920 E	1,687	1986	2	MOD HS-20	10	1	159	157	42.0	45.5
I- 920 W	1,688	1986	2	MOD HS-20	10	1	159	157	42.0	45.5
I- 921 E	1,017	1986	2	MOD HS-20	0	1	151	149	42.0	45.5
I- 921 W	1,018	1986	2	MOD HS-20	0	1	151	149	42.0	45.5
I- 923 E	2,062	1988	2	MOD HS-20	0	3	93	35	42.0	44.0
I- 923 W	2,062	1988	2	MOD HS-20	0	3	93	35	42.0	44.0
H- 993	12,670	1986	4	MOD HS-20	0	4	200	72	70.0	82.3
I- 1000	4,435	1986	1	MOD HS-20	9	4	228	82	24.0	26.0
I- 1001	6,900	1986	1	MOD HS-20	24	4	238	81	24.0	26.0
H- 1003	63,270	1986	6	MOD HS-20	33	3	218	108	108.0	110.0
I- 1005 E	25,653	1986	2	MOD HS-20	10	3	155	85	39.2	42.0

Table 3-1 (Continued). Database of Nevada Bridges with Protection Systems.

BRIDGE NUMBER	CURRENT PROTECTION SYSTEM				PREVIOUS PROTECTION SYSTEM			
	PROTECTIVE SYSTEM	BID COST	PAY UNIT	DATE INSTALLED*	PROTECTIVE SYSTEM	BID COST	PAY UNIT	DATE INSTALLED*
I- 878	WATERPROOFING	\$0.69	SQ.FT.	1979 (1832)	PAINT WATERPROOF	\$2.46	SQ.FT.	1979 (1832)
I- 882	WATERPROOFING	\$0.69	SQ.FT.	1979 (1832)	(NONE)			
I- 892	WATERPROOFING	\$0.70	SQ.FT.	1978 (1767)	(NONE)			
I- 896	WATERPROOFING	\$0.68	SQ.FT.	1978 (1683)	(NONE)			
I- 901	WATERPROOFING	\$0.51	SQ.FT.	1979 (1763)	(NONE)			
I- 908	WATERPROOFING	\$1.00	SQ.FT.	1983 (1975)	(NONE)			
I- 909 E	WATERPROOFING	\$1.00	SQ.FT.	1983 (1975)	(NONE)			
I- 909 W	WATERPROOFING	\$1.00	SQ.FT.	1983 (1975)	(NONE)			
B- 911 E	WATERPROOFING	\$1.00	SQ.FT.	1983 (1975)	(NONE)			
B- 911 W	WATERPROOFING	\$1.00	SQ.FT.	1983 (1975)	(NONE)			
H- 912 E	WATERPROOFING	\$1.00	SQ.FT.	1983 (1975)	(NONE)			
H- 912 W	WATERPROOFING	\$1.00	SQ.FT.	1983 (1975)	(NONE)			
H- 914 E	WATERPROOFING	\$1.00	SQ.FT.	1983 (1975)	(NONE)			
H- 914 W	WATERPROOFING	\$1.00	SQ.FT.	1983 (1975)	(NONE)			
I- 915	SPRAY WATERPROOF	\$35.00	GAL.	1989 (2327)	(NONE)			
G- 919 E	LSDC OVERLAY	\$25.00	CU.YD.	1980 (1833)	(NONE)			
G- 919 W	LSDC OVERLAY	\$25.00	CU.YD.	1980 (1833)	(NONE)			
I- 920 E	LSDC OVERLAY	\$25.00	CU.YD.	1980 (1833)	(NONE)			
I- 920 W	LSDC OVERLAY	\$25.00	CU.YD.	1980 (1833)	(NONE)			
I- 921 E	LSDC OVERLAY	\$25.00	CU.YD.	1980 (1833)	(NONE)			
I- 921 W	LSDC OVERLAY	\$25.00	CU.YD.	1980 (1833)	(NONE)			
I- 923 E	PC OVERLAY (ASPHALT)	\$55.00	CU.FT.	1991 (2407)	(NONE)			
I- 923 W	PC OVERLAY (ASPHALT)	\$55.00	CU.FT.	1991 (2407)	(NONE)			
H- 993	WATERPROOFING	\$0.80	SQ.FT.	1982 (1946)	(NONE)			
I- 1000	LSDC OVERLAY	\$100.00	CU.YD.	1984 (2032)	WATERPROOFING	\$0.80	SQ.FT.	1972 (1459)
I- 1001	LSDC OVERLAY	\$100.00	CU.YD.	1984 (2032)	WATERPROOFING	\$0.80	SQ.FT.	1972 (1459)
H- 1003	WATERPROOFING	\$0.88	SQ.FT.	1974 (1513)	(NONE)			
I- 1005 E	LSDC OVERLAY	\$115.00	CU.YD.	1986 (2139)	WATERPROOFING	\$0.48	SQ.FT.	1973 (1476)

*Number in parenthesis is Nevada Department of Transportation contract number.

Table 3-1 (Continued). Database of Nevada Bridges with Protection Systems.

BRIDGE NUMBER	ROUTE	MILEPOST	STRUCTURE NAME AND DESCRIPTIVE LOCATION	STRUCTURE TYPE	YEAR BUILT
I- 1005 W	FAI 080	WA 16.09	ROCK BLVD. INTERCHANGE	CONCRETE BOX GIRDER	1968
I- 1006 E	FAI 080	WA 16.79	PYRAMID INTERCHANGE	CONCRETE BOX GIRDER	1969
I- 1006 W	FAI 080	WA 16.79	PYRAMID INTERCHANGE	CONCRETE BOX GIRDER	1969
I- 1007 E	FAI 080	WA 17.57	EAST McCARREN INTERCHANGE	CONCRETE BOX GIRDER	1964
I- 1007 W	FAI 080	WA 17.57	EAST McCARREN INTERCHANGE	CONCRETE BOX GIRDER	1964
I- 1008	FAI 080	WA 19.69	VISTA INTERCHANGE	CONCRETE BOX GIRDER	1985
I- 1010	FAI 080	WA 15.55	RAMP 24 OVER KIETZKE LANE	CONCRETE BOX GIRDER	1969
B- 1066 E	FAI 080	EL 7.69	HUMBOLDT R.-CARLIN CANYON. #1	STEEL GIRDER	1971
B- 1066 W	FAI 080	EL 7.69	HUMBOLDT R.-CARLIN CANYON. #1	STEEL GIRDER	1971
I- 1086	FAI 080	WA 14.86	I-580 INTERCHANGE	CONCRETE BOX GIRDER	1969
I- 1086	FAI 580	WA 25.83	I-80 INTERCHANGE	CONCRETE BOX GIRDER	1969
I- 1087	FAI 080	WA 14.88	RAMP 14	CONCRETE BOX GIRDER	1969
I- 1088	FAI 080	WA 14.90	RAMP 15	CONCRETE BOX GIRDER	1969
I- 1089	FAP 395	WA 26.42	ODDIE INTERCHANGE	CONCRETE BOX GIRDER	1967
H- 1090	FAP 395	WA 26.83	WEDEKIND GRADE SEPARATION	CONCRETE BOX GIRDER	1967
H- 1091 N	FAP 395	WA 27.41	CLEAR ACRE GRADE SEPARATION	CONCRETE BOX GIRDER	1967
G- 1092 N	FAP 395	WA 30.04	PANTHER VALLEY U.P.R.R. OVERPASS	PRECAST CONCRETE BOX	1967
G- 1092 S	FAP 395	WA 30.04	PANTHER VALLEY U.P.R.R. OVERPASS	PRECAST CONCRETE BOX	1967
I- 1093 N	FAP 395	WA 30.31	PANTHER VALLEY INTERCHANGE	CONCRETE DECK SLAB	1967
B- 1111 E	FAI 080	EL 8.10	HUMBOLDT R.-CARLIN CANYON. #2	STEEL GIRDER	1971
B- 1111 W	FAI 080	EL 8.10	HUMBOLDT R.-CARLIN CANYON. #2	STEEL GIRDER	1971
B- 1112 E	FAI 080	EL 9.06	HUMBOLDT R.-CARLIN CANYON. #3	STEEL GIRDER	1971
B- 1112 W	FAI 080	EL 9.06	HUMBOLDT R.-CARLIN CANYON. #3	STEEL GIRDER	1971
B- 1113 E	FAI 080	EL 9.33	HUMBOLDT R.-CARLIN CANYON. #4	STEEL GIRDER	1971
B- 1113 W	FAI 080	EL 9.33	HUMBOLDT R.-CARLIN CANYON. #4	STEEL GIRDER	1971
I- 1147 E	FAI 080	PE 63.00	DUN GLEN INTERCHANGE	CONCRETE DECK SLAB	1967
I- 1147 W	FAI 080	PE 63.00	DUN GLEN INTERCHANGE	CONCRETE DECK SLAB	1967
I- 1149	FAI 580	WA 25.74	RAMP 14 W-N	CONCRETE BOX GIRDER	1969

Table 3-1 (Continued). Database of Nevada Bridges with Protection Systems.

BRIDGE NUMBER	ADT	ADT YEAR	LANES ON BRIDGE	DESIGN LOAD	SKEW ANGLE	NO OF SPANS	STRUCT LENGTH	MAX. SPAN LENGTH	WIDTH CURB-CURB	WIDTH OUT-OUT
I- 1005 W	25,653	1986	2	MOD HS-20	10	3	155	85	44.4	48.0
I- 1006 E	17,182	1986	2	MOD HS-20	0	3	109	42	39.2	42.2
I- 1006 W	17,183	1986	2	MOD HS-20	0	3	109	42	39.0	42.0
I- 1007 E	8,160	1986	2	MOD HS-20	0	4	182	47	52.5	55.5
I- 1007 W	8,160	1986	2	MOD HS-20	0	4	182	47	88.0	91.0
I- 1008	5,015	1986	4	MOD HS-20	0	4	175	54	26.0	31.0
I- 1010	63,270	1986	2	MOD HS-20	23	4	183	56	23.2	26.2
B- 1066 E	2,728	1987	2	MOD HS-20	0	3	320	130	29.9	36.7
B- 1066 W	2,728	1987	2	MOD HS-20	0	3	320	130	29.9	36.7
I- 1086	32,800	1986	6	MOD HS-20	7	4	247	78	46.0	47.0
I- 1086	32,800	1986	6	MOD HS-20	7	4	247	78	45.0	94.0
I- 1087	11,460	1986	1	MOD HS-20	0	4	228	79	24.0	26.0
I- 1088	10,900	1986	1	MOD HS-20	9	4	233	84	38.0	40.0
I- 1089	44,150	1986	5	MOD HS-20	0	4	182	70	84.0	86.0
H- 1090	43,350	1986	4	MOD HS-20	30	4	103	60	74.0	76.0
H- 1091 N	14,993	1986	2	MOD HS-20	6	3	102	60	40.0	42.0
G- 1092 N	13,325	1986	2	MOD HS-20	17	5	208	45	40.0	42.0
G- 1092 S	13,325	1986	2	MOD HS-20	17	5	208	55	40.0	42.0
I- 1093 N	12,775	1986	2	MOD HS-20	49	4	183	70	40.0	42.0
B- 1111 E	2,728	1987	2	MOD HS-20	0	3	370	152	29.9	36.6
B- 1111 W	2,728	1987	2	MOD HS-20	0	3	370	152	29.9	36.6
B- 1112 E	2,728	1987	2	MOD HS-20	0	3	320	130	42.0	44.0
B- 1112 W	2,728	1987	2	MOD HS-20	0	3	320	130	42.0	44.0
B- 1113 E	2,728	1987	2	MOD HS-20	0	3	370	152	42.0	44.0
B- 1113 W	2,728	1987	2	MOD HS-20	0	3	370	152	42.0	44.0
I- 1147 E	2,398	1987	2	MOD HS-20	0	3	105	42	40.0	42.0
I- 1147 W	2,398	1987	2	MOD HS-20	0	3	105	42	40.0	42.0
I- 1149	9,810	1984	7	MOD HS-20	32	3	144	66	45.0	106.0

Table 3-1 (Continued). Database of Nevada Bridges with Protection Systems.

BRIDGE NUMBER	CURRENT PROTECTION SYSTEM				PREVIOUS PROTECTION SYSTEM			
	PROTECTIVE SYSTEM	BID COST	PAY UNIT	DATE INSTALLED*	PROTECTIVE SYSTEM	BID COST	PAY UNIT	DATE INSTALLED*
I- 1005 W	LSDC OVERLAY	\$115.00	CU.YD.	1987 (2139)	WATERPROOFING	\$0.48	SQ.FT.	1973 (1476)
I- 1006 E	WATERPROOFING	\$0.88	SQ.FT.	1974 (1513)	(NONE)			
I- 1006 W	WATERPROOFING	\$0.88	SQ.FT.	1974 (1513)	(NONE)			
I- 1007 E	WATERPROOFING	\$1.05	SQ.FT.	1974 (1511)	(NONE)			
I- 1007 W	WATERPROOFING	\$1.05	SQ.FT.	1974 (1511)	(NONE)			
I- 1008	LSDC OVERLAY	\$117.00	CU.YD.	1985 (2046)	(NONE)			
I- 1010	WATERPROOFING	\$0.88	SQ.FT.	1974 (1513)	(NONE)			
B- 1066 E	WATERPROOFING	\$0.55	SQ.FT.	1974 (1486)	(NONE)			
B- 1066 W	WATERPROOFING	\$0.55	SQ.FT.	1974 (1486)	(NONE)			
I- 1086	LSDC OVERLAY	\$100.00	CU.YD.	1984 (2032)	WATERPROOFING	\$0.80	SQ.FT.	1972 (1459)
I- 1086	LSDC OVERLAY	\$100.00	CU.YD.	1984 (2032)	(NONE)			
I- 1087	LSDC OVERLAY	\$100.00	CU.YD.	1984 (2032)	WATERPROOFING	\$0.80	SQ.FT.	1972 (1459)
I- 1088	LSDC OVERLAY	\$100.00	CU.YD.	1984 (2032)	WATERPROOFING	\$0.80	SQ.FT.	1972 (1459)
I- 1089	LSDC OVERLAY	\$100.00	CU.YD.	1984 (2032)	WATERPROOFING	\$0.88	SQ.FT.	1974 (1513)
I- 1090	LSDC OVERLAY	\$100.00	CU.YD.	1984 (2032)	WATERPROOFING	\$0.88	SQ.FT.	1974 (1513)
H- 1091 N	LSDC OVERLAY	\$100.00	CU.YD.	1984 (2032)	WATERPROOFING	\$0.88	SQ.FT.	1974 (1513)
G- 1092 N	LSDC OVERLAY	\$100.00	CU.YD.	1984 (2032)	WATERPROOFING	\$0.88	SQ.FT.	1974 (1513)
G- 1092 S	LSDC OVERLAY	\$100.00	CU.YD.	1984 (2032)	WATERPROOFING	\$0.88	SQ.FT.	1974 (1513)
I- 1093 N	LSDC OVERLAY	\$100.00	CU.YD.	1984 (2032)	WATERPROOFING	\$0.88	SQ.FT.	1974 (1513)
B- 1111 E	WATERPROOFING	\$0.55	SQ.FT.	1974 (1486)	(NONE)			
B- 1111 W	WATERPROOFING	\$0.55	SQ.FT.	1974 (1486)	(NONE)			
B- 1112 E	WATERPROOFING	\$0.55	SQ.FT.	1974 (1486)	(NONE)			
B- 1112 W	WATERPROOFING	\$0.55	SQ.FT.	1974 (1486)	(NONE)			
B- 1113 E	WATERPROOFING	\$0.55	SQ.FT.	1974 (1486)	(NONE)			
B- 1113 W	WATERPROOFING	\$0.55	SQ.FT.	1974 (1486)	(NONE)			
I- 1147 E	PC OVERLAY (ASPHALT)	\$43.00	CU.FT.	1991 (2393)	WATERPROOFING	\$0.75	SQ.FT.	1979 (1819)
I- 1147 W	PC OVERLAY (ASPHALT)	\$43.00	CU.FT.	1991 (2393)	WATERPROOFING	\$0.75	SQ.FT.	1979 (1819)
I- 1149	LSDC OVERLAY	\$100.00	CU.YD.	1984 (2032)	(NONE)			

*Number in parenthesis is Nevada Department of Transportation contract number.

Table 3-1 (Continued). Database of Nevada Bridges with Protection Systems.

BRIDGE NUMBER	ROUTE	MILEPOST	STRUCTURE NAME AND DESCRIPTIVE LOCATION	STRUCTURE TYPE	YEAR BUILT
I- 1159 E	FAI 080	EL 98.67	PEQUOP INTERCHANGE	CONCRETE VOIDED SLAB	1973
I- 1159 W	FAI 080	EL 98.67	PEQUOP INTERCHANGE	CONCRETE VOIDED SLAB	1973
I- 1161 E	FAI 080	PE 19.06	RODGERS CANAL	STEEL GIRDER	1976
I- 1161 W	FAI 080	PE 19.06	RODGERS CANAL	STEEL GIRDER	1976
H- 1162 E	FAI 080	WA 12.04	STOKER GRADE SEPARATION	CONCRETE BOX GIRDER	1966
H- 1162 W	FAI 080	WA 12.04	STOKER GRADE SEPARATION	CONCRETE BOX GIRDER	1966
I- 1171	FAP 395	WA 25.95	RAMP N-E & N-W OVER 9TH ST.	CONCRETE BOX GIRDER	1969
I- 1172	FAP 395	WA 25.96	N-S FREEWAY & 9TH ST.	CONCRETE BOX GIRDER	1969
H- 1199	FAI 080	WA 12.73	VINE GRADE SEPARATION	STEEL BOX GIRDER	1973
H- 1205	FAI 080	EL 5.87	VIVIAN GRADE SEPARATION	PRESTRESSED BOX GIRDER	1976
G- 1233 L	FAI 580	WA 25.59	S.P.T.CO. & 4TH ST. W-S	STEEL GIRDER	1971
G- 1233 R	FAI 580	WA 25.59	S.P.T.CO. & 4TH ST. S-W	STEEL GIRDER	1971
G- 1233	FAI 580	WA 25.59	S.P.T.CO. & 4TH ST. N-S	STEEL GIRDER	1971
H- 1234	FAI 580	WA 25.42	TRUCKEE RIVER, KIETZKE LN.	STEEL GIRDER	1971
H- 1256 E	FAI 080	HU 11.66	WEST STRIP GRADE SEPARATION	CONCRETE BOX GIRDER	1970
H- 1256 W	FAI 080	HU 11.66	WEST STRIP GRADE SEPARATION	CONCRETE BOX GIRDER	1970
I- 1301 E	FAI 080	WA 10.68	WEST McCARREN INTERCHANGE	CONCRETE BOX GIRDER	1977
I- 1301 W	FAI 080	WA 10.68	WEST McCARREN INTERCHANGE	CONCRETE BOX GIRDER	1977
I- 1305	FAP 395	WA 27.18	NORTH McCARRAN INTERCHANGE	PRECAST CONCRETE GIRDER	1971
I- 1306	FAP 395	WA 28.84	PARR INTERCHANGE	PRECAST CONCRETE GIRDER	1971
I- 1511 E	FAI 080	EL 69.72	ALAZON INTERCHANGE	CONCRETE BOX GIRDER	1977
I- 1511 W	FAI 080	EL 69.72	ALAZON INTERCHANGE	CONCRETE BOX GIRDER	1977
H- 1512 E	FAI 080	EL 73.46	SHOSHONE GRADE SEPARATION	CONCRETE BOX GIRDER	1977
H- 1512 W	FAI 080	EL 73.46	SHOSHONE GRADE SEPARATION	CONCRETE BOX GIRDER	1977

Table 3-1 (Continued). Database of Nevada Bridges with Protection Systems.

BRIDGE NUMBER	ADT	ADT YEAR	LANES ON BRIDGE	DESIGN LOAD	SKEW ANGLE	NO OF SPANS	STRUCT LENGTH	MAX. SPAN LENGTH	WIDTH CURB-CURB	WIDTH OUT-OUT
I- 1159 E	2,072	1988	2	MOD HS-20	30	3	150	58	50.0	52.0
I- 1159 W	2,072	1988	2	MOD HS-20	30	3	150	58	50.0	52.0
I- 1161 E	3,090	1989	2	MOD HS-20	30	1	73	68	42.0	45.0
I- 1161 W	3,090	1989	2	MOD HS-20	30	1	73	68	42.0	45.0
H- 1162 E	12,543	1986	2	MOD HS-20	15	3	152	68	40.0	42.0
H- 1162 W	12,543	1986	2	MOD HS-20	15	3	152	68	40.0	42.0
I- 1171	9,440	1986	2	MOD HS-20	46	3	163	82	36.0	38.0
I- 1172	39,100	1986	6	MOD HS-20	12	4	200	65	92.0	94.0
H- 1199	7,500	1986	2	MOD HS-20	0	5	770	207	32.0	39.0
H- 1205	150	1987	2	MOD HS-20	0	2	255	130	32.0	34.8
G- 1233 L	11,700	1986	2	MOD HS-20	99	6	450	95	38.0	40.0
G- 1233 R	11,700	1986	1	MOD HS-20	99	6	460	95	24.0	26.0
G- 1233	12,200	1984	6	MOD HS-20	34	6	460	95	44.0	47.0
H- 1234	76,800	1986	8	MOD HS-20	99	3	495	180	58.5	118.0
H- 1256 E	2,710	1987	2	MOD HS-20	35	3	210	82	42.0	44.0
H- 1256 W	2,710	1987	2	MOD HS-20	35	3	210	82	42.0	44.0
I- 1301 E	10,985	1986	2	MOD HS-20	30	1	183	180	42.0	45.0
I- 1301 W	10,985	1986	2	MOD HS-20	30	1	183	180	42.0	45.0
I- 1305	24,445	1986	4	MOD HS-20	25	2	258	96	88.0	96.5
I- 1306	3,470	1986	2	MOD HS-20	20	2	257	96	48.0	50.5
I- 1511 E	1,957	1986	2	MOD HS-20	0	1	105	103	42.0	45.5
I- 1511 W	1,958	1986	2	MOD HS-20	0	1	105	103	42.0	45.5
H- 1512 E	1,832	1986	2	MOD HS-20	0	1	122	120	42.0	45.5
H- 1512 W	1,833	1986	2	MOD HS-20	0	1	122	120	42.0	45.5

Table 3-1 (Continued). Database of Nevada Bridges with Protection Systems.

BRIDGE NUMBER	CURRENT PROTECTION SYSTEM				PREVIOUS PROTECTION SYSTEM			
	PROTECTIVE SYSTEM	BID COST	PAY UNIT	DATE INSTALLED*	PROTECTIVE SYSTEM	BID COST	PAY UNIT	DATE INSTALLED*
I- 1159 E	LMC OVERLAY	NOT AVAILABLE	NOT AVAILABLE	1974 (1421)	(NONE)			
I- 1159 W	LMC OVERLAY	NOT AVAILABLE	NOT AVAILABLE	1974 (1421)	(NONE)			
I- 1161 E	LMC OVERLAY	NOT AVAILABLE	NOT AVAILABLE	1972 (1600)	(NONE)			
I- 1161 W	LMC OVERLAY	NOT AVAILABLE	NOT AVAILABLE	1972 (1600)	(NONE)			
H- 1162 E	WATERPROOFING	\$0.80	SQ.FT.	1982 (1937)	(NONE)			
H- 1162 W	WATERPROOFING	\$0.80	SQ.FT.	1982 (1937)	(NONE)			
I- 1171	LSDC OVERLAY	\$100.00	CU.YD.	1984 (2032)	WATERPROOFING	\$0.80	SQ.FT.	1972 (1459)
I- 1172	LSDC OVERLAY	\$100.00	CU.YD.	1984 (2032)	WATERPROOFING	\$0.80	SQ.FT.	1972 (1459)
H- 1199	SPRAY WATERPROOF	\$0.40	SQ.FT.	1985 (2037)	(NONE)			
H- 1205	WATERPROOFING	\$0.68	SQ.FT.	1978 (1683)	(NONE)			
G- 1233 L	LSDC OVERLAY	\$400.00	CU.YD.	1983 (1980)	(NONE)			
G- 1233 R	LSDC OVERLAY	\$400.00	CU.YD.	1983 (1980)	(NONE)			
G- 1233	LSDC OVERLAY	\$400.00	CU.YD.	1983 (1980)	(NONE)			
H- 1234	LSDC OVERLAY	\$400.00	CU.YD.	1983 (1980)	(NONE)			
H- 1256 E	WATERPROOFING	\$0.66	SQ.FT.	1974 (1517)	(NONE)			
H- 1256 W	WATERPROOFING	\$0.66	SQ.FT.	1974 (1517)	(NONE)			
I- 1301 E	WATERPROOFING	\$0.80	SQ.FT.	1977 (1703)	(NONE)			
I- 1301 W	WATERPROOFING	\$0.80	SQ.FT.	1977 (1703)	(NONE)			
I- 1305	LSDC OVERLAY	\$100.00	CU.YD.	1985 (2032)	(NONE)			
I- 1306	LSDC OVERLAY	\$100.00	CU.YD.	1984 (2032)	(NONE)			
I- 1511 E	LSDC OVERLAY	\$25.00	CU.YD.	1981 (1833)	(NONE)			
I- 1511 W	LSDC OVERLAY	\$25.00	CU.YD.	1981 (1833)	(NONE)			
H- 1512 E	LSDC OVERLAY	\$25.00	CU.YD.	1980 (1833)	(NONE)			
H- 1512 W	LSDC OVERLAY	\$25.00	CU.YD.	1980 (1833)	(NONE)			

*Number in parenthesis is Nevada Department of Transportation contract number.

Chapter 4

Comparison of the Engineering Properties of Polyester-Styrene Polymer Concrete and Portland Cement Concrete

4.1 Introduction

This chapter is concerned with the use of polyester-styrene polymer concrete as a bridge deck overlay material. Polymer concrete overlays provide durable and wear-resistant surfaces for portland cement concrete bridge decks, and can be formulated to provide low water and chloride permeabilities.¹⁵

The bond between the polymer concrete overlay and the portland cement concrete substrate is generally stronger than the strength of the portland cement concrete itself, resulting in a composite section with distinct areas of different physical properties. In order to study the effects of composite action and the behavioral differences between portland cement concrete and polymer concrete, a knowledge of the material properties of polymer concrete must be obtained. This chapter presents an overview of the engineering properties of polyester-styrene polymer concrete and offers a comparison of these properties to those of conventional portland cement concrete.

4.2 What are Polymers?

"Plastic products" is what usually comes to mind when one hears the term "polymer," but polymers embody a broader list of materials than just the familiar ones: nylon clothing; PVC pipe, bottles, and record albums; polyethylene bags; and polystyrene fast-food containers. DNA, leather, and natural rubber are also polymers. Polymers are composed of long chain-like molecules consisting of repeating basic units called monomers.²³

The polymer binders typically used for polymer concrete bridge deck overlays include acrylic resins, polyester resins, and epoxies. This study is concerned with a binder composed of unsaturated isophthalic polyester dissolved in a styrene monomer.

4.3 Hydration, Polymerization, and Binder Mechanisms

Portland cement concrete is a mixture of coarse and fine aggregates, portland cement, water, entrapped or entrained air, and frequently, various admixtures proportioned, mixed, and cured to develop the required hardened properties. The primary function of the mixing water is to allow the calcium silicate molecules in the cement particles to undergo a chemical reaction, called hydration, to produce calcium hydroxide and calcium silicate hydrate. The engineering properties of concrete, such as setting and hardening, strength, and dimensional stability, depend primarily on the calcium silicate hydrate gel.²⁴

In hardened portland cement concrete, the calcium silicate hydrate particles form dense, bonded aggregations between the other crystalline phases and the remaining unhydrated cement grains. These particles also adhere to the coarse and fine aggregates, cementing everything together.

Polymerization, often called "curing" or "hardening," is the process of forming long polymer chains from individual monomer molecules.²⁵ Polymerization is an exothermic chemical reaction in which chain growth occurs as a result of the presence of reactive molecules, called free-radicals.

Polymer concrete is a mixture of coarse and fine aggregate and a polymeric binder which replaces the portland cement/water binder of conventional concrete. Upon subsequent polymerization of the initiated binder, a hardened concrete mass results. In contrast to the hydrated cement, which consists of separate binder particles cemented together, polymer binders represent a continuous phase—the binder is essentially one piece, with the aggregate locked inside.

4.4 Typical Mix Designs

To highlight differences between the mix proportions in a typical portland cement concrete mix and a polyester-styrene polymer concrete mix, an example of each is presented in this section, as well as the descriptions of polyester-styrene concretes from previous research projects.

4.4.1 Portland Cement Concrete

A typical mix design for portland cement concrete²⁶ consists of the following material proportions:

Portland cement, Type I or II	560 lb/yd ³
Coarse aggregate (¾ inch maximum)	1710 lb/yd ³
Fine aggregate (fineness modulus = 2.8)	1075 lb/yd ³
Water-cement ratio.....	0.50
Air content	6.0 percent

This mixture was laboratory tested and yielded a compressive strength of 3300 psi after 7 days, and over 4000 psi after 28 days.

4.4.2 Polymer Concrete

A typical polyester-styrene polymer concrete mix design²⁷ for bridge deck overlays consists of the following components:

Unsaturated polyester in styrene monomer	12 percent by weight
Methyl ethyl ketone peroxide initiator	0.8 percent of resin
Cobalt naphthenate promoter.....	0.4 percent of resin
γ-methacryloxypropyltrimethoxysilane coupler	1.0 percent of resin
Combined coarse and fine aggregate	88 percent by weight

4.4.3 Polymer Concretes from Previous Research

The properties of polymer concrete discussed in the remainder of this chapter were derived from four research projects. This section presents descriptions of the mix designs which were used to develop the results.

In a paper presented at the First International Congress on Polymer Concrete, held in London in 1976, K. Kobayashi and T. Ito discussed the properties of an unsaturated polyester resin concrete.²⁸ This concrete consisted of 11 percent (by weight) unsaturated polyester (61 percent) in styrene monomer (39 percent). Methyl ethyl ketone peroxide (MEKP) and cobalt octenate were used as the initiator/promoter system, and γ -methacryloxypropyltrimethoxysilane was used as a silane coupling agent. The maximum aggregate size used was 3/4-inch. Concrete specimens were cured at 68°F for the first 24 hours, followed by an additional 15 hours at 158°F. This elevated temperature resulted in a significant increase in compressive strength of the polymer concrete, compared to the other test projects. The concrete produced had the following properties:

Compressive strength, f'_c	20,000 psi
Splitting tensile strength, f_{ct}	1600 psi
Modulus of elasticity, E_c	4.4×10^6 psi

Another paper, by R. C. Valore, Jr. and D. J. Naus, presented at the First International Congress on Polymer Concrete was based on combinations of rigid, resilient, flexible, and "low shrinkage" polyester resins.²⁹ The unsaturated polyester resin contained styrene monomers in amounts of 20 to 40 percent by weight. Methyl ethyl ketone peroxide and cobalt naphthenate were used as the initiator/promoter system, the maximum aggregate size was 3/8-inch, and no silane coupling agent was employed. The concrete properties were as follows:

Compressive strength, f'_c	9000 - 16,100 psi
Splitting tensile strength, f_{ct}	1400 - 2300 psi
Modulus of elasticity, E_c	$1.2 - 4.6 \times 10^6$ psi

C. Vipulanandan and E. Paul performed laboratory testing on both epoxy and polyester polymer concretes.³⁰ A variety of aggregate combinations were used, but the majority of testing for polyester systems was performed using a concrete composed of 15 percent (by weight) unsaturated polyester-styrene binder with Ottawa 20-30 sand aggregate. Several curing methods were employed to evaluate effects on strength properties; the methods included a 24-hour cure at room temperature followed by 24 hours at room temperature or at various elevated temperatures. All testing was performed after the 2-day curing period. As was the case with the Kobayashi and Ito research, the specimens cured at elevated temperatures exhibited higher strength characteristics. Typical properties for the polymer concretes tested were:

Compressive strength, f'_c	7000 - 10,000 psi
Splitting tensile strength, f_{ct}	450 - 1300 psi
Modulus of elasticity, E_c	$0.7 - 1.0 \times 10^6$ psi

The fourth set of data was published by the California Department of Transportation.³¹ No information is available as to the actual concrete composition; however, the resin loading was specified as 11 percent by weight, using 3/8-inch maximum aggregate size. Properties were described as follows:

Compressive strength, f'_c	7500 psi
Modulus of rupture, f_r	2000 psi
Modulus of elasticity, E_c	$1.6 - 2.4 \times 10^6$ psi

4.5 Principle Properties

4.5.1 Compressive Strength

Compressive strength is the measured maximum resistance to axial loading, expressed as force per unit of cross-sectional area. Because most concretes are comparatively weaker in tension than compression, concrete structures are usually designed so that the concrete is in compression; thus, the compressive strength, f'_c , is an important property of hardened concrete.³² The 28-day compressive strength of a typical structural portland cement concrete is in the range of 4000 psi to 6000 psi, as measured in the laboratory using 6-inch diameter by 12-inch high cylindrical specimens. As shown by the research projects described in the previous section, polyester-styrene polymer concretes have compressive strengths which range from 7000 psi to 20,000 psi, depending on resin formulation, amount of initiator and promoter, and temperature.

4.5.2 Modulus of Elasticity

For many materials, strain is directly proportional to stress up to a certain limit. The constant value of stress divided by strain is known as the modulus of elasticity, and is an indication of the stiffness or resistance to movement of a material. Even though most concretes do not possess a perfectly linear relationship between stress and strain, an approximate value is often used because the modulus of elasticity is a convenient parameter. Figure 4-1 shows typical stress-strain relationships for portland cement concrete and illustrates the range of polyester-styrene polymer concretes that can be formulated.

An empirical formula for the modulus of elasticity in compression has been developed for portland cement concrete and is given in the ACI building code:³³

$$E_c = 33 w^{1.5} \sqrt{f'_c},$$

in which w is the unit weight of the concrete in lb/ft^3 , and f'_c is the concrete compressive strength in psi.

Similar relationships were derived for polyester-styrene polymer concrete by Valore and Naus and by Vipulanandan and Paul. Valore and Naus' equation²⁹ is based on compressive strength testing of 3-inch diameter by 6-inch high cylindrical specimens:

$$E_c = 17 w^{1.5} \sqrt{f'_c}.$$

C. Vipulanandan and E. Paul's equation³⁰ is based on the least-squares fit of their data for polyester-styrene concrete made with Ottawa 20-30 sand:

$$E_c = 10,200 \sqrt{f'_c}.$$

Table 4-1 presents a summary of calculated versus several measured values of E_c for the polymer concrete. Note that Valore and Naus' equation appears to be relatively accurate compared with the other researcher's measured values, with the exception of Vipulanandan and Paul. Conversely, the Vipulanandan and Paul equation appears accurate only with their own observations. This may be the result of their particular concrete mixture: the use of Ottawa 20-30 sand requires a greater resin content than would be necessary with a blend of coarse and fine aggregates. With increasing resin content, the concrete's properties begin to be influenced more by the resin properties and less by the aggregate properties. Since the cured resin exhibits a lower modulus of elasticity than the concrete, additional resin content in the concrete will tend to lower the concrete's modulus of elasticity. Figure 4-2 graphically presents the differences between the Valore and Naus equation and the Vipulanandan and Paul equation. The Valore and Naus curve was generated using a unit weight, w , value of 145 lb/ft^3 , a typical value for concretes made with a blend of coarse and fine aggregates. Note, also, that the Vipulanandan and Paul curve is for concrete with a unit weight of 124 lb/ft^3 .

Based on the Valore and Naus equation, for the same compressive strengths and unit weights of concrete, the portland cement concrete is almost twice as stiff as the polymer concrete. For the typical values of $f'_c = 4000$ psi for portland cement concrete and $f'_c = 8000$ psi for polyester-styrene concrete, the values of E_c are approximately 3.6×10^6 psi and 2.6×10^6 psi, respectively.

4.5.3 Splitting Tensile Strength

The strength of concrete in tension is a major factor in the extent and size of cracking in structures. The tensile strengths of portland cement concretes and polymer concretes are typically determined using the split-cylinder test, a method based on the theory of elasticity for a homogeneous material in a biaxial state of stress.³⁴ A cylindrical specimen, typically 6 inches in diameter by 12 inches long, is placed in the testing machine lying on its side and a compressive load is applied uniformly along the length of the cylinder; the cylinder will split in half when the tensile strength is reached. The tensile strength of portland cement concrete has been empirically found to be related to the compressive strength:³³

$$f_{ct} = 6.7 \sqrt{f'_c}.$$

In their research program, R.C. Valore, Jr. and D. J. Naus performed split-cylinder tests on polyester-styrene polymer concrete using 3-inch diameter by 6-inch long specimens loaded at a rate of less than 2 ksi per minute. The results revealed that a relationship similar to that of portland cement concrete held for polyester-styrene concrete.²⁹

$$f_{ct} = 14 \sqrt{f'_c}.$$

Based on testing of 1-1/2 inch diameter specimens of polyester-styrene polymer concrete made with Ottawa 20-30 sand, Vipulanandan and Paul determined that a linear relationship between splitting tensile strength and compressive strength existed:³⁰

$$f_{ct} = 0.1 f'_c.$$

Table 4-1 lists a comparison of calculated f_{ct} values to laboratory measured values. Both the Valore and Naus equation and the Vipulanandan and Paul equation give the same result for the Kobayashi and Ito test results, overestimating splitting tensile strength by approximately 20 percent; however, the Valore and Naus equation is a significantly better fit with their own data than is the Vipulanandan and Paul equation. Figure 4-3 presents a comparison of the Valore and Naus equation and the Vipulanandan and Paul equation for splitting tensile strength. Both equations provide similar results in the compressive strength range $f'_c = 18,000$ to $20,000$ psi. Below this, significant differences occur, with the greatest difference occurring at approximately $f'_c = 5000$ psi, where the Vipulanandan and Paul equation produces a result one-half the value of the Valore and Naus equation. Values for splitting tensile strength which are omitted from Table 4-1 indicate that measured data was not reported in the respective researcher's literature.

Using the Valore and Naus equation, for a given value of compressive strength, polyester-styrene polymer concrete has a tensile strength more than twice that of conventional portland cement concrete. Because polymer concretes generally have compressive strengths greater than portland cement concrete, a significant difference in splitting tensile strength is realized (a factor of approximately three): 1250 psi for polyester-styrene concrete with $f'_c = 8000$ psi, compared to 425 psi for portland cement concrete with $f'_c = 4000$ psi.

4.5.4 Modulus of Rupture

Tensile strength in flexure, known as modulus of rupture, is important when considering cracking and deflection of bridge decks. The modulus of rupture, f_r , is calculated using the flexure formula, $f = Mc/I$, where M is the bending moment applied to a prismatic specimen, c is the distance from the neutral axis to the extreme tension fiber, and I is the moment of inertia of the specimen in the direction of bending. The standard modulus of rupture specimen is a 6-inch by 6-inch by 18-inch beam. After moist-curing for seven days, the specimen is tested to failure using a third-point flexure loading system. The third-point loading test generally results in a higher tensile strength value than the split-cylinder test, primarily because the compressive stress distribution is not linear when tensile failure is imminent as is assumed in the computation of the nominal Mc/I stress.³⁴ It is generally accepted that an average value for the modulus of rupture in portland cement concrete may be calculated using the following formula:³³

$$f_r = 7.5 \sqrt{f'_c}.$$

Flexural strength values for polyester-styrene concrete were determined by Valore and Naus, using third-point bending tests with 2-inch by 2-inch by 12-inch prismatic specimens. Based on this testing a relationship for polyester-styrene concrete was derived:²⁹

$$f_r = 25 \sqrt{f'_c}.$$

A comparison of measured values to those calculated using this formula shows that the formula estimates the modulus of elasticity with reasonable accuracy. Table 4-1 shows this comparison. Other researchers listed in Table 4-1 did not report measured values for modulus of rupture, so the accuracy of the Valore and Naus equation has not been cross-verified.

Using typical values for portland cement concrete, $f'_c = 4000$ psi, and polyester-styrene concrete, $f'_c = 8000$ psi, the resulting flexural strengths are 335 psi and 2235 psi, respectively. On the average, polyester-styrene concrete has over 6.5 times the flexural strength of portland cement concrete.

4.6 Other Properties

4.6.1 Thermal Expansion Characteristics

Thermal expansion of portland cement concrete is affected by mix proportions, moisture content, age of the concrete, and coefficients of thermal expansion of the individual concrete components. For a given moisture content and concrete mix, the coefficient of thermal expansion of the aggregate is the most significant parameter. The coefficient of thermal expansion for hardened portland cement concrete, α , typically ranges from $3.5 \times 10^{-6}/^{\circ}\text{F}$ to $6.5 \times 10^{-6}/^{\circ}\text{F}$; when a precise value is not required, $5.5 \times 10^{-6}/^{\circ}\text{F}$ is usually used.³⁵

The coefficient of thermal expansion for rigid, cured polyester-styrene resin is approximately $40 \times 10^{-6}/^{\circ}\text{F}$. For flexible polymer concrete, the thermal expansion coefficient approaches $13.3 \times 10^{-6}/^{\circ}\text{F}$, and for rigid polymer concrete, the coefficient approaches $7.7 \times 10^{-6}/^{\circ}\text{F}$.²⁹ The rigidity (or flexibility) of a polyester-styrene system is dependent upon the resin formulation. The difference between values of the thermal expansion coefficient for the polymer concrete and the unfilled resin can be attributed to the thermal expansion coefficients of the aggregate, as with portland cement concrete.

Polyester-styrene polymer concrete used for bridge deck overlay purposes usually incorporates a more flexible resin. Thus, the resulting thermal expansion coefficient, α , is equal to approximately $13 \times 10^{-6}/^{\circ}\text{F}$,²⁹ which is somewhat greater than twice that of portland cement concrete.

4.6.2 Rate of Strength Gain

The rate of strength gain is another important property, determining when formwork may be removed and the structure self-supporting, when the structure can support additional loads and, for bridge decks, when the bridge can be reopened to traffic. Figure 4-4 shows a plot of strength versus time after placement; Figure 4-5 shows the same plot on a logarithmic time scale to better illustrate the rapid strength gain of the polymer concrete. Portland cement concrete which has been moist-cured typically reaches 100 percent of its design strength in 28 days, but continues to gain strength as additional hydration occurs. Polyester-styrene polymer concrete typically reaches its full compressive strength within 2 to 10 days, but generally has sufficient strength (approximately 4000 psi) to allow reopening of the bridge deck within 4 to 6 hours after overlay placement.

4.6.3 Sensitivity of Strength to Temperature

It is generally assumed that the strength of portland cement concrete does not appreciably change over the relatively narrow temperature range from 0°F to 140°F. This is backed by research³⁶ which shows that the strength of concrete made with siliceous aggregate may actually increase slightly before degrading at extremely high temperatures (greater than 800°F).

Because the polymer concrete's polyester-styrene binder is a plastic resin, it does not enjoy such freedom from strength degradation. Test results show that strength decreases almost linearly from 100 percent at 73°F to 75 percent at 140°F.^{28,37} Following the same trend, another research project noted a 27 percent decrease in compressive strength when testing temperature was increased from 72°F to 250°F.³⁰ Figure 4-6 illustrates the relationship between temperature and compressive strength.

4.6.4 Shrinkage

Shrinkage of concrete in beams and slabs may have an effect on deflection. Shrinkage in an unrestrained plain concrete member would merely shorten it without causing curvature or stress.³⁴ However, in the presence of steel reinforcement, the bond between the steel and concrete will restrain the shrinkage locally, resulting in curvature in the member. The effect is similar in a polyester-styrene polymer concrete bridge deck overlay: shrinkage is restrained at the overlay/deck bond surface and unrestrained at the top surface. This can result in significant stresses at the bond interface.

The shrinkage stresses developed in a restrained member can be determined knowing the modulus of elasticity and the shrinkage strain: $\sigma_{sh} = E_c \epsilon_{sh}$. ACI Committee 209 has recommended that the following expression be used for determining shrinkage strain for any time, t , after age 7 days for moist-cured portland cement concrete:³⁴

$$\epsilon_{sh} = \frac{t}{35 + t} (\epsilon_{sh})_u,$$

where ϵ_{sh} is the shrinkage strain at any time t after initial curing, t is the time in days after curing, and $(\epsilon_{sh})_u$ is the ultimate shrinkage strain. The average value suggested for $(\epsilon_{sh})_u$ is 800×10^{-6} inch/inch for 40 percent relative humidity, but the range extends from 415×10^{-6} to over 1000×10^{-6} .³⁴ Shrinkage in portland cement concrete is caused by moisture loss; typically, 90 percent of the shrinkage will have occurred at the end of one year.

In contrast, shrinkage in polyester-styrene polymer concrete is a result of the volume reduction due to the chemical reaction, i.e., the cross-linking of polymer chains, which occurs during polymerization.^{17,38} Figure 4-7 illustrates the shrinkage stresses that developed in rigid and flexible polyester concrete specimens that were restrained from shrinking. At the present time, there are no research data available to determine a

numerical relationship to quantify shrinkage stress and strain for polyester-styrene concrete as there are for portland cement concrete.

4.6.5 Creep

Creep is the property by which a material continues to deform with time under sustained loads within the elastic range. The resulting inelastic deformation increases at a lower rate during the time of loading.

In portland cement concrete, the mechanism of creep may be due to any one or a combination of the following: crystalline flow in the aggregate and hardened cement paste, plastic flow of the cement paste surrounding the aggregate, closing of internal voids, and the flow of water out of the cement gel due to external load and drying.³⁴ Factors affecting the magnitude of creep are the constituents, proportions such as water content and water/cement ratio, curing temperature and humidity, age at loading, duration of loading, magnitude of stress, surface to volume ratio of the member, and slump. A general prediction method uses a standard creep coefficient equation for a concrete with 4 inches or less slump, 40 percent relative humidity, moist cured, and which is loaded at the age of 7 days.³⁴

$$C_t = \frac{\text{creep strain}}{\text{initial elastic strain}}$$

$$C_t = \frac{t^{0.6}}{10 + t^{0.6}} C_u$$

where t is the duration of loading (days) and C_u is the ultimate creep coefficient. The typical range for C_u is 1.3 to 4.15, with an average of 2.35.³⁴ A plot of this equation is shown in Figure 4-8.

The mechanism for creep in polyester-styrene concrete is mainly viscous flow of the polymer resin and has been found to be dependent on temperature, loading stress, time duration of loading, and volume fraction of resin.³⁹ In their research, N.

Dharmarajan and C. D. Armeniades developed a method for determining the creep compliance for specific resin concrete mixtures. Creep compliance is defined as the ratio of the creep strain to the applied constant stress:³⁹

$$J(t, T, \sigma, \nu) = \frac{\epsilon_{crp}}{\sigma}$$

This equation can be converted to a form such as is used for portland cement concrete by substituting $\sigma = E_c \epsilon_{initial}$ for σ and rearranging the above equation:

$$\epsilon_{crp} = E_c \epsilon_{initial} J(t, T, \sigma, \nu),$$

$$\frac{\epsilon_{crp}}{\epsilon_{initial}} = E_c J(t, T, \sigma, \nu),$$

$$C_t = E_c J(t, T, \sigma, \nu).$$

Several of the parameters required in the creep compliance function, J , must be determined in the laboratory using the specific polymer concrete under consideration; at the current time values for general application have not been determined.

The research also shows that stable creep in polyester-styrene concrete occurs up to a stress-to-strength ratio of 0.6 regardless of resin content. Higher stresses resulted in catastrophic creep, with failure occurring within only a few hours.³⁹

Research performed by R. D. Browne, M. Adams and E. L. French also showed a temperature dependence.³⁸ Figure 4-9 shows the effect of temperature on the creep of portland cement concrete and two polymer concretes loaded to a stress-to-strength ratio of 17 percent. It can be seen that, after 100 days at 68°F, the flexible polyester has a strain approximately nine times greater than the portland cement concrete. At an elevated temperature of 150°F, the rigid polymer concrete fails after only five days. These results indicate that polyester-styrene concrete may not be suitable for structural applications; however, in thin sections (such as bridge deck overlays), where the resultant

deformation is very small, creep and sustained load indentation have not been found to be a problem.³⁸

4.7 Summary

Polymer concrete is a mixture of coarse and fine aggregate and a polymeric binder which replaces the portland cement/water binder of conventional concrete. Upon subsequent polymerization, a hardened concrete mass results. In contrast to hydrated cement, the polymer binder represents a continuous phase—essentially one piece of material, with the aggregate locked inside.

Polyester-styrene concrete was found to have a higher compressive strength and higher tensile and flexural strengths than portland cement concrete. The modulus of elasticity of polyester-styrene polymer concrete can vary greatly from that of portland cement concrete. Additionally, the coefficient of thermal expansion, amount of shrinkage, and creep were found to be greater in polymer concrete than in conventional concrete. Polyester-styrene concrete was found to gain compressive strength much more rapidly than portland cement concrete, but the polymer suffers a reduction in strength as temperature increases, exhibiting a 25 percent decrease in strength for a temperature change from 73°F to 140°F.

Table 4-1. Comparison of Empirical Formulae to Measured Values for Polyester-Styrene Polymer Concretes.

	Compressive Strength, f'_c (ksi)	Modulus of Elasticity, E_c (ksi)		Splitting Tensile Strength, f_{ct} (ksi)		Modulus of Rupture, f_r (ksi)
		$17w^{1.5}\sqrt{f'_c}$ (ksi)	$10,200\sqrt{f'_c}$ (ksi)	$14\sqrt{f'_c}$ (ksi)	$0.1f'_c$ (ksi)	
Jerzak 1990	Measured	1.6 - 2.4 × 10 ³				2.0
	Calculated	2.44 × 10 ³				2.2
	Meas./Calc.	0.66 - 0.98		1.82 - 2.73		0.91
Vipulanandan and Paul 1990	Measured	0.7 - 1.0 × 10 ³		0.4 - 1.3		
	Calculated	2.0-2.3×10 ³	0.9-1.0×10 ³	1.17 - 1.4	0.7 - 1.0	
	Meas./Calc.	0.35-0.43	0.8-1.0	0.34 - 0.93	0.57 - 1.3	
Kobayashi and Ito 1976	Measured	4.4 × 10 ³		1.60		
	Calculated	4.0 × 10 ³	1.44 × 10 ³	1.98	2.0	
	Meas./Calc.	1.1	3.1	0.81	0.80	
Valore and Naus 1976	Measured	1.2 - 4.6 × 10 ³		1.40 - 2.30		
	Calculated	2.8-3.8×10 ³	1.0-1.3×10 ³	1.30 - 1.80	0.90 - 1.61	
	Meas./Calc.	0.4 - 1.2	1.2 - 3.54	1.1 - 1.33	1.6 - 1.4	

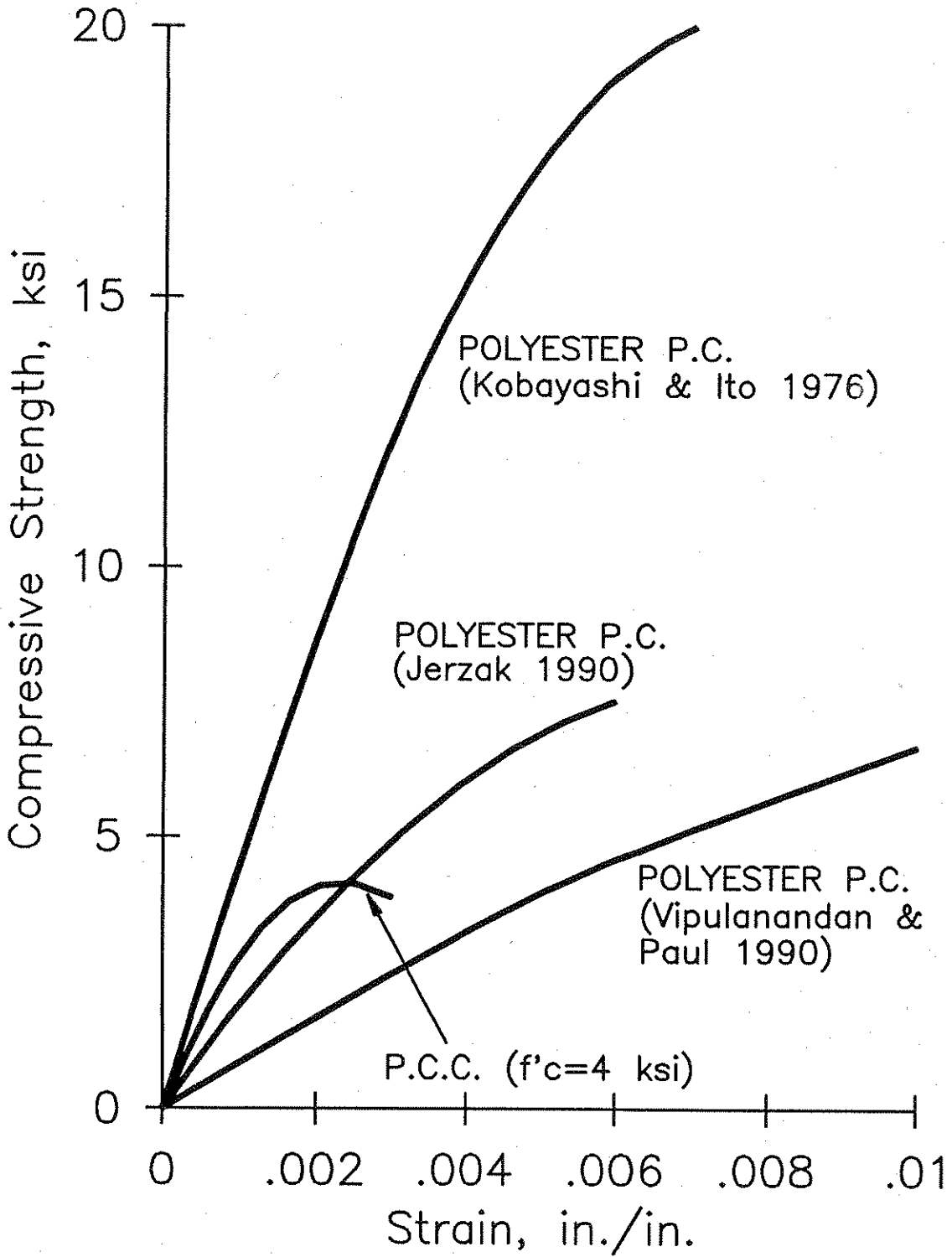


Figure 4-1. Stress-Strain Curves for Polyester-Styrene Polymer Concrete and Portland Cement Concrete (After Refs. 28, 30, and 31).

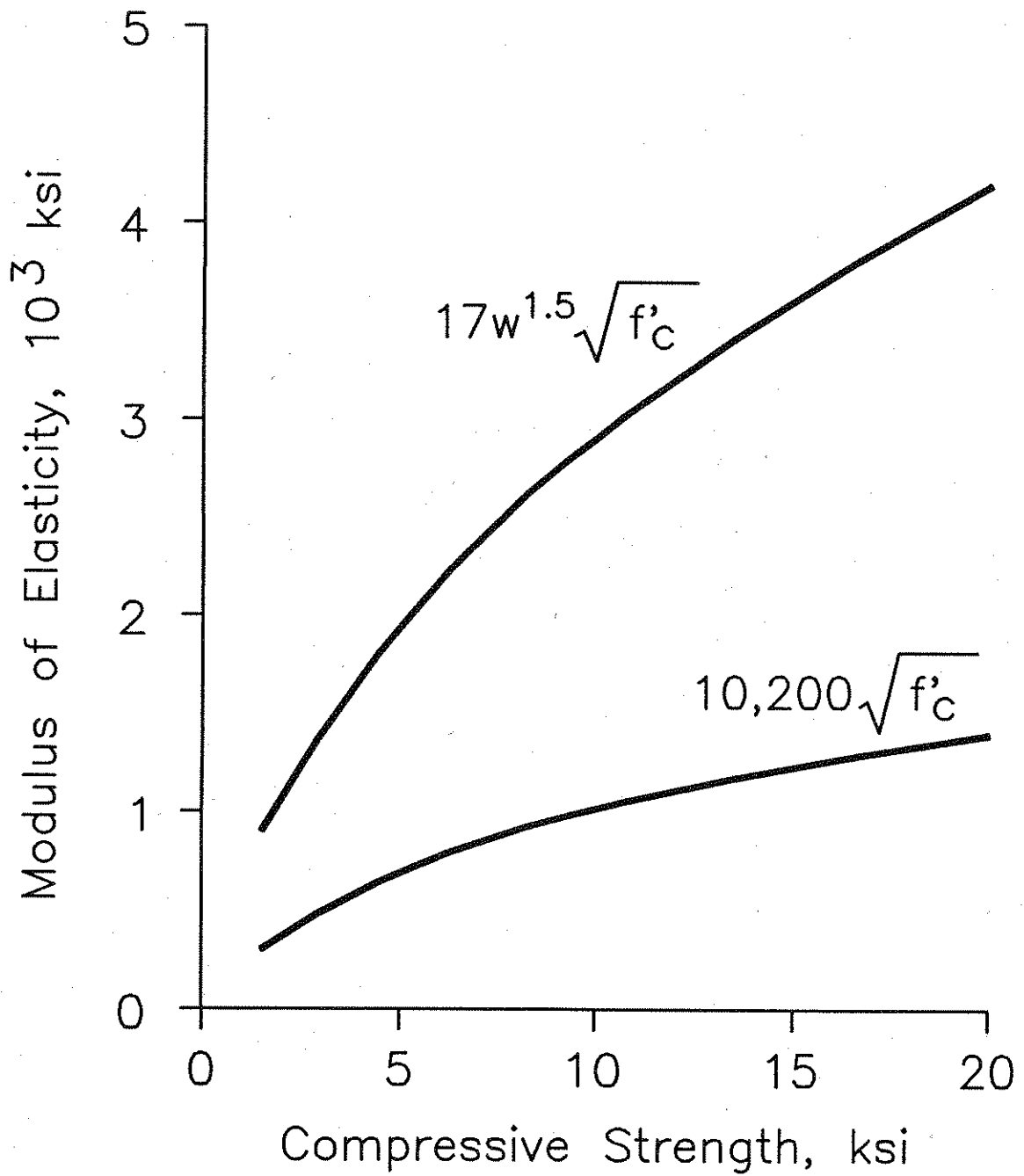


Figure 4-2. Comparison of Empirical Relationships between Compressive Strength and Modulus of Elasticity for Polyester-Styrene Concrete (after Refs. 29 and 30).

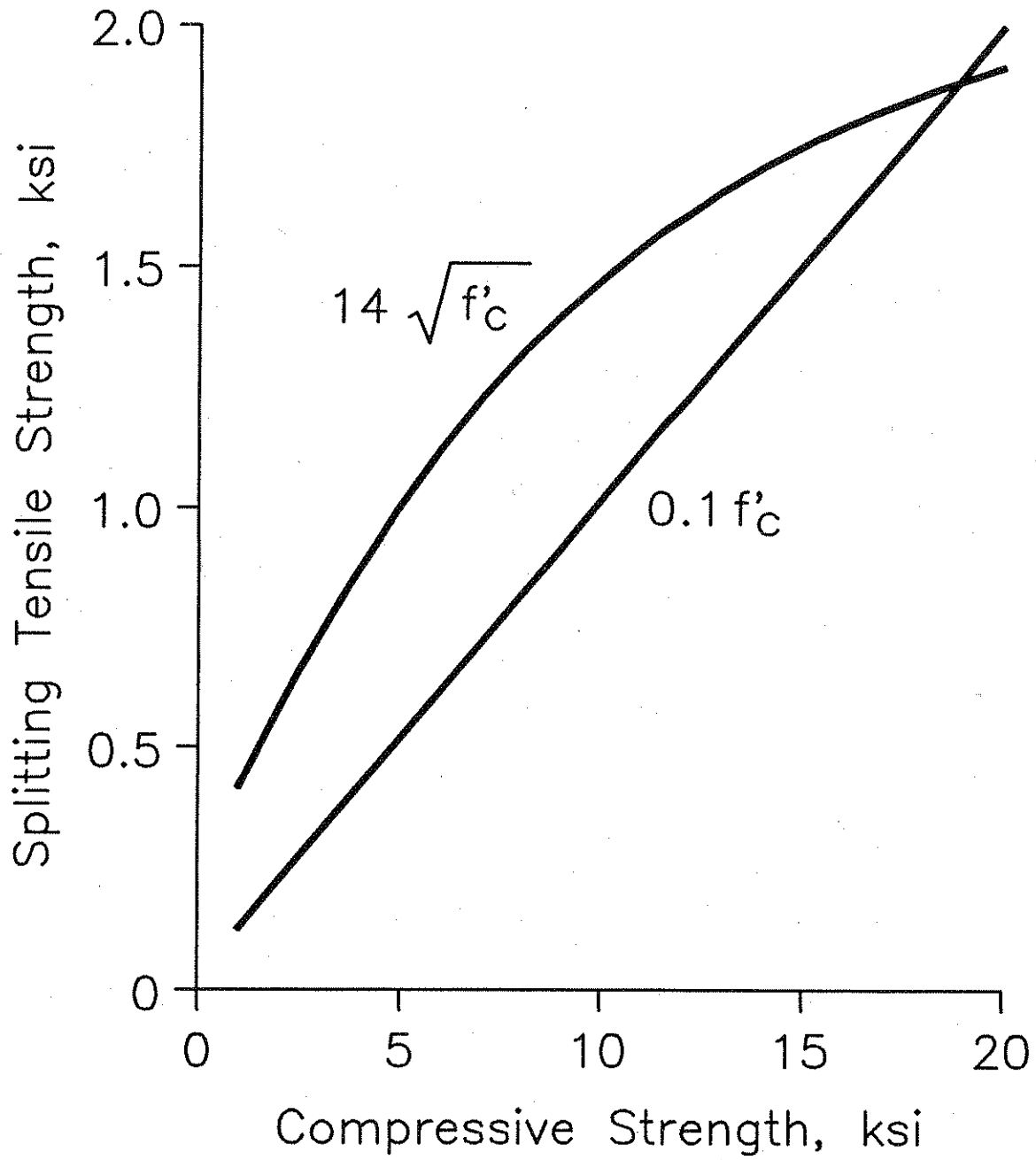


Figure 4-3. Comparison of Empirical Relationships between Compressive Strength and Splitting Tensile Strength for Polyester-Styrene Concrete (after Refs. 29 and 30).

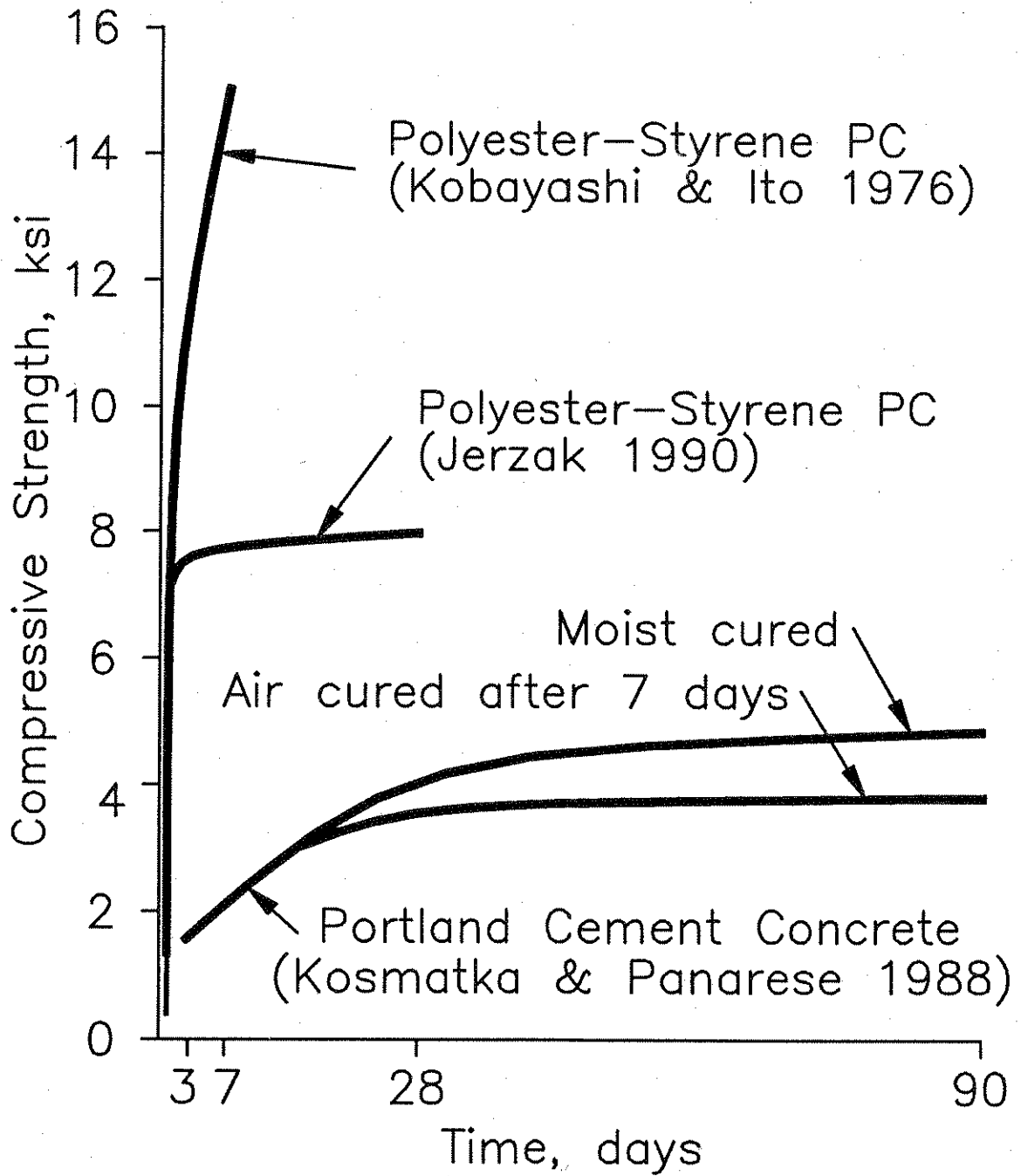


Figure 4-4. Early Strength Gain of Polyester-Styrene Polymer Concrete and Portland Cement Concrete (After Refs. 24, 28, and 31).

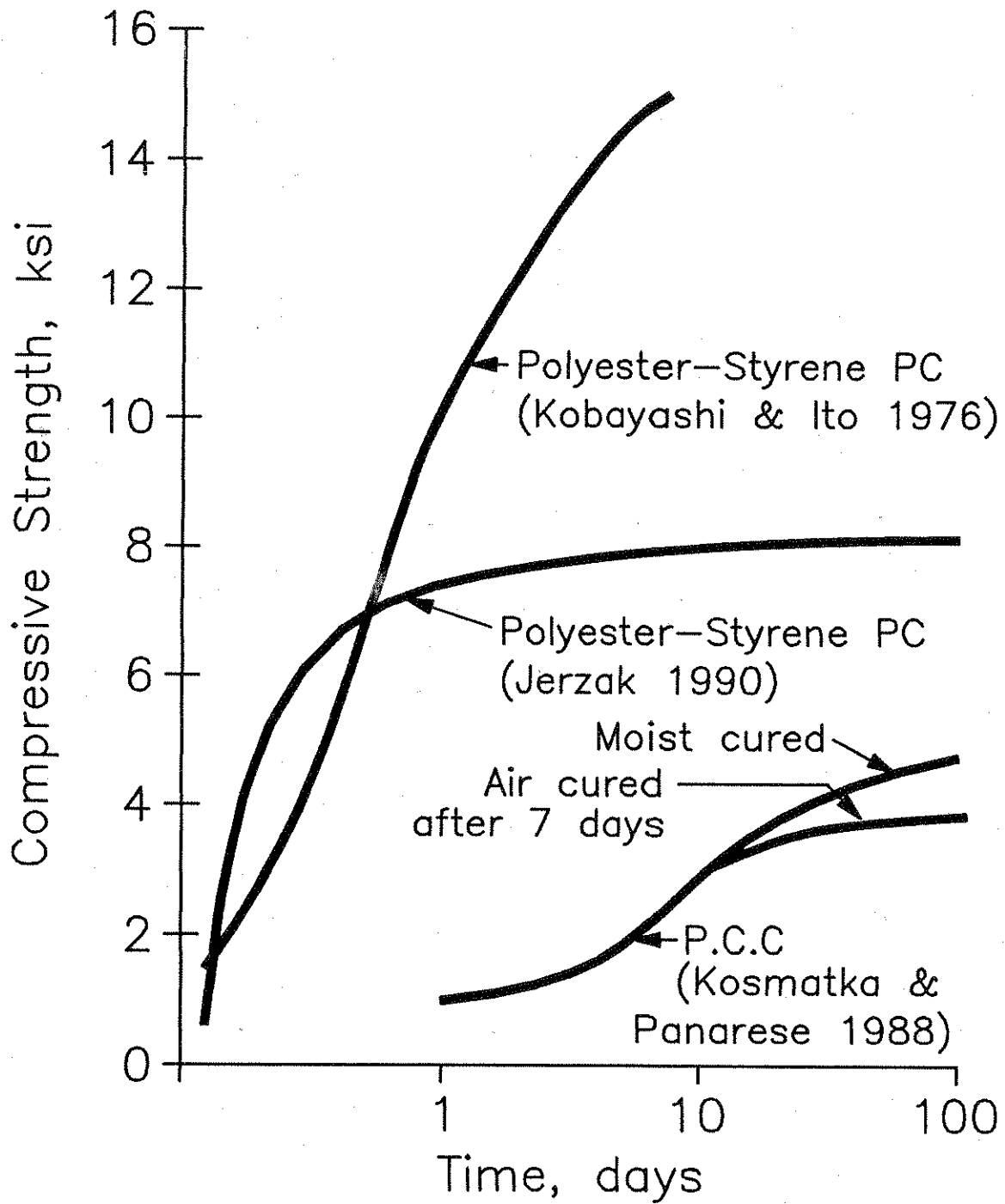


Figure 4-5. Early Strength Gain of Polyester-Styrene Polymer Concrete and Portland Cement Concrete (logarithmic scale) (After Refs. 24, 28, and 31).

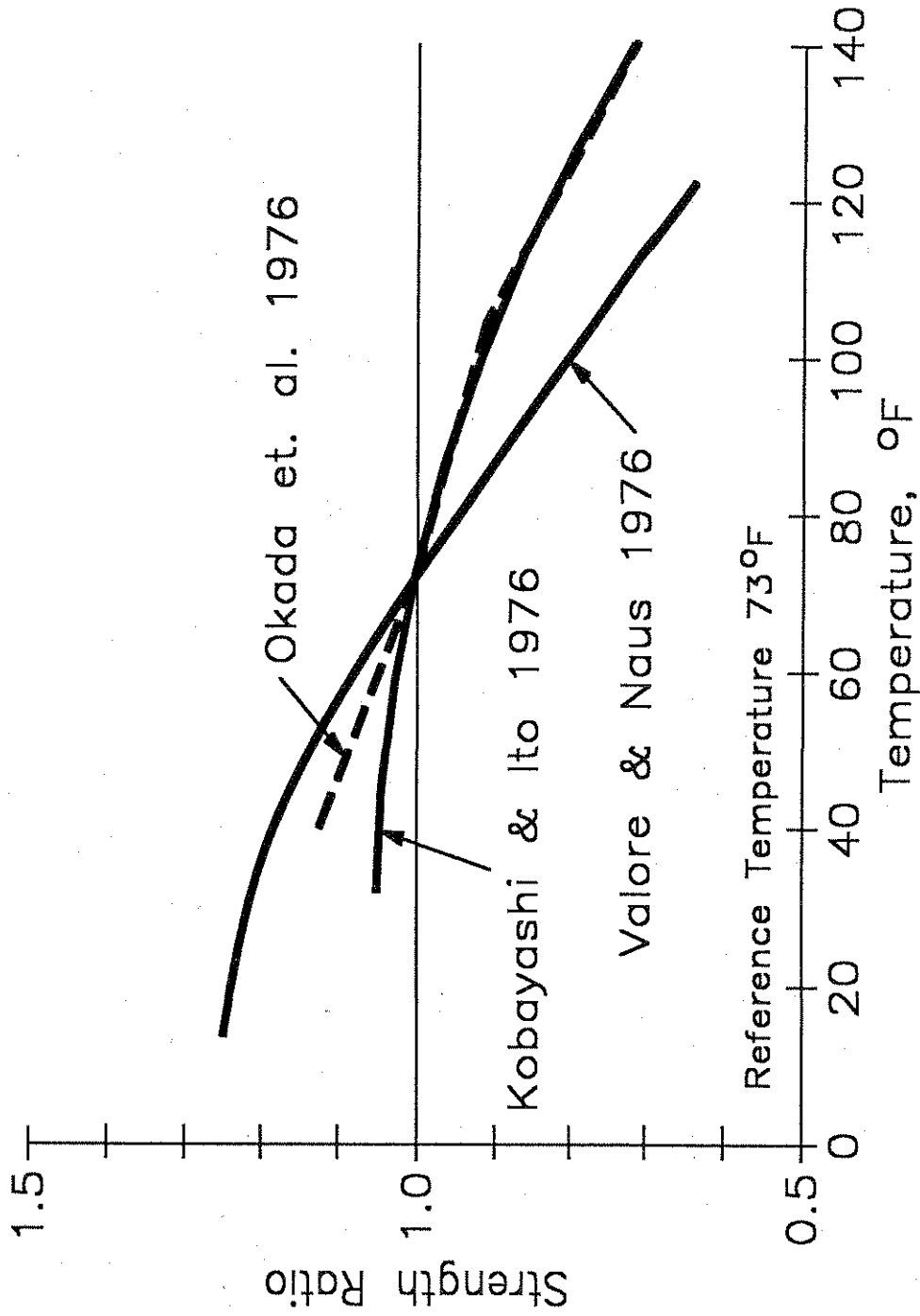


Figure 4-6. Sensitivity of Polyester-Styrene Polymer Concrete Compressive Strength to Temperature (After Refs. 28, 29, and 37).

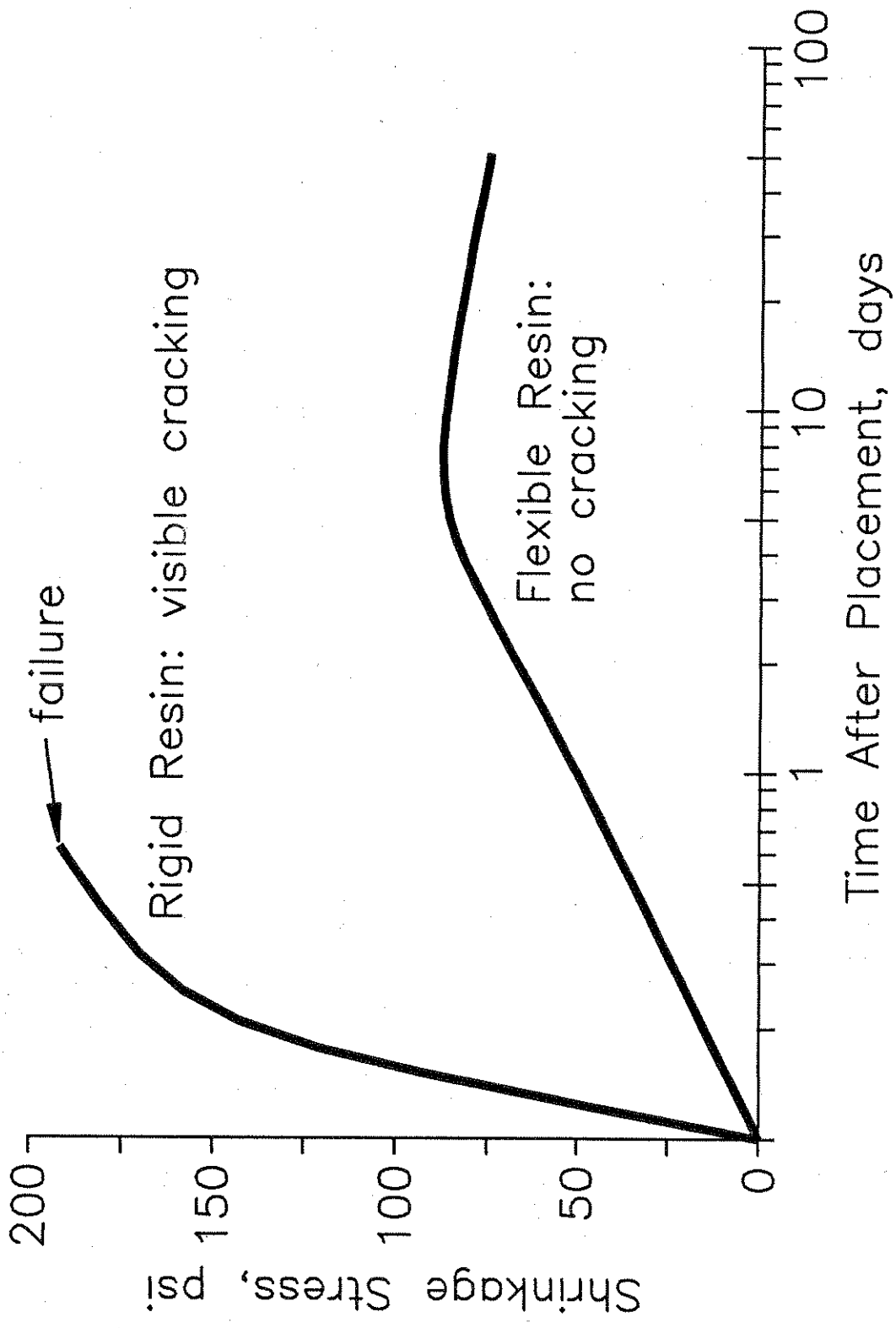


Figure 4-7. Restrainted Shrinkage Stress of Two Polyester-Styrene Concretes (after Ref. 38).

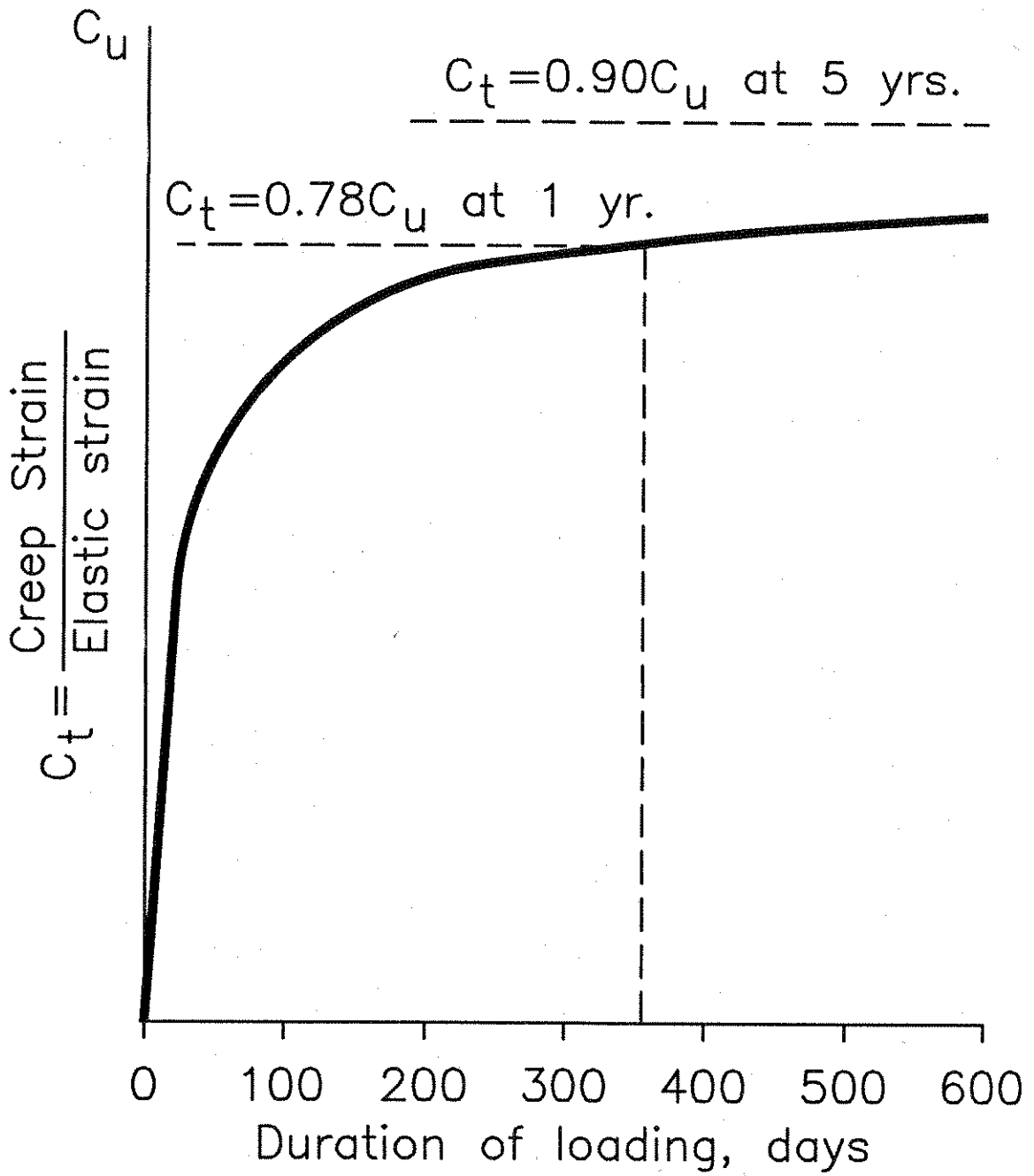


Figure 4-8. Standard Creep Coefficient Variation for Portland Cement Concrete with Duration of Loading (after Ref. 34).

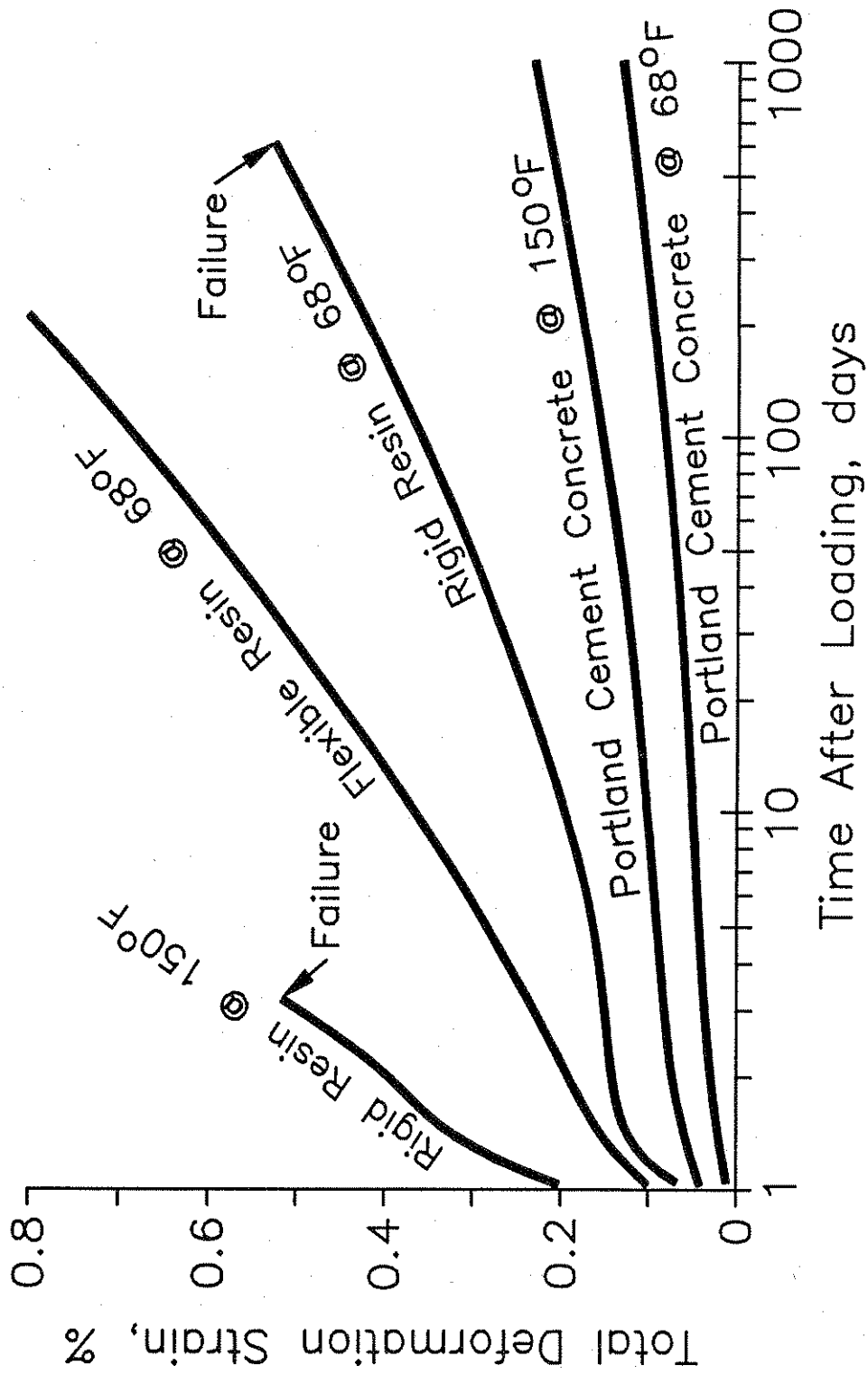


Figure 4-9. Compressive Creep of Polyester-Styrene Polymer Concretes and Portland Cement Concretes Loaded at Stress/Strength Ratio of 17 percent (after Ref. 38).

Chapter 5

Thermal Compatibility between Portland Cement Concrete and Polyester-Styrene Polymer Concrete

5.1 Introduction

The bond between a polymer concrete overlay and the portland cement concrete bridge deck is generally stronger than the portland cement concrete itself, resulting in a composite section with distinct areas of different physical properties. Because the polyester-styrene concrete and the portland cement concrete exhibit different values of coefficient of thermal expansion, α , and modulus of elasticity, E , composite action under temperature change raises a concern. To ensure against overlay failure, either debonding or cracking, thermal performance was examined using two finite element models.

5.2 Temperature Loads on Highway Bridges

The effects of air temperature, wind, humidity, intensity of solar radiation, and types of material combine to cause thermal loading in bridge decks.⁴⁰ There are two basic temperature cycles: diurnal and seasonal. The diurnal cycle usually begins in the early morning hours, just before dawn, when the air temperature reaches a minimum value. Solar radiation causes the air temperature to rise until the daily peak is reached, usually in the mid-afternoon, several hours before sunset. The air temperature then drops to a low reached before dawn the next morning. Clouds, which shade the area or produce precipitation, and the arrival of new air masses, either warmer or cooler, can affect the diurnal. The seasonal temperature cycle results from changes in the sun's relative position and distance from the earth.⁴⁰

There are generally two daily extreme conditions of temperature distribution within the bridge deck. In the first extreme, the top and bottom surfaces of the deck have different temperatures. This temperature differential is greatest in the afternoon, under the influence of direct solar radiation. During the night, the bridge deck slowly loses the

heat built up during the previous day. Because a temperature difference is required to cause a transfer of heat, the deck temperature lags the decreasing air temperature. When the air temperature passes its lowest point and begins to increase, shortly after dawn, it is possible to reach a point at which the air temperature is the same as the bridge deck top and bottom surface temperatures, and a uniform temperature exists in the deck.⁴⁰ This uniform, or isothermal, condition forms the second extreme.

The American Association of State Highway and Transportation Officials (AASHTO) recommends that highway bridges be designed to accommodate stresses or movements resulting from temperature variations.⁴¹ For concrete structures located in cold climates, the specified range is from 35°F above to 45°F below the assumed erection temperature.

For this study, the specified temperatures were assumed to represent the air temperature, and thus the surface temperature in the shaded area on the underside of the bridge deck. For each of the temperature extremes, 35°F increase and 45°F decrease, two conditions were examined: the isothermal case, where temperatures throughout the deck section are the same, and the case where a temperature differential exists between the top and bottom surfaces of the deck. The 35°F increase cases were assumed to represent summer conditions, and the 45°F decrease cases were assumed to represent winter conditions.

Several attempts have been made to quantify the temperature gradient that exists within a bridge deck. Most research appears to be concerned with gradients through box-girder type structures, since these are more susceptible to thermal effects than solid slab decks. However, in their paper, M. Elbadry and A. Ghali show a comparison of temperature gradients for various slab thicknesses and box-girder section depths.⁴² Figure 5-1(a) illustrates the gradient in a 0.25 m (10-inch) slab, based on summer climatological conditions in Calgary, Canada. A simplified temperature gradient was

assumed for this research, as shown in Figure 5-1(b). The simplified gradient is a second-order parabola with the axis of symmetry coincident with the bottom fiber of the deck slab. The general equation has the form:

$$T(y) = \frac{\Delta T}{h^2} y^2 + T_o,$$

where $T(y)$ is the temperature at point y , ΔT is the temperature differential between the top and the bottom of the deck in degrees Fahrenheit, h is the slab thickness in inches, y is the distance in inches above the bottom of the deck slab, and T_o is the temperature at the bottom of the slab. In the absence of more accurate temperature data for Nevada bridges, a ΔT of 25°F in summer was assumed. The winter ΔT was assumed to be 15°F.

5.3 Concrete Properties

The engineering properties for the polyester-styrene polymer concrete overlays and the portland cement concrete bridge decks used in the finite element models are shown in Table 5-1. Typical structural portland cement concrete used in Nevada is an air-entrained concrete with a specified minimum compressive strength, f'_c , of 4000 psi. The modulus of Elasticity, E , was calculated to be 3.64×10^6 psi using the empirical relationship:³³

$$E_c = 33 w^{1.5} \sqrt{f'_c}.$$

The modulus of rupture, f_r , value of 475 psi was based on the relationship:³³

$$f_r = 7.5 \sqrt{f'_c}.$$

A value of 5.0×10^{-6} /°F for the material's coefficient of thermal expansion was used to account for the basalt-type aggregates commonly used in Nevada.⁴³ The unit weight and poisson's ratio values were assumed to be 145 lb/ft³ and 0.25, respectively.

The polyester-styrene polymer concrete used for the bridge deck overlay was assumed to have a compressive strength of 7500 psi.³¹ The modulus of elasticity value, $E = 2.57 \times 10^6$ psi, and the modulus of rupture value, $f_r = 2165$ psi, were based on the following empirical relationships:²⁹

$$E_c = 17 w^{1.5} \sqrt{f'_c}, \text{ and}$$

$$f_r = 25 \sqrt{f'_c}.$$

A coefficient of thermal expansion value of $13.0 \times 10^{-6} / ^\circ\text{F}$, representative of flexible resins, was chosen.²⁹ The unit weight and poisson's ratio were assumed to be the same as the portland cement concrete: 145 lb/ft³ and 0.25, respectively.

5.4 Thermal Compatibility Modeling

5.4.1 Description of Models

For this analysis, the bridge deck was considered to be a one-way slab, with live loads, dead loads, and thermal loads acting in the deck's transverse direction. This assumption was made because the transverse direction generally controls the slab design. Two finite element models were chosen to be representative of typical structures found in Nevada. The first model, Model 1, consists of an 8-inch thick concrete slab with a ¾-inch polyester-styrene polymer concrete overlay. A span of 8 feet was chosen to represent a typical distance between supports in the transverse direction for an 8-inch slab. Model 2 was based on an actual bridge that is scheduled to receive a polymer concrete overlay. This bridge (B-1111E/W) is located on Interstate 80 in Elko County, Nevada, and carries traffic over the Humboldt River east of the Carlin Canyon tunnels. This bridge is a 370-foot, 3-span composite steel girder, concrete slab structure with a maximum span length of 152 feet. Figure 5-2 shows the deck cross-section for the

eastbound structure. This model has a 9.5 inch thick deck and an $\frac{3}{4}$ -inch overlay. The span between supports is 12.5 feet. Both models have a beam width of 1 foot.

A multi-span support arrangement, shown in Figure 5-3(b), was used for both finite element models to minimize end effects in the analysis. The assumption of a pin-type support at the center of the beam allows us to take advantage of symmetry, requiring only half of the structure for the finite element mesh. This concept, illustrated in Figure 5-3(c), reduces the complexity of the models, and significantly decreases computation time.

Figure 5-4 illustrates the three end restraint conditions which were considered. The first condition, in which all three supports are rigidly fixed, represents a deck with very stiff supports. In the second condition, the center and right supports are rollers, allowing both rotation and translation. These two end restraint conditions were intended to model the extreme cases under temperature loading, the first to produce the maximum axial stresses in the materials, and the second to produce the highest interface shear stresses. A third restraint condition, a cantilever beam, was examined to ensure that the first two cases did indeed represent the extremes. Analysis demonstrated that the cantilever model was slightly less critical than the roller-support restraints, for producing interface shears, and not critical at all, compared to the completely fixed condition, for producing axial stresses.

For each end restraint condition, four temperature loading cases were examined in Model 1. These included a 35°F increase with temperature constant through the section, a 35°F increase with an additional 25°F differential temperature imposed across the section, a 45°F decrease, with a constant temperature through the deck, and a 45°F decrease with an imposed temperature differential, the top surface being 15°F warmer. Analysis demonstrated that the controlling load cases were the 35°F increase with the additional thermal gradient and the 45°F isothermal decrease. Since these controlled in

the first model, a decision was made to include only these two loading cases when analyzing Model 2.

The finite element meshes consist of 594 nodes with 256 three-dimensional solid elements for Model 1 and 902 nodes with 400 three-dimensional solid elements for Model 2. Figures 5-5 and 5-6 illustrate the finite element meshes which were used. The analysis was performed on an IBM®-compatible personal computer using Celestial Software's Images-3D™, a commercial finite element package.⁴⁴

5.4.2 Generalized ACI Ultimate Strength Method

To check whether the stresses determined by the finite element analysis are low enough to preclude an overlay failure, such as cracking or debonding, allowable limits must be determined. Allowable unfactored stress limits were calculated using a generalized approach to the American Concrete Institute (ACI) ultimate strength design method.³³ While highway bridges are typically designed according to American Association of State Highway and Transportation Officials (AASHTO) guidelines, the ACI Building Code forms the basis for many of the AASHTO provisions.

The procedure for the ultimate strength method is two-step. First, the ultimate capacity of the structure is determined as the nominal capacity multiplied by a strength reduction factor. Second, the appropriate combination of loads is multiplied by load factors. The ultimate strength must then be greater than the factored loads. If the ultimate strength is less than the applied factored loads, the design is unacceptable.

5.4.2.1 Compression in Portland Cement Concrete

In general, compressive stresses develop in the portland cement concrete bridge deck as temperature increases. As the bridge deck warms, the material tends to expand, resulting in thermal strains. If the movement is restrained, thermal stresses will develop.

One assumption that is made in the ultimate strength method is that at the nominal moment capacity, the stress in the tension reinforcing steel is equal to its yield strength, and the stress in the compression concrete is equal to $0.85 f'_c$, where f'_c is the compressive strength of the concrete. For this research, it was assumed that the bridge deck was designed according to ACI-318 Eq. 9-1:³³

$$U = 1.4D + 1.7L,$$

where U is the required strength, D is the applied dead load moment, and L is the applied live load moment. It was assumed that the structure was designed with no additional conservatism, i.e., the design strength is equal to the required strength:

$$\phi M_n = 1.4 M_D + 1.7 M_L,$$

or

$$\phi 0.85 f'_c = 1.4D + 1.7L,$$

where D is the extreme compression fiber stress due to the applied dead load, and L is the extreme compression fiber stress due to the applied live load.

ACI-318 Eq. 9-5 can then be employed to determine the inherent reserve capacity for thermal stresses:

$$U = 0.75 (1.4D + 1.4T + 1.7L),$$

where U is the required strength, D is the applied dead load, T is the applied thermal load, and L is the applied live load. If we again assume the required strength is equal to the extreme compression fiber limit, $\phi 0.85 f'_c$, and substitute $\phi 0.85 f'_c$ for $1.4D + 1.7L$, we obtain

$$\phi 0.85 f'_c = 0.75 (\phi 0.85 f'_c + 1.4T_c),$$

which can be rearranged:

$$0.85 \phi f'_c = 0.75 (0.85 \phi f'_c) + 1.05 T_c,$$

$$T_c = \frac{0.25 (0.85 \phi f'_c)}{1.05},$$

finally yielding,

$$T_c = 0.2 \phi f'_c.$$

Since the thermal load acts as an axial load in combination with flexure, the value for the strength reduction factor, ϕ , is 0.70. Substituting this value gives

$$T_c = 0.14 f'_c. \tag{5-1}$$

For portland cement concrete with a compressive strength, f'_c , of 4000 psi, Eq. (5-1) produces an allowable unfactored compressive stress due to temperature equal to 560 psi.

5.4.2.2 Tension in Portland Cement Concrete

In general, tensile stresses develop in the bridge deck as temperature decreases. In this study, tension capacity of portland cement concrete is neglected. It is assumed that the concrete would crack, and that the reinforcing steel would carry the tensile load. This assumption was necessary because design methods ignore the tensile strength of concrete for tension and flexure cases.³³

5.4.2.3 Compression in Polyester-Styrene Polymer Concrete

For both Model 1 and Model 2, it was assumed that the polyester-styrene polymer concrete overlay was placed on the bridge deck after the structure was already in service, i.e., as a retrofit. The overlay was assumed to be a non-structural member, carrying none

of the structure's dead load or live load. Given this assumption, the equation that controls the required strength is ACI-318 Eq. 9-6:

$$U = 1.4 (D + T).$$

Since $D = 0$ and $U = 0.85 \phi f'_c$, we have

$$0.85 \phi f'_c = 1.4 T_c.$$

Rearranging the equation, we obtain

$$T_c = 0.607 \phi f'_c.$$

Substituting the strength reduction factor for compression, $\phi = 0.70$, gives

$$T_c = 0.425 f'_c. \tag{5-2}$$

The compressive strength of polyester-styrene polymer concrete decreases nearly linearly as temperature is increased. It was assumed that at elevated temperature compressive strength would decrease by 25 percent.²⁸ At elevated temperatures, Eq. (5-2) produces an allowable unfactored compressive stress due to temperature equal to 2390 psi for polyester-styrene concrete with a compressive strength of 7500 psi.

5.4.2.4 Tension in Polyester-Styrene Polymer Concrete

It is important to note that the ACI-318 building code gives no guidance for tensile stresses in concrete, since the tensile strength of concrete is ignored in design.³³ However, unlike tension in the portland cement concrete bridge deck, tension in the overlay material cannot be ignored. There is no steel reinforcement in the typical polyester-styrene polymer concrete overlay, and cracking of the overlay cannot be tolerated, since cracking can destroy the overlay's integrity.

An estimate for allowable tensile loading due to temperature decrease was made using ACI-318 Eq. 9-6. The required strength is set equal to the design strength, which is assumed to be equal to the modulus of rupture, f_r , multiplied by the strength reduction factor, ϕ :

$$\phi f_r = 1.4 (D + T).$$

The modulus of rupture value was chosen for use instead of the splitting tensile strength because the modulus of rupture represents a tensile failure in bending, the result of a direct tensile load at the fiber under consideration. Tensile failure in the splitting tensile strength test is the indirect result of an applied compressive load.

The value for dead load, D , is zero, since the overlay is not a structural member. This produces

$$\phi f_r = 1.4 T_t.$$

Substituting the value for the strength reduction factor for tension, $\phi = 0.90$, and rearranging yields:

$$T_t = 0.64 f_r. \tag{5-3}$$

For polyester-styrene polymer concrete, modulus of rupture is equal to:²⁹

$$f_r = 25 \sqrt{f'_c}.$$

Therefore, for polyester-styrene concrete with a compressive strength, f'_c , of 7500 psi and a modulus of rupture, f_r , of 2165 psi, Eq. (5-3) gives an allowable unfactored tensile stress due to temperature equal to 1385 psi.

5.4.2.5 Interface Shear

Shear stresses develop along the interface plane when temperature changes, due to the different values of coefficient of thermal expansion, α , and modulus of elasticity, E , for polyester-styrene polymer concrete and portland cement concrete. When an overlay fails, it usually exhibits local debonding as a result of tensile failure in the portland cement concrete substrate.

To determine the allowable tensile stresses in the substrate, and thus the allowable interface shear, we can use Eq. (5-3), derived previously:

$$T_t = 0.64 f_r. \quad (5-3, \text{repeated})$$

ACI-318 Eq. 9-9 was used to calculate modulus of rupture:

$$f_r = 7.5 \sqrt{f'_c}.$$

For portland cement concrete with a compressive strength, f'_c , of 4000 psi and a modulus of rupture, f_r , of 475 psi, Eq. (5-3) gives an allowable unfactored interface shear stress due to temperature equal to 305 psi. For polyester-styrene polymer concrete with a compressive strength, f'_c , of 7500 psi and a modulus of rupture, f_r , of 2165 psi, Eq. (5-3) gives an allowable unfactored interface shear stress due to temperature equal to 1385 psi.

5.4.3 AASHTO Design Loads

In order to perform an accurate analysis to determine allowable stresses, actual design dead and live load moments were calculated. The dead load consists of the weight of the deck and an assumed additional weight equivalent to 3 inches of asphalt concrete.⁸ The dead load per square foot of deck area, w_d , can be calculated as

$$w_d = 150 \text{ lb/ft}^3 \left(\frac{8 \text{ in} + 3 \text{ in}}{12 \text{ in/ft}} \right) = 138 \text{ lb/ft}^2, \text{ for Model 1,}$$

and

$$w_d = 150 \text{ lb/ft}^3 \left(\frac{9.5 \text{ in} + 3 \text{ in}}{12 \text{ in/ft}} \right) = 156 \text{ lb/ft}^2, \text{ for Model 2.}$$

For design purposes, the deck is assumed to be continuous over the supports. The dead load moment, M_D , is assumed to be the same for the positive moment region in the center of the span and for the negative moment region over the supports:

$$M_D = \frac{w_d l^2}{10}.$$

Substituting $w_d = 138 \text{ lb/ft}^2$ and $l = 8 \text{ ft}$ for Model 1 and $w_d = 156 \text{ lb/ft}^2$ and $l = 12 \text{ ft}$ for Model 2, we obtain

$$M_D = 880 \text{ lb-ft,}$$

and

$$M_D = 2440 \text{ lb-ft,}$$

for Model 1 and Model 2, respectively.

The live load moment was calculated using AASHTO HS20-44 loading, according to Section 3.24.3, Case A, of the AASHTO bridge code.⁴¹ The live load moment, M_L , can be calculated using the formula

$$M_L = \left(\frac{S + 2}{32} \right) P_{20},$$

where S is the modified span length, in accordance with Section 3.24.1.2(b), of the AASHTO bridge code, and P_{20} is the load on one rear wheel of the HS20 truck ($P_{20} = 16,000 \text{ lb}$). For this analysis, S was assumed to be 8 feet for Model 1 and was calculated to be 12.0 feet for Model 2. Section 3.24.3.1, of the AASHTO bridge code, requires a continuity factor of 0.8 for slabs continuous over 3 or more supports. An impact factor of 30 percent, per AASHTO Section 3.8.2, was also included:

$$M_L = \left(\frac{8 + 2}{32} \right) (16,000 \text{ lb}) (0.8) (1.3) = 5200 \text{ lb-ft, for Model 1,}$$

and

$$M_L = \left(\frac{12 + 2}{32}\right)(16,000 \text{ lb})(0.8)(1.3) = 7280 \text{ lb-ft, for Model 2.}$$

Knowing the design loads, we can now determine the design strength of the structure, and the reserve capacity available for temperature loading.

5.4.4 AASHTO Service Load Method

5.4.4.1 Compression in Portland Cement Concrete

Compression in the portland cement concrete is a result of a combination of bending moment and compressive axial stress caused by an increase in temperature. The extreme fiber stress, f , in the bridge deck caused by applied moments can be determined using the relationship

$$f = \frac{M c}{I},$$

where M is the applied moment, c is the distance from the neutral axis to the extreme compression fiber, and I is the deck's moment of inertia.

Based on the design dead load, $M_D = 880$ lb-ft, and the design live load, $M_L = 5200$ lb-ft, the extreme compression fiber stresses for Model 1 were found to be

$$f_D = 83 \text{ psi, and}$$

$$f_L = 372 \text{ psi.}$$

For Model 2, with a design dead load, M_D , of 2440 lb-ft and a design live load, M_L , equal to 7280 lb-ft, the extreme compression fiber stresses are

$$f_D = 162 \text{ psi, and}$$

$$f_L = 386 \text{ psi.}$$

The dead load stresses are assumed to be present in the bridge deck prior to overlay placement. The live load stresses were calculated based on the composite section.

To determine Model 1 and Model 2 deck section reserve capacity for thermal stresses, AASHTO load combination Group IV was employed:

$$1.25 (0.4 f'_c) \geq D + L + T_c, \quad (5-4)$$

where f'_c is the compressive strength of the concrete, D is the compressive stress caused by dead loads, L is the live load stress, and T_c is the compressive stress due to temperature increase.

Substituting into Eq. (5-4) the appropriate values for f'_c , D , and L for the two models, the equation yields an allowable compressive stress due to temperature, T_c , of 1545 psi for Model 1 and 1452 psi for Model 2.

5.4.4.2 Compression in Polyester-Styrene Polymer Concrete

The overlay was assumed to carry no dead load, but live load is present due to composite action between the deck and the overlay. Based on the design live load for Model 1, $M_L = 5200$ lb-ft, the extreme fiber stress in the overlay was found to be

$$f_L = 447 \text{ psi.}$$

For Model 2, the extreme fiber compressive stress was found to be

$$f_L = 450 \text{ psi,}$$

for a design dead load moment, M_D , of 7280 lb-ft.

AASHTO load combination Group IV was used to determine the overlays' reserve capacity for thermal stresses:

$$1.25 (0.4 f'_c) \geq D + L + T_c, \quad (5-4, \text{repeated})$$

where f'_c is the compressive strength of the polyester-styrene polymer concrete, D is the compressive stress caused by the dead load ($D = 0$), L is the live load stress, and T_c is the compressive stress caused by a temperature increase.

Because the compressive strength of polyester-styrene polymer concrete decreases as temperature is increased, an f'_c value of 5625 psi was used instead of the assumed value of 7500 psi, representing a 25 percent decrease in strength. Substituting f'_c and f_L , and solving for T_c , Eq. (5-5) produces an allowable thermal compressive stress equal to 2366 psi for Model 1, and 2363 psi for Model 2.

5.4.4.3 Tension in Polyester-Styrene Polymer Concrete

The AASHTO service load design method does not address the issue of direct tension in a member, choosing, as does the ACI-318 building code, to neglect the tensile strength of concrete.⁴¹ Tension in the overlay material cannot be neglected, however, since cracking in the overlay can destroy its integrity, allowing air, water, and chlorides an unimpeded path to the deck and the reinforcing steel.

AASHTO does provide a limit of 21 percent of the modulus of rupture for extreme fiber stress in tension for a plain concrete member undergoing flexure.⁴¹ Using this limit, Eq. (5-4) can be rewritten:

$$1.25 (0.21 f_r) \geq D + L + T_c.$$

The dead load, D , and the live load, L , were assumed to be zero. Even though the overlay is subjected to live loads due to the composite action of the section, the live load is not continuously present; the assumption of no live load produces a more conservative temperature stress limit. With dead load and live load both zero, the equation reduces to:

$$1.25 (0.21 f_r) = T_c \quad (5-5)$$

Substituting the value $f_r = 2165$ psi, and rearranging, we obtain an allowable tensile stress due to temperature equal to 568 psi.

5.4.4.4 Interface Shear

Because of the tensile nature of overlay shear failures, such as debonding, Eq. (5-5) was used to determine an allowable shear stress value. For portland cement concrete with a compressive strength, f'_c , of 4000 psi and a modulus of rupture, f_r , of 475 psi, Eq. (5-5) gives an allowable interface shear stress due to temperature equal to 125 psi. For polyester-styrene polymer concrete with a compressive strength, f'_c , of 7500 psi and a modulus of rupture, f_r , of 2165 psi, Eq. (5-5) gives an allowable interface shear due to temperature equal to 568 psi. At elevated temperatures, where $f'_c = 5625$ psi and $f_r = 1875$ psi, the allowable interface shear decreases to 492 psi.

5.4.5 AASHTO Ultimate Strength Method

Allowable temperature stresses were also determined using the AASHTO ultimate strength method of analysis, even though the bridge of Model 2 was not designed using this philosophy. This was performed primarily as a check against the service load analysis, but would be applicable to similar bridges which may have been designed using the ultimate strength method. Generally, a structure designed for service loads will prove adequate when an ultimate strength analysis is performed. The reverse, however, is often not the case, since the service load method is more conservative. It was possible in this analysis to perform more exact calculations, rather than generalizing stresses as for the ACI method, because the actual design loads were available. In order to perform the method's calculations for Model 1, the reinforcing steel had to be designed for a typical 8-inch slab.

5.4.5.1 Compression in Portland Cement Concrete

The general procedure for the AASHTO ultimate strength method is the same as that for the ACI-318 method: the ultimate capacity of the structure is determined as the nominal capacity multiplied by a strength reduction factor, and the appropriate combination of loads is multiplied by load factors.⁴¹ The ultimate strength must then be greater than the factored loads for the design to be acceptable. In the design of the 8-inch thick slab, AASHTO load combination Group I was used to determine the ultimate moment capacity required:

$$\phi M_n = 1.3 [D + 1.67 L].$$

Substituting $D = 880$ lb-ft and $L = 5200$ lb-ft for Model 1, the minimum required ultimate moment capacity is $\phi M_n = 12,433$ lb-ft.

The ultimate moment capacity, ϕM_n , can also be expressed as:⁴¹

$$\phi M_n = \phi \left[A_s f_y d \left(1 - 0.6 \frac{\rho f_y}{f'_c} \right) \right],$$

where ϕ is the strength reduction factor, 0.90, A_s is the area of tensile steel in the section, f_y is the yield strength of the steel reinforcement, d is the depth of the tension reinforcement, ρ is the section's steel ratio, which is equal to A_s/bd , and f'_c is the concrete's compressive strength.

The unknown area of reinforcing steel for Model 1 was determined by substituting the known values for ϕM_n , f_y , f'_c , and b , and the assumed value for d into the equation. Using the reinforcing steel thus determined, the actual ultimate moment capacity for Model 1 was calculated:

$$\phi M_n = 12,500 \text{ lb-ft.}$$

The ultimate moment capacity for Model 2 was calculated in the same manner, using the actual bridge design parameters, and was found to be:

$$\phi M_n = 20,600 \text{ lb-ft.}$$

For Model 2, $D = 2440$ lb-ft and $L = 7280$ lb-ft; therefore, the minimum required ultimate moment capacity is $\phi M_n = 19,000$ lb-ft.

To determine the allowable axial compression caused by a temperature increase, it was necessary to determine the axial load–moment interaction relationship, also known as the strength interaction relationship, for the transformed composite section. This involved determining three points on the interaction curve: pure compression, pure bending, and the balanced strain condition.

The formula for pure compression is:⁴¹

$$\phi P_o = \phi [0.85 f'_c (A_g - A_{st}) + A_{st} f_y],$$

where ϕP_o is the ultimate compressive strength for a section with no applied moment, A_g is the gross cross-sectional area, A_{st} is the area of longitudinal (axial) steel in the cross section, and f_y is the yield strength of the steel reinforcement.

In the case of pure flexure, i.e., without any applied axial force, the ultimate moment capacity is what we have seen before, except that ϕ is equal to 0.70:

$$\phi M_o = \phi \left[A_s f_y d \left(1 - 0.6 \frac{\rho f_y}{f'_c} \right) \right].$$

At the balanced strain condition, the tension reinforcement reaches the strain corresponding to its yield strength, just as the concrete in compression reaches its assumed ultimate strain of 0.003. The compressive strength, ϕP_b , and the moment strength, ϕM_b , at the balanced strain condition are given by the equations:⁴¹

$$\phi P_b = \phi [0.85 f'_c b a_b + A'_s f'_s + A_s f_y],$$

$$\phi M_b = \phi [0.85 f'_c b a_b \left(d - d'' - \frac{a_b}{2} \right) + A'_s f'_s (d - d' - d'') + A_s f_y d''],$$

where

$$a_b = \left(\frac{87,000}{87,000 + f_y} \right) \beta_1 d, \text{ and}$$

$$f'_s = 87,000 \left[1 - \left(\frac{d'}{d} \right) \left(\frac{87,000 + f_y}{87,000} \right) \right] \leq f_y.$$

ϕ is again 0.70, and β_1 is 0.85 for 4000 psi compressive strength concrete.

Using these equations, the following values were obtained for Model 1:

$$\phi P_o = 278,600 \text{ lb for pure compression,}$$

$$\phi M_o = 10,800 \text{ lb-ft for pure bending, and}$$

$$\phi P_b = 97,800 \text{ lb, and}$$

$$\phi M_b = 33,300 \text{ lb-ft at the balanced strain condition.}$$

The following values were calculated for Model 2:

$$\phi P_o = 334,000 \text{ lb for pure compression,}$$

$$\phi M_o = 17,400 \text{ lb-ft for pure bending, and}$$

$$\phi P_b = 127,800 \text{ lb, and}$$

$$\phi M_b = 47,600 \text{ lb-ft at the balanced strain condition.}$$

Figures 5-7 and 5-8 show the resulting load-moment interaction diagrams for Model 1 and Model 2, respectively. A straight line was assumed to connect the

calculated points on the curve, a conservative assumption since these lines fall on the inside of where the actual curve would lie. In the range of compressive stresses greater than the balanced stress the section is controlled by compression; a load-moment combination exceeding the interaction curve will result in a compressive failure (crushing) of the concrete, rather than a tensile failure of the steel reinforcement. For Model 1, the relationship for this region, assumed to be linear, is

$$\phi P = 278,600 - 5.429 \phi M, \quad (5-6)$$

where ϕP is the factored axial compression limit in pounds, and ϕM is the factored applied moment in lb-ft. Since the AASHTO Group IV total factored moment, ϕM_{D+L} , applied to the structure is 7900 lb-ft, Eq. (5-6) yields a maximum allowable factored axial compressive load, ϕP , equal to 235,700 lb.

For Model 2, the relationship is given by:

$$\phi P = 334,000 - 4.332 \phi M. \quad (5-7)$$

The total factored moment, ϕM_{D+L} , applied to the structure is 12,640 lb-ft; therefore, Eq. (5-7) produces a maximum allowable factored axial compressive load, ϕP , equal to 279,200 lb.

To determine the allowable temperature stresses, the AASHTO Group IV load combination is used:

$$\phi P \geq 1.3 [D + L + T].$$

Dead loads and live loads do not produce axial forces. Normal stresses due to bending are accounted by moments in the interaction relationship. The equation can thus be reduced and rearranged to yield

$$T_c = \left(\frac{\phi P}{1.3} \right) \frac{1}{A_g}, \quad (5-8)$$

where T_c is the allowable unfactored compressive stress due to temperature increase, ϕP is the maximum allowable factored compression load, obtained from the interaction diagram, and A_g is the gross section area, required to convert axial load into axial stress. Substituting the values for ϕP and A_g into Eq. (5-8), we obtain an unfactored compressive stress allowable limit equal to 1770 psi for Model 1 and 1785 psi for Model 2.

5.4.5.2 Compression in Polyester-Styrene Polymer Concrete

The overlay was assumed to have been placed on the bridge deck after the structure was subjected to the dead load, that is, the overlay carries no dead load. However, because of composite action between the bridge deck and the overlay, the overlay will be subjected to live loads.

The axial load-moment interaction relationships for the composite section, described previously, were used to determine the allowable axial compression, due to temperature, in the presence of live load moments. The interaction relationships are:

$$\phi P = 278,600 - 5.429 \phi M, \text{ for Model 1, and} \quad (5-6, \text{ repeated})$$

$$\phi P = 334,000 - 4.332 \phi M, \text{ for Model 2.} \quad (5-7, \text{ repeated})$$

The total applied moment for Model 1, using the AASHTO Group IV load combination, is 6760 lb-ft. Eq. (5-6) yields a maximum allowable factored axial compressive load, ϕP , of 30,120 lb. For Model 2, the total applied moment is 9460 lb-ft; Eq. (5-7) produces a maximum allowable factored axial load of 31,040 lb. These loads apply to the actual cross-sectional area of the overlay.

These allowable loads were calculated using the transformed composite section, where the polyester-styrene polymer concrete was transformed into an equal region of portland cement concrete, based on the modular ratio, $n = E_{pspc}/E_{pcc}$, and are

independent of the compressive strength of the polyester-styrene concrete. To account for the compressive strength of the overlay material, maximum allowable compressive loads were also determined assuming the overlay to be in a state of pure compression. Under this assumption, the maximum factored compressive load, ϕP_c , in the overlay is given by the equation:⁴¹

$$\phi P_c = \phi [0.85 f'_c (A_g - A_{st}) + A_{st} f_y],$$

where A_g is the gross section area under consideration, A_{st} is the area of reinforcing steel in the section, and f_y is the yield strength of the steel reinforcement. The overlay is an unreinforced section, so the equation can be reduced to

$$\phi P_c = \phi [0.85 f'_c (A_g)].$$

Substituting the values for our two models, we obtain the maximum allowable factored loads:

$$\phi P_c = 30,120 \text{ lb for Model 1, and}$$

$$\phi P_c = 30,100 \text{ lb for Model 2.}$$

These values are for polyester-styrene concrete at elevated temperatures, which is assumed to decrease compressive strength by 25 percent.

The maximum allowable factored loads are the lower of the two sets of calculated values:

$$\phi P_c = 30,120 \text{ lb for Model 1, and}$$

$$\phi P_c = 30,100 \text{ lb for Model 2.}$$

Eq. (5-8), derived previously, was used to determine the allowable unfactored compressive stress due to an increase in temperature:

$$T_c = \left(\frac{\phi P_c}{1.3} \right) \frac{1}{A_g} \quad (5-8, \text{repeated})$$

Substituting the values for ϕP_c and A_g , we obtained an allowable unfactored compressive stress due to temperature increase equal to 2575 psi at elevated temperatures, for both Model 1 and Model 2.

5.4.5.3 Tension in Polyester-Styrene Polymer Concrete

There is no specific guidance in the AASHTO ultimate strength design method for determining the strength of members under direct tension. Because tensile failure in the overlay material cannot be allowed, it was assumed that the ultimate tensile load, ϕP_t , is equal to

$$\phi P_t = \phi (f_r A_g), \text{ or}$$

$$\phi f_t = \phi f_r,$$

where ϕf_t is the ultimate tensile strength and f_r is the material's modulus of rupture. Substituting $\phi = 0.90$ and $f_r = 2165$ psi, we obtained an ultimate tensile strength value of 1950 psi.

AASHTO load combination Group IV was used to determine the allowable temperature load:

$$\phi P \geq 1.3 [D + L + T].$$

The dead load, D , and the live load, L , were assumed to be zero. Even though the overlay is subjected to live loads due to the composite action of the section, the live load is not continuously present; therefore, the assumption of no live load produces a more

conservative temperature stress limit. With dead load and live load both zero, and rearranging the equation to solve for T , the equation becomes:

$$T_t = \frac{\phi f_t}{1.3}, \quad (5-9)$$

where T_t is the maximum allowable unfactored stress caused by a decrease in temperature, ϕ is the strength reduction factor, 0.90, and f_t is the tensile strength of the polyester-styrene concrete, assumed to be equal to the modulus of rupture, f_r .

Substituting the appropriate values into Eq. (5-9), we obtained an allowable unfactored tensile stress value of 1500 psi.

5.4.5.4 Interface Shear

There is no simple method, using AASHTO ultimate strength design, for determining allowable interface shear.⁴¹ Shear strength methods are typically used for determining vertical shear in beams, thus the equations for shear involve the cross-sectional area and the section's shear reinforcement. Horizontal shear is considered for composite sections; however, this requires steel dowels to transfer the shear stresses, something that is not present in bridge deck overlays. To estimate the tensile strength of the portland cement or polyester-styrene concrete under the influence of interface shear, we assume that the ultimate tensile strength, ϕf_t , is equal to

$$\phi f_t = \phi f_r. \quad (5-10)$$

For portland cement concrete with a compressive strength, f'_c , of 4000 psi, and a modulus of rupture, f_r , equal to 475 psi, Eq. (5-10) yielded an ultimate strength of 428 psi. For 7500 psi compressive strength polyester-styrene polymer concrete, with a modulus of rupture of 2165 psi, Eq. (5-10) produced an ultimate strength of 1949 psi.

The allowable tensile stress due to interface shear can then be calculated using Eq. (5-9), shown previously:

$$T_t = \frac{\phi f_t}{1.3} \quad (5-9, \text{ repeated})$$

Substituting the appropriate values for f_t , this equation produces an allowable unfactored interface shear stress of 330 psi for the portland cement concrete, and 1500 psi for the polyester-styrene polymer concrete at room temperature. At elevated temperature, where the compressive strength of polyester-styrene is assumed to be 5625 psi, the allowable unfactored interface shear stress is 1300 psi.

5.5 Results

The fully restrained finite element model, shown in Figure 5-4(a) resulted in the largest compressive and tensile stresses in the portland cement concrete and polyester-styrene concrete for both Model 1 and Model 2. The beam continuous over the two roller supports, illustrated in Figure 5-4(b), resulted in the largest interface shear values, near the right support. In both Model 1 and Model 2, the cantilever condition produced nearly the same interface shear values at the extreme right end, but was otherwise not a limiting case.

Results of the finite element analysis for the various end restraint conditions and temperature loading cases are shown in Tables 5-2 through 5-13 for Model 1, and in Tables 5-14 through 5-19 for Model 2. These tables list axial stress values and interface shear stress values for selected locations on the model. Positive axial stress values indicate tension, negative values indicate compression. The limiting values are indicated by a box surrounding the value.

A comparison of the stresses obtained from the finite element analysis to the allowable unfactored stresses for Model 1 is shown in Table 5-20. All finite element analysis results are less than their associated allowable values, with the following exceptions: for the 35°F temperature increase case, compression in the portland cement concrete exceeds the allowable value calculated by the ACI ultimate strength method and

interface shear in the portland cement concrete exceeds the allowable value calculated using the AASHTO service load method. For the 45°F temperature decrease, tension in the polyester-styrene polymer concrete exceeds the allowable values for all three methods of calculation; the interface shear in the portland cement concrete also exceeds the allowable value, as calculated using the AASHTO service load method.

Table 5-21 lists the comparison of the finite element analysis results to the allowable unfactored stresses for Model 2. All finite element analysis results are less than their associated allowable values, with the following exceptions: the portland cement concrete in compression, for the 35°F increase case, is excessive when compared to the ACI ultimate strength method allowable stress, and the interface shear is excessive compared to the AASHTO service load method. Also, the polyester-styrene polymer concrete in tension, for the 45°F decrease case, exceeds the allowable stress values for all three methods.

It is important to note that the tension values for polyester-styrene polymer concrete and the compression values for portland cement concrete, which exceeded allowable values in both Model 1 and Model 2, were the result of the fixed end restraint condition. In these situations, the values generated in the finite element analysis were independent of the other material, since the interface shear was nearly zero. Field installations to date have not shown problems, which may indicate that the stiffness of the fixed restraints was overly conservative, and not representative of actual field conditions.

All interface shear values which exceeded allowable values exceeded only the value calculated by the AASHTO service load method. This may be a result of an overly conservative estimate of tensile strength, which was limited to 21 percent of the modulus of rupture.

The presence of finite element analysis results which exceed the allowable limits indicate that problem areas may be present; these areas bear watching in field

installations, even though no problems have been noted to date. This is especially important where the polyester-styrene overlay is concerned, since cracking in the overlay cannot be tolerated.

5.6 Summary

The bond between the polymer concrete overlay and the portland cement concrete deck results in composite action in a section with distinct areas of different physical properties. Because the polyester-styrene concrete and the portland cement concrete exhibit different values of coefficient of thermal expansion, α , and modulus of elasticity, E , composite action under temperature change raises a concern.

The effects of air temperature, wind, humidity, intensity of solar radiation, and types of material combine to cause thermal loading in bridge decks. There are generally two daily extreme conditions of temperature distribution within a bridge deck. In the first extreme, the top and bottom surfaces of the deck have different temperatures. This temperature differential is greatest in the afternoon, under the influence of direct solar radiation. During the night, the bridge deck slowly loses the heat built up during the previous day. When the air temperature passes its lowest point and begins to increase, shortly after dawn, it is possible to reach a point at which the air temperature is the same as the bridge deck top and bottom surface temperatures, and a uniform temperature exists in the deck. This uniform condition forms the second extreme.

The American Association of State Highway and Transportation Officials recommends that highway bridges be designed to accommodate stresses or movements resulting from temperature variations. For concrete structures located in cold climates, the specified range is from 35°F above to 45°F below the assumed erection temperature. For each of these temperature extremes, two conditions were examined in this study: the isothermal case, where temperatures throughout the deck section are the same, and the case where a temperature differential exists between the top and bottom surfaces of the

deck. The 35°F increase cases were assumed to represent summer conditions, and the 45°F decrease cases were assumed to represent winter conditions. A simplified temperature gradient was assumed for this research: a second-order parabola with the axis of symmetry coincident with the bottom fiber of the deck slab.

Two finite element models were examined to determine the thermal compatibility between the overlay and the bridge deck. The first model was designed to represent an 8-inch thick bridge deck with a ¾-inch polyester-styrene overlay, and an 8-foot span between girders. The second model was based on an actual bridge. The finite element model for this bridge consists of a 9.5-inch thick slab with a span length of 12.5 feet. This model also had a ¾-inch polyester-styrene overlay.

For each model, three end restraint conditions were considered: fixed ends at all supports; a fixed support at the left end, with roller supports to the right; and a cantilever beam. The first two end restraint conditions were intended to model the extreme cases under temperature loading, the first to produce the maximum axial stress in the materials, and the second to produce the highest interface shear. The cantilever was examined to ensure that the first two cases were indeed the extreme cases. Analysis confirmed that the cantilever model was not critical.

A comparison of the stresses obtained from the finite element analysis to the allowable unfactored stresses was presented. Most finite element analysis results were less than their associated allowable values, indicating acceptable performance. However, some exceptions were present in both models: compression in the portland cement concrete due to increasing temperature and tension in the overlay material due to decreasing temperature.

Even though no problems have been noted to date, the presence of finite element analysis results which exceed the allowable limits indicate that problem areas may be present; these areas bear watching in field installations. This is especially important

where the polyester-styrene overlay is concerned, since cracking in the overlay cannot be tolerated.

Table 5-1. Engineering Properties of Materials used in the Finite Element Models.

	Polyester-Styrene Polymer Concrete	Portland Cement Concrete
Compressive Strength, f'_c	7500 psi	4000 psi
Modulus of Elasticity, E	2.57×10^6 psi	3.64×10^6 psi
Modulus of Rupture, f_r	2165 psi	475 psi
Coefficient of Thermal Expansion, α	13.0×10^{-6} /°F	5.0×10^{-6} /°F
Unit Weight, w_c	145 lb/ft ³	145 lb/ft ³
Poisson's Ratio, ν	0.25	0.25

Table 5-2. Finite Element Analysis Results for Model 1: All Supports Fixed; 35°F Temperature Increase with 25°F Thermal Gradient Across Deck.

		Left Span				Right Span				
		Left Support	Left Quarter-span	Mid-span	Right Quarter-span	Center Support	Left Quarter-span	Mid-span	Right Quarter-span	Right Support
Polymer Concrete Overlay	Top Fiber Stress, psi	-2286	-2287	-2287	-2287	-2286	-2287	-2287	-2287	-2286
	Bottom Fiber Stress, psi	-2209	-2210	-2210	-2210	-2209	-2210	-2210	-2210	-2209
	Interface Shear, psi	0	0	0	0	0	0	0	0	0
PCC Bridge Deck	Interface Shear, psi	0	0	0	0	0	0	0	0	0
	Top Fiber Stress, psi	-893	-895	-895	-895	-893	-895	-895	-895	-893
	Bottom Fiber Stress, psi	-685	-690	-690	-690	-685	-690	-690	-690	-685

Table 5-3. Finite Element Analysis Results for Model 1: All Supports Fixed; 35°F Isothermal Temperature Increase.

		Left Span				Right Span				
		Left Support	Left Quarter-span	Mid-span	Right Quarter-span	Center Support	Left Quarter-span	Mid-span	Right Quarter-span	Right Support
Polymer Concrete Overlay	Top Fiber Stress, psi	-1345	-1345	-1345	-1345	-1345	-1345	-1345	-1345	-1345
	Bottom Fiber Stress, psi	-1351	-1351	-1351	-1351	-1351	-1351	-1351	-1351	-1351
	Interface Shear, psi	0	0	0	0	0	0	0	0	0
PCC Bridge Deck	Interface Shear, psi	0	0	0	0	0	0	0	0	0
	Top Fiber Stress, psi	-563	-564	-564	-564	-563	-564	-564	-564	-563
	Bottom Fiber Stress, psi	-661	-663	-663	-663	-661	-663	-663	-663	-661

Table 5-4. Finite Element Analysis Results for Model 1: All Supports Fixed; 45°F Temperature Decrease with 15°F Thermal Gradient Across Deck.

		Left Span				Right Span				
		Left Support	Left Quarter-span	Mid-span	Right Quarter-span	Center Support	Left Quarter-span	Mid-span	Right Quarter-span	Right Support
Polymer Concrete Overlay	Top Fiber Stress, psi	1164	1165	1165	1165	1164	1165	1165	1165	1164
	Bottom Fiber Stress, psi	1222	1222	1222	1222	1222	1222	1222	1222	1222
	Interface Shear, psi	0	0	0	0	0	0	0	0	0
PCC Bridge Deck	Interface Shear, psi	0	0	0	0	0	0	0	0	0
	Top Fiber Stress, psi	526	526	526	526	526	526	526	526	526
	Bottom Fiber Stress, psi	835	836	836	836	835	836	836	836	835

Table 5-5. Finite Element Analysis Results for Model 1: All Supports Fixed; 45°F Isothermal Temperature Decrease.

	Left Span				Right Span				
	Left Support	Left Quarter-span	Mid-span	Right Quarter-span	Center Support	Left Quarter-span	Mid-span	Right Quarter-span	Right Support
Top Fiber Stress, psi	1729	1729	1729	1729	1729	1729	1729	1729	1729
Bottom Fiber Stress, psi	1736	1737	1737	1737	1736	1737	1737	1737	1736
Interface Shear, psi	0	0	0	0	0	0	0	0	0
Interface Shear, psi	0	0	0	0	0	0	0	0	0
Top Fiber Stress, psi	724	725	725	725	724	725	725	725	724
Bottom Fiber Stress, psi	850	852	852	852	850	852	852	852	850

Table 5-6. Finite Element Analysis Results for Model 1: Left Support Fixed, Rollers at Center and Right Supports; 35°F Temperature Increase with 25°F Thermal Gradient Across Deck.

	Left Span				Right Span				
	Left Support	Left Quarter-span	Mid-span	Right Quarter-span	Center Support	Left Quarter-span	Mid-span	Right Quarter-span	Right Support
Top Fiber Stress, psi	-1614	-1645	-1683	-1722	-1761	-1663	-1544	-1413	-890
Bottom Fiber Stress, psi	-1541	-1569	-1604	-1639	-1673	-1581	-1473	-1359	-985
Interface Shear, psi	1	0	1	1	0	0	6	15	170
Interface Shear, psi	2	2	2	1	0	5	7	14	199
Top Fiber Stress, psi	48	12	-34	-80	-123	-11	124	248	522
Bottom Fiber Stress, psi	141	174	223	271	327	196	50	-98	-108

Table 5-7. Finite Element Analysis Results for Model 1: Left Support Fixed, Rollers at Center and Right Supports; 35°F Isothermal Temperature Increase.

	Left Span				Right Span				
	Left Support	Left Quarter-span	Mid-span	Right Quarter-span	Center Support	Left Quarter-span	Mid-span	Right Quarter-span	Right Support
Polymer Concrete Overlay	Top Fiber Stress, psi	-834	-844	-858	-872	-886	-809	-759	-492
	Bottom Fiber Stress, psi	-841	-851	-863	-876	-888	-816	-773	-589
	Interface Shear, psi	0	0	0	0	0	3	8	98
PCC Bridge Deck	Interface Shear, psi	1	1	1	0	0	3	8	112
	Top Fiber Stress, psi	157	145	128	112	97	183	224	340
	Bottom Fiber Stress, psi	19	31	48	65	85	-14	-66	-53

Table 5-8. Finite Element Analysis Results for Model 1: Left Support Fixed, Rollers at Center and Right Supports; 45°F Temperature Decrease with 15°F Thermal Gradient Across Deck.

	Left Span				Right Span				
	Left Support	Left Quarter-span	Mid-span	Right Quarter-span	Center Support	Left Quarter-span	Mid-span	Right Quarter-span	Right Support
Top Fiber Stress, psi	604	606	609	612	615	608	599	584	394
Bottom Fiber Stress, psi	662	664	666	668	671	664	655	643	520
Interface Shear, psi	0	0	0	0	0	1	2	7	81
Interface Shear, psi	0	0	0	0	0	1	2	6	92
Top Fiber Stress, psi	-267	-265	-262	-258	-255	-263	-271	-273	-329
Bottom Fiber Stress, psi	50	48	44	41	37	46	56	67	35

Table 5-9. Finite Element Analysis Results for Model 1: Left Support Fixed, Rollers at Center and Right Supports; 45°F Isothermal Temperature Decrease.

		Left Span				Right Span				
		Left Support	Left Quarter-span	Mid-span	Right Quarter-span	Center Support	Left Quarter-span	Mid-span	Right Quarter-span	Right Support
Polymer Concrete Overlay	Top Fiber Stress, psi	1072	1086	1103	1121	1139	1094	1040	976	633
	Bottom Fiber Stress, psi	1081	1094	1110	1126	1141	1100	1049	994	757
	Interface Shear, psi	1	0	0	0	0	2	4	11	124
PCC Bridge Deck	Interface Shear, psi	1	1	1	1	0	3	4	10	144
	Top Fiber Stress, psi	-202	-186	-165	-144	-124	-175	-236	-288	-438
	Bottom Fiber Stress, psi	-24	-40	-62	-84	-109	-50	17	85	68

Table 5-10. Finite Element Analysis Results for Model 1: Cantilever Beam—Left Support Fixed, Center and Right Supports Free; 35°F Temperature Increase with 25°F Thermal Gradient Across Deck.

		Left Span				Right Span				
		Left Support	Left Quarter-span	Mid-span	Right Quarter-span	Center	Left Quarter-span	Mid-span	Right Quarter-span	Right End
Polymer Concrete Overlay	Top Fiber Stress, psi	-1293	-1294	-1294	-1294	-1294	-1294	-1293	-1280	-876
	Bottom Fiber Stress, psi	-1248	-1248	-1248	-1248	-1247	-1246	-1244	-1238	-972
	Interface Shear, psi	0	0	0	0	1	1	3	12	168
PCC Bridge Deck	Interface Shear, psi	0	0	0	0	0	1	2	10	195
	Top Fiber Stress, psi	423	422	422	422	421	421	418	403	537
	Bottom Fiber Stress, psi	-259	-263	-263	-263	-263	-263	-263	-263	-131

Table 5-11. Finite Element Analysis Results for Model 1: Cantilever Beam—Left Support Fixed, Center and Right Supports Free; 35°F Isothermal Temperature Increase.

	Left Span				Right Span				
	Left Support	Left Quarter-span	Mid-span	Right Quarter-span	Center	Left Quarter-span	Mid-span	Right Quarter-span	Right End
Top Fiber Stress, psi	-720	-720	-720	-720	-720	-720	-720	-712	-487
Bottom Fiber Stress, psi	-737	-737	-737	-737	-736	-736	-734	-730	-584
Interface Shear, psi	0	0	0	0	0	1	2	7	96
Interface Shear, psi	0	0	0	0	0	1	2	6	111
Top Fiber Stress, psi	291	290	290	290	290	290	288	279	346
Bottom Fiber Stress, psi	-123	-125	-125	-125	-125	-125	-125	-125	-61

Table 5-12. Finite Element Analysis Results for Model 1: Cantilever Beam—Left Support Fixed, Center and Right Supports Free; 45°F Temperature Decrease with 15°F Thermal Gradient Across Deck.

	Left Span				Right Span				
	Left Support	Left Quarter-span	Mid-span	Right Quarter-span	Center	Left Quarter-span	Mid-span	Right Quarter-span	Right End
Top Fiber Stress, psi	582	582	582	582	582	582	582	575	393
Bottom Fiber Stress, psi	641	641	641	641	641	640	639	635	519
Interface Shear, psi	0	0	0	0	0	1	2	6	80
Interface Shear, psi	0	0	0	0	0	1	2	6	92
Top Fiber Stress, psi	-294	-294	-294	-293	-293	-293	-291	-284	-397
Bottom Fiber Stress, psi	78	78	78	78	78	78	78	78	37

Table 5-13. Finite Element Analysis Results for Model 1: Cantilever Beam—Left Support Fixed, Center and Right Supports Free; 45°F Isothermal Temperature Decrease.

		Left Span				Right Span				
		Left Support	Left Quarter-span	Mid-span	Right Quarter-span	Center	Left Quarter-span	Mid-span	Right Quarter-span	Right End
Polymer Concrete Overlay	Top Fiber Stress, psi	925	925	925	926	926	926	925	915	627
	Bottom Fiber Stress, psi	947	948	947	947	947	946	944	939	751
	Interface Shear, psi	0	0	0	0	0	1	2	9	123
PCC Bridge Deck	Interface Shear, psi	0	0	0	0	0	1	2	8	142
	Top Fiber Stress, psi	-374	-373	-373	-373	-373	-372	-370	-359	-445
	Bottom Fiber Stress, psi	158	160	160	160	160	160	160	160	79

Table 5-14. Finite Element Analysis Results for Model 2: All Supports Fixed; 35°F Temperature Increase with 25°F Thermal Gradient Across Deck.

		Left Span				Right Span				
		Left Support	Left Quarter-span	Mid-span	Right Quarter-span	Center Support	Left Quarter-span	Mid-span	Right Quarter-span	Right Support
Polymer Concrete Overlay	Top Fiber Stress, psi	-2309	-2310	-2310	-2310	-2309	-2309	-2310	-2311	-2311
	Bottom Fiber Stress, psi	-2242	-2243	-2243	-2243	-2242	-2243	-2243	-2244	-2244
	Interface Shear, psi	0	0	0	0	0	0	0	0	0
PCC Bridge Deck	Interface Shear, psi	0	0	0	0	0	0	0	0	0
	Top Fiber Stress, psi	-916	-918	-918	-918	-916	-918	-919	-919	-919
	Bottom Fiber Stress, psi	-683	-688	-688	-688	-683	-687	-688	-687	-681

Table 5-15. Finite Element Analysis Results for Model 2: All Supports Fixed; 45°F Isothermal Temperature Decrease.

		Left Span				Right Span				
		Left Support	Left Quarter-span	Mid-span	Right Quarter-span	Center Support	Left Quarter-span	Mid-span	Right Quarter-span	Right Support
Polymer Concrete Overlay	Top Fiber Stress, psi	1735	1735	1735	1735	1735	1735	1735	1735	1735
	Bottom Fiber Stress, psi	1741	1742	1742	1742	1741	1742	1742	1742	1742
	Interface Shear, psi	0	0	0	0	0	0	0	0	0
PCC Bridge Deck	Interface Shear, psi	0	0	0	0	0	0	0	0	0
	Top Fiber Stress, psi	730	730	730	730	730	730	731	731	731
	Bottom Fiber Stress, psi	846	848	848	848	846	848	848	848	845

Table 5-16. Finite Element Analysis Results for Model 2: Left Support Fixed, Rollers at Center and Right Supports; 35°F Temperature Increase with 25°F Thermal Gradient Across Deck.

		Left Span				Right Span				
		Left Support	Left Quarter-span	Mid-span	Right Quarter-span	Center Support	Left Quarter-span	Mid-span	Right Quarter-span	Right Support
Polymer Concrete Overlay	Top Fiber Stress, psi	-1647	-1683	-1718	-1752	-1787	-1694	-1561	-1538	-1117
	Bottom Fiber Stress, psi	-1584	-1618	-1650	-1683	-1716	-1626	-1511	-1461	-1150
	Interface Shear, psi	0	1	1	1	2	5	15	31	105
PCC Bridge Deck	Interface Shear, psi	1	1	1	1	2	3	15	29	127
	Top Fiber Stress, psi	-11	-32	-74	-116	-153	-27	77	231	444
	Bottom Fiber Stress, psi	131	171	216	260	312	174	42	-95	-145

Table 5-17. Finite Element Analysis Results for Model 2: Left Support Fixed, Rollers at Center and Right Supports; 45°F Isothermal Temperature Decrease.

	Left Span				Right Span				
	Left Support	Left Quarter-span	Mid-span	Right Quarter-span	Center Support	Left Quarter-span	Mid-span	Right Quarter-span	Right Support
Top Fiber Stress, psi	1088	1103	1118	1132	1147	1110	1045	1062	793
Polymer Concrete Overlay Bottom Fiber Stress, psi	1096	1110	1124	1138	1153	1116	1061	1057	864
Interface Shear, psi	0	0	0	1	1	4	11	24	76
Interface Shear, psi	0	0	1	1	1	3	11	23	91
PCC Bridge Deck Top Fiber Stress, psi	-183	-164	-147	-130	-115	-169	-205	-280	-385
Bottom Fiber Stress, psi	-18	-35	-54	-72	-94	-36	19	77	86

Table 5-18. Finite Element Analysis Results for Model 2: Cantilever Beam—Left Support Fixed, Center and Right Supports Free; 35°F Temperature Increase with 25°F Thermal Gradient Across Deck.

		Left Span				Right Span				
		Left Support	Left Quarter-span	Mid-span	Right Quarter-span	Center	Left Quarter-span	Mid-span	Right Quarter-span	Right End
Polymer Concrete Overlay	Top Fiber Stress, psi	-1353	-1354	-1354	-1353	-1354	-1362	-1333	-1415	-1099
	Bottom Fiber Stress, psi	-1312	-1313	-1313	-1314	-1316	-1319	-1300	-1348	-1134
	Interface Shear, psi	0	0	0	1	2	7	14	33	103
PCC Bridge Deck	Interface Shear, psi	0	0	0	0	2	6	12	32	124
	Top Fiber Stress, psi	366	365	365	366	368	374	351	379	464
	Bottom Fiber Stress, psi	-243	-247	-247	-247	-247	-248	-247	-250	-170

Table 5-19. Finite Element Analysis Results for Model 2: Cantilever Beam—Left Support Fixed, Center and Right Supports Free; 45°F Isothermal Temperature Decrease.

	Left Span				Right Span				
	Left Support	Left Quarter-span	Mid-span	Right Quarter-span	Center	Left Quarter-span	Mid-span	Right Quarter-span	Right End
Top Fiber Stress, psi	965	965	965	965	965	971	950	1010	785
Bottom Fiber Stress, psi	982	982	983	983	985	987	973	1009	858
Interface Shear, psi	0	0	0	0	1	5	10	24	75
Interface Shear, psi	0	0	0	0	1	4	9	24	90
Top Fiber Stress, psi	-332	-331	-331	-332	-334	-338	-321	-341	-393
Bottom Fiber Stress, psi	139	141	141	141	141	141	140	142	97

Table 5-20. Comparison of Finite Element Analysis Results and Calculated Allowable Stresses for Model 1.

			Finite Element Analysis Result (psi)	Allowable Stress		
				ACI Ultimate Strength Method (psi)	AASHTO Methods	
					Service Load Method (psi)	Ultimate Strength Method (psi)
35°F Temperature Increase	Polyester-Styrene Polymer Concrete	f_{axial}	-2287	-2390	-2366	-2575
		f_{shear}	170	1200	492	1300
	Portland Cement Concrete	f_{axial}	-895	-560	-1545	-1770
		f_{shear}	199	305	125	330
45°F Temperature Decrease	Polyester-Styrene Polymer Concrete	f_{axial}	+1737	+1385	+568	+1500
		f_{shear}	124	1385	568	1500
	Portland Cement Concrete	f_{axial}	+852	N/C	N/C	N/C
		f_{shear}	144	305	125	330

N/C — Not Considered

Table 5-21. Comparison of Finite Element Analysis Results and Calculated Allowable Stresses for Model 2.

			Allowable Stress			
			Finite Element Analysis Result (psi)	ACI Ultimate Strength Method (psi)	AASHTO Methods	
					Service Load Method (psi)	Ultimate Strength Method (psi)
35°F Temperature Increase	Polyester-Styrene Polymer Concrete	<i>f_{axial}</i>	-2311	-2390	-2363	-2575
		<i>f_{shear}</i>	105	1200	492	1300
	Portland Cement Concrete	<i>f_{axial}</i>	-919	-560	-1452	-1785
		<i>f_{shear}</i>	127	305	125	330
45°F Temperature Decrease	Polyester-Styrene Polymer Concrete	<i>f_{axial}</i>	+1742	+1385	+568	+1500
		<i>f_{shear}</i>	76	1385	568	1500
	Portland Cement Concrete	<i>f_{axial}</i>	+848	N/C	N/C	N/C
		<i>f_{shear}</i>	91	305	125	330

N/C — Not Considered

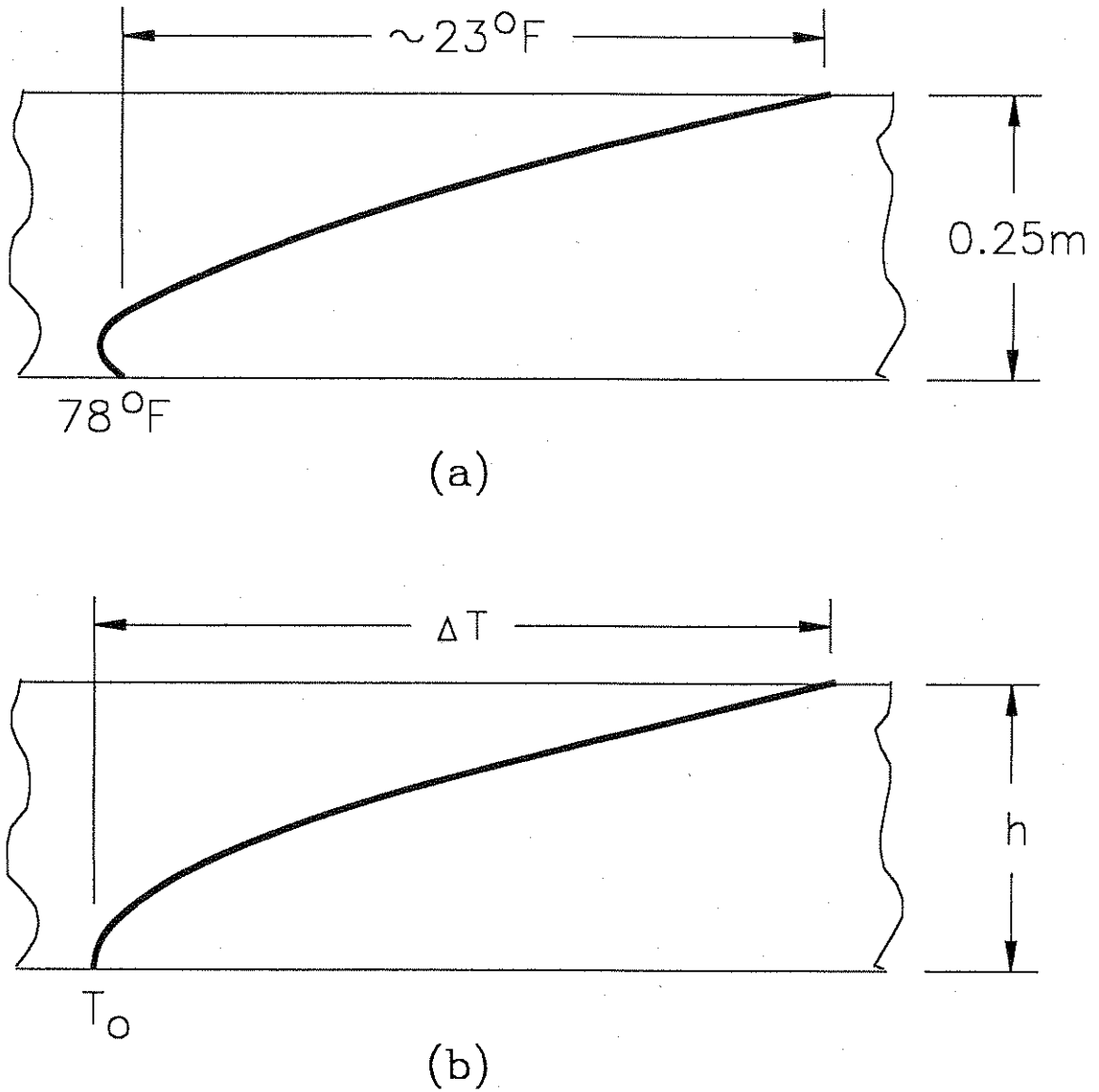


Figure 5-1. (a) Actual Temperature Gradient through Slab Bridge Deck (after Ref. 42).
 (b) Simplified Parabolic Gradient used in the Analysis.

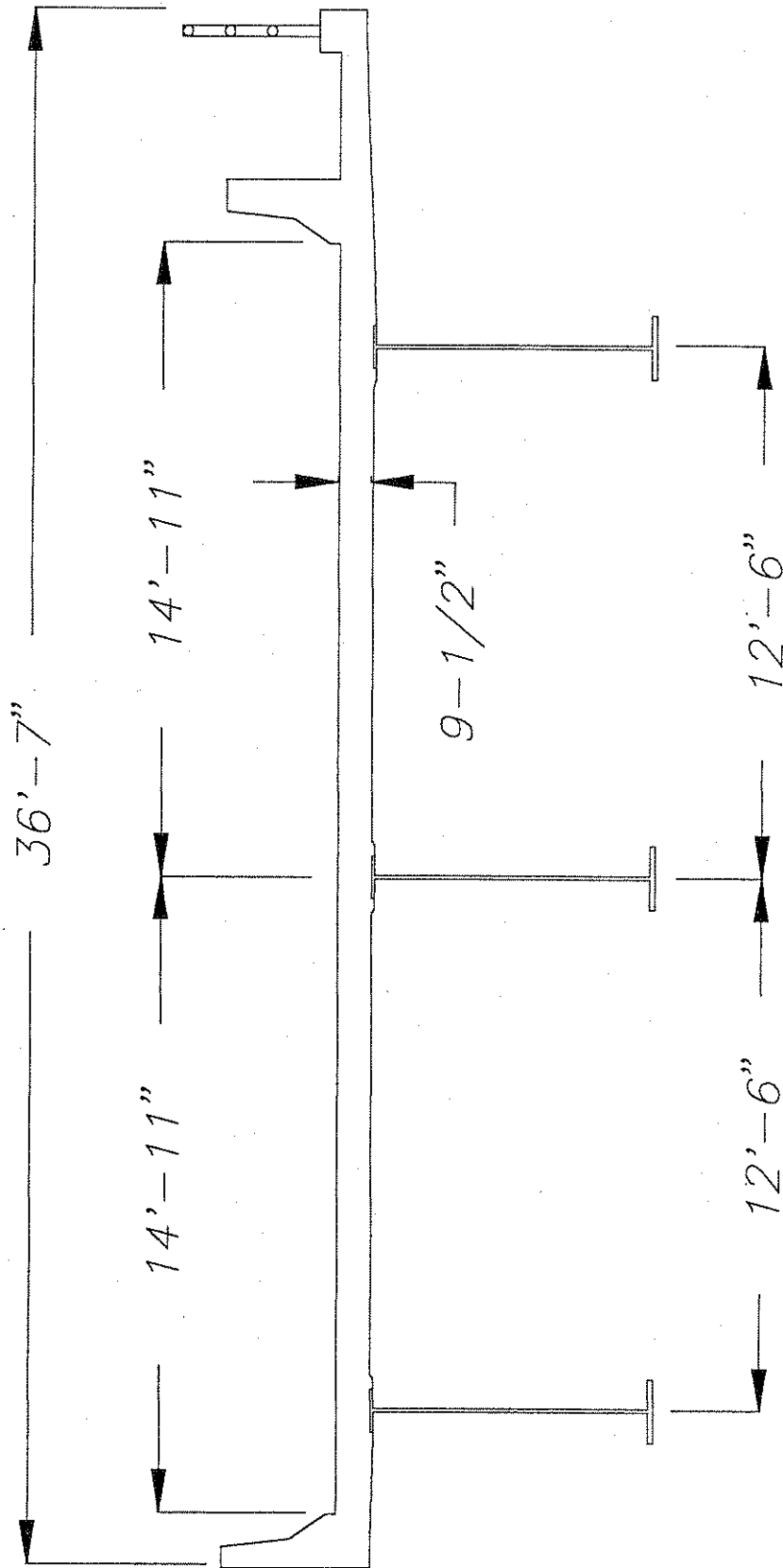


Figure 5-2. Deck Section of Humboldt River Bridge used for the Second Finite Element Model.

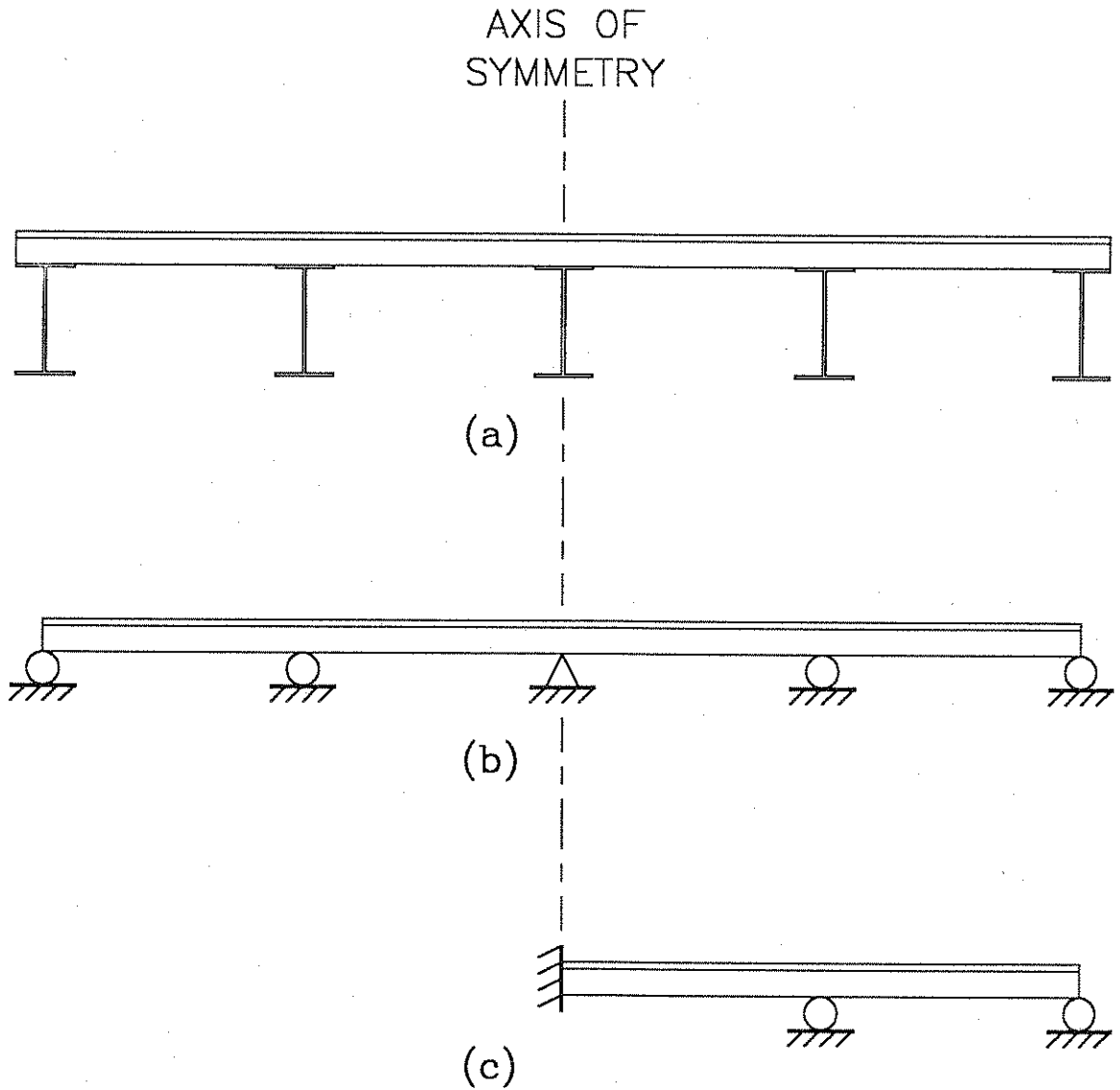
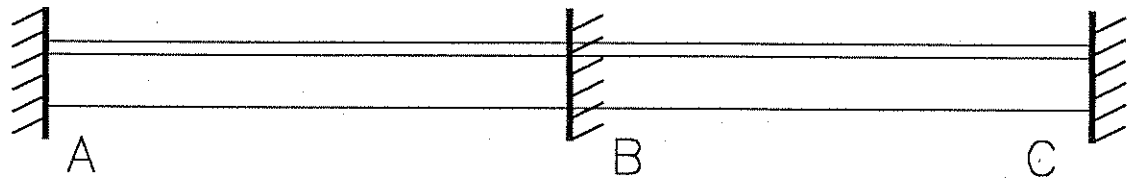
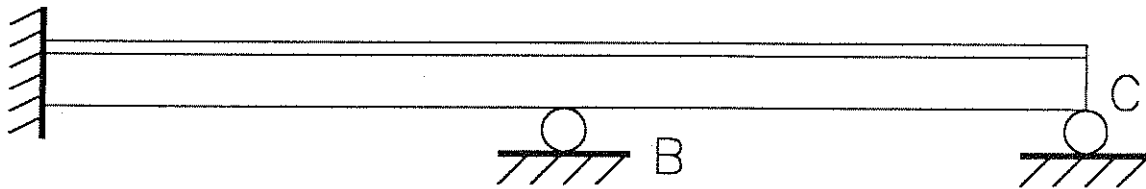


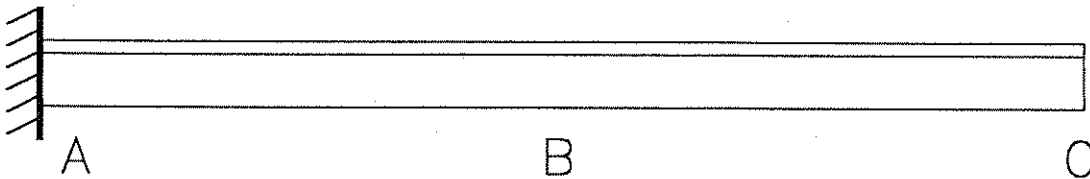
Figure 5-3. (a) Cross-Sectional View of Deck. (b) Multiple Span Model used to Minimize End Effects. (c) Symmetric Nature of Model Allows the use of only Half of the Structure for the Finite Element Analysis.



(a)



(b)



(c)

Figure 5-4. End Restraint Conditions used in the Finite Element Models: (a) Fixed Restraints at Nodes A, B, and C, (b) Roller Supports at Nodes B and C, and (c) Cantilever.

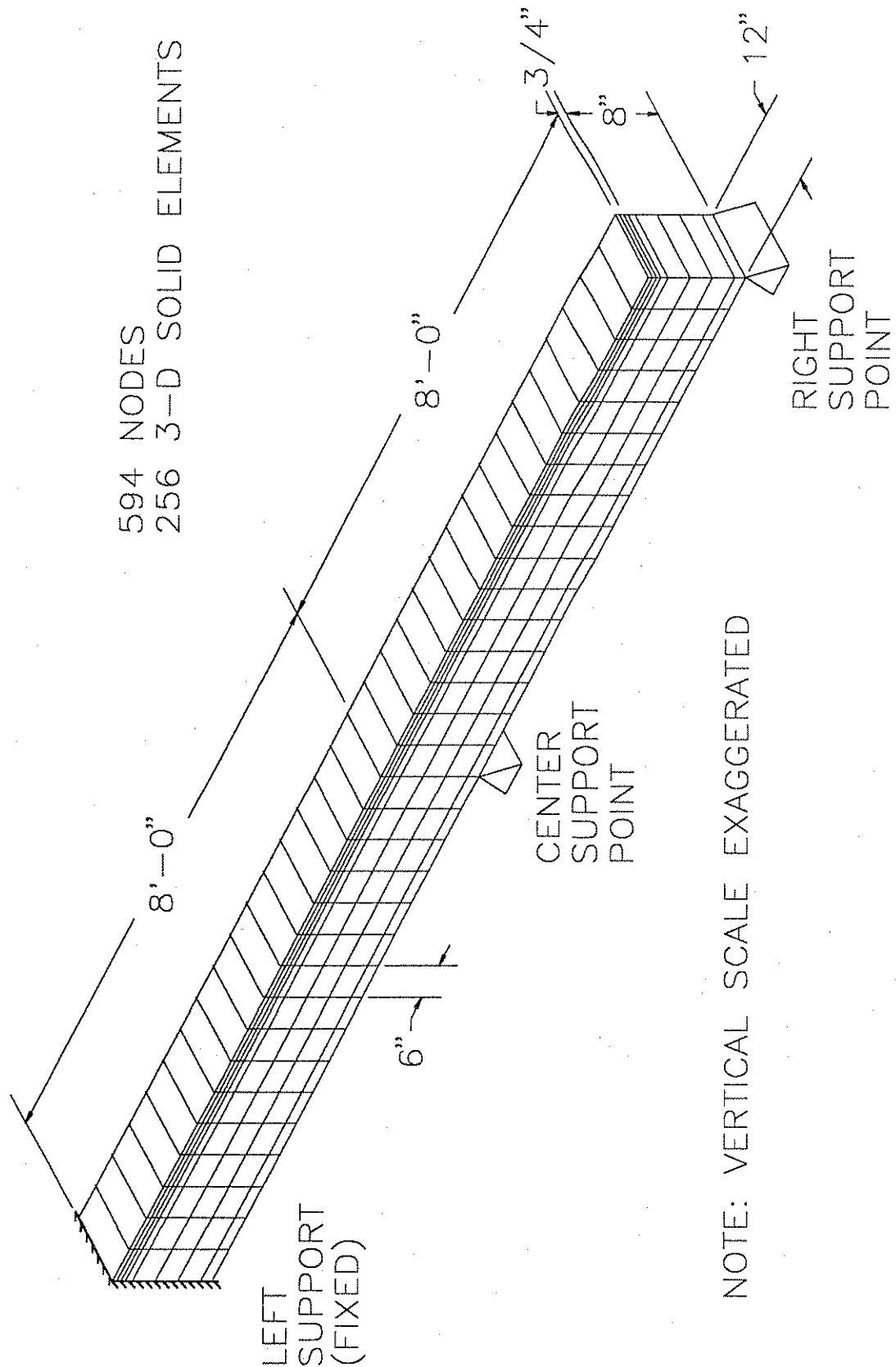


Figure 5-5. Finite Element Mesh for Model 1.

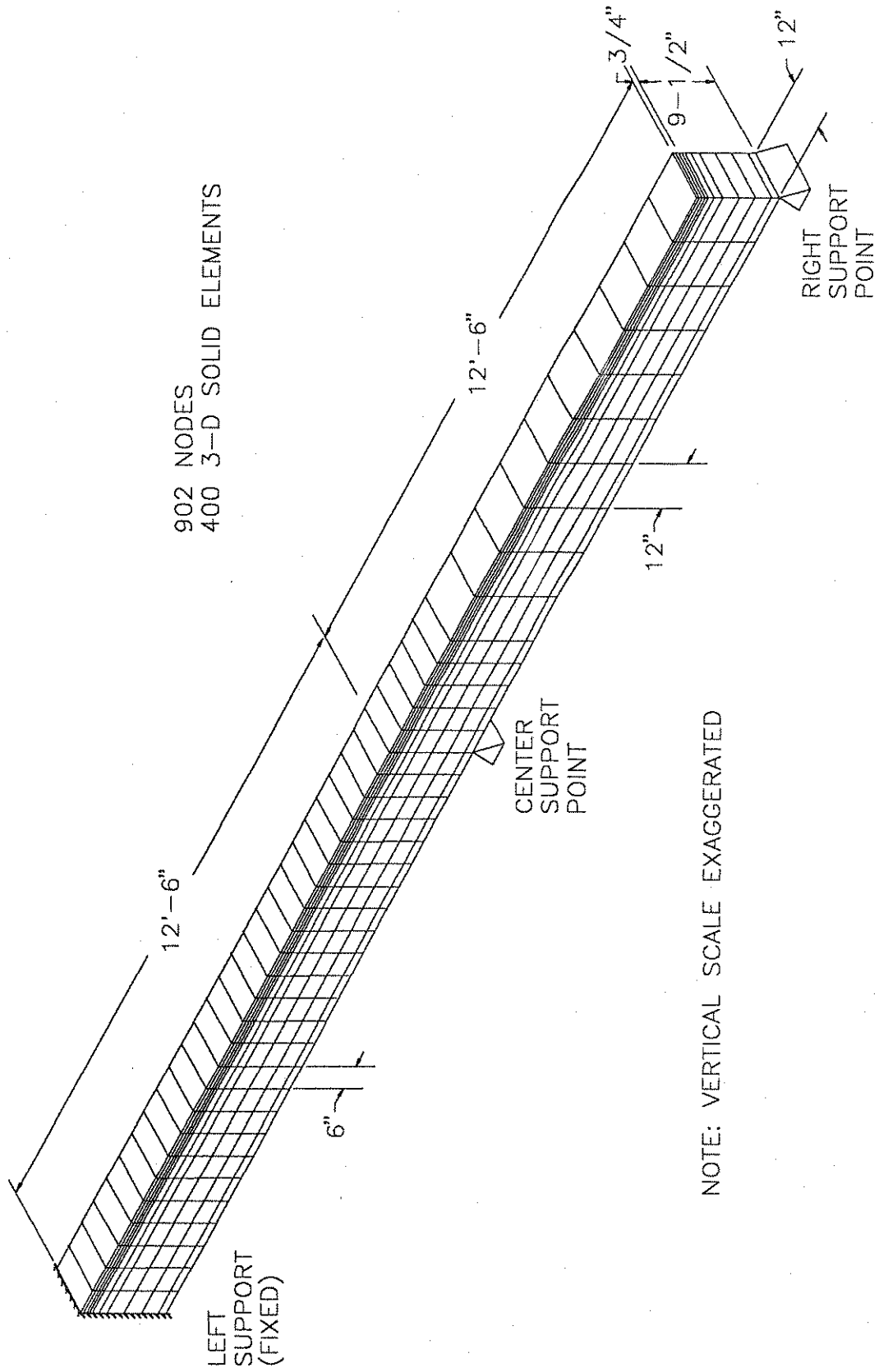


Figure 5-6. Finite Element Mesh for Model 2.

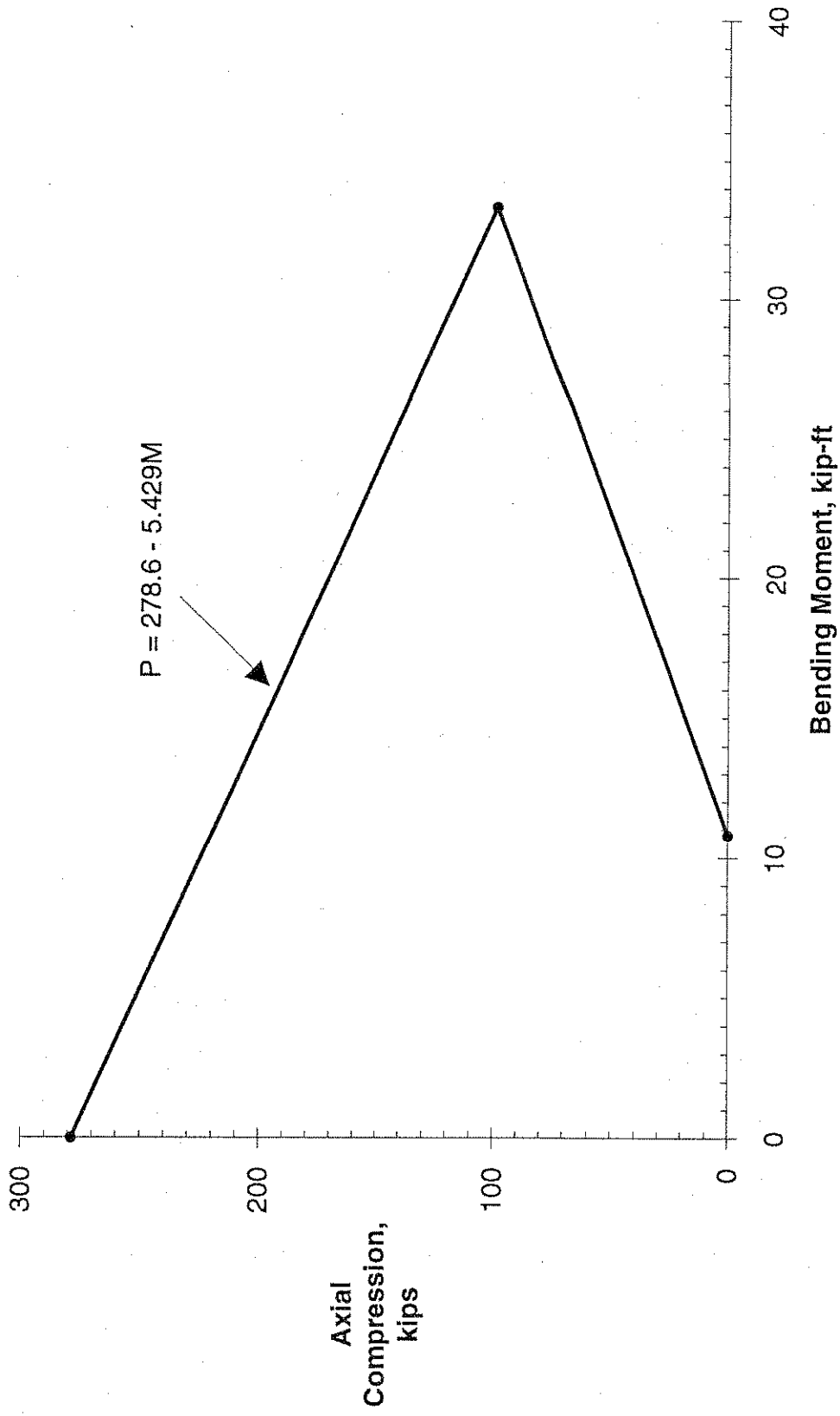


Figure 5-7. Strength Interaction Diagram for Model 1.

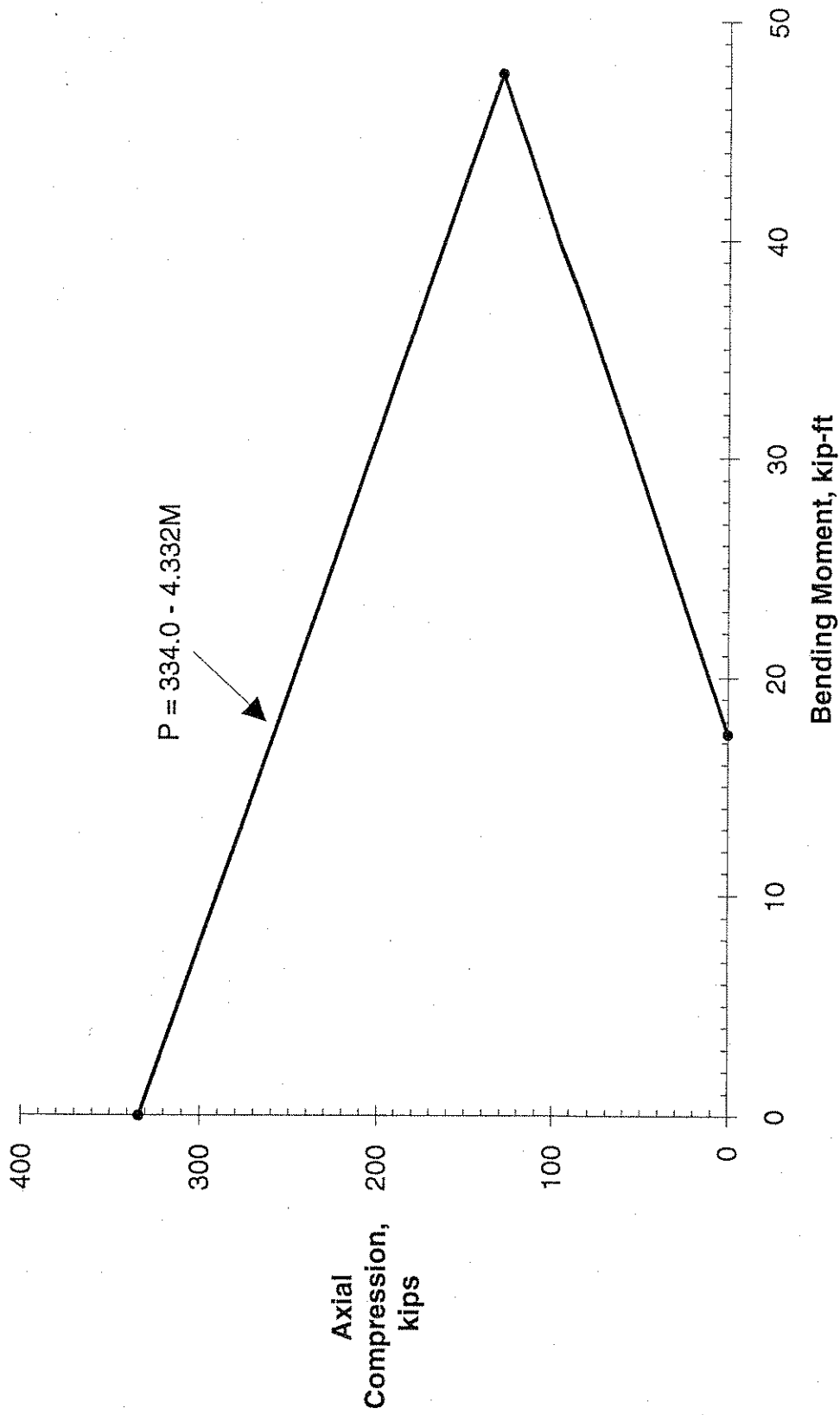


Figure 5-8. Strength Interaction Diagram for Model 2.

Chapter 6

Summary and Conclusions

6.1 Summary

Several methods are available to protect bridge decks from chloride and water intrusion, including cathodic protection systems, epoxy-coated reinforcing steel, polymer impregnation of the deck, impermeable membranes with asphalt concrete overlays, latex-modified concrete overlays, low-slump dense concrete overlays, and polymer concrete overlays. As an aid in determining which of the various methods have been used in Nevada, a database of bridges with installed protective systems was compiled. This database is also expected to serve as a reference for the comparison of protective system performance in the future.

Polyester-styrene polymer concrete overlays have recently gained favor with the Nevada Department of Transportation. Polyester-styrene overlays have been placed on several bridges in Nevada over the last two years, and several more are planned for the near future.

In order to study the physical differences between the portland cement concrete bridge deck and the polyester-styrene polymer concrete overlay, a knowledge of the material properties of polyester-styrene concrete was obtained from available research. The literature review showed that polyester-styrene polymer concrete has a higher compressive strength than portland cement concrete. Tensile and flexural strengths were also greater than for portland cement concrete, and were found to show a dependence on the square root of compressive strength, similar to portland cement concrete: $14 \sqrt{f'_c}$ and $25 \sqrt{f'_c}$ for splitting tensile strength and modulus of rupture, respectively, compared to $6.7 \sqrt{f'_c}$ and $7.5 \sqrt{f'_c}$ for portland cement concrete. The modulus of elasticity also showed a dependence on the square root of compressive strength: $17 w^{1.5} \sqrt{f'_c}$ versus $33 w^{1.5} \sqrt{f'_c}$. The coefficient of thermal expansion for polymer concrete made with a

flexible polyester resin was found to be approximately 13×10^{-6} inch/inch-°F, slightly more than twice that of portland cement concrete. Shrinkage and creep appear to be higher in polymer concrete than in conventional concrete, but quantitative methods for determining these parameters were not available. Polyester-styrene concrete gains compressive strength much more rapidly than portland cement concrete, but the polymer suffers a reduction in strength as temperature increases, exhibiting a 25 percent decrease over a temperature range of 73°F to 140°F.

Because polyester-styrene polymer concrete and portland cement concrete were found to exhibit different values for coefficient of thermal expansion and modulus of elasticity, composite action under temperature change is of concern. To ensure against overlay failure, thermal performance was examined using two finite element models. The first model was designed to represent an 8-inch thick bridge deck with an 8-foot span between girders. The second model was based on an actual bridge, with a 9.5-inch thick slab and a span length of 12.5 feet. Both models included a ¾-inch polyester-styrene overlay. For each model, three end restraint conditions were considered: fixed ends at all supports; a fixed support at the left end, with roller supports to the right; and a cantilever beam. Each model was subjected to a temperature increase of 35°F and a temperature decrease of 45°F, as recommended by the American Association of State Highway and Transportation Officials. The 35°F increase was accompanied by a 25°F differential temperature through the deck, representing warm daytime conditions; the 45°F decrease case was assumed to have a constant temperature through the deck, representing cold nighttime conditions.

A comparison of the stresses obtained from the finite element analysis to the allowable unfactored stresses was made to ensure thermal compatibility between the polymer concrete overlay and the bridge deck. Most finite element analysis results were less than their associated allowable values; however, some exceptions were present in

both models: compression in the portland cement concrete due to increasing temperature and tension in the overlay material due to decreasing temperature.

6.2 Conclusions

It appears that polyester-styrene polymer concrete is an effective bridge deck overlay material, exhibiting high compressive and tensile strengths, and should continue to be used by the Nevada Department of Transportation.

Most stresses from the thermal compatibility finite element analysis were less than their allowable values, indicating acceptable performance; however, some excessive stresses were present. Even though no problems with polymer concrete overlays have been noted to date, the presence of excessive finite element results indicates that problem areas may be present; these areas need to be carefully observed in field installations.

Previous research indicates that an entire range of polyester-styrene concrete properties exists, depending on resin formulation, aggregate properties, mixture design, and curing method. Because of the wide range of concretes possible, laboratory determination of the properties of the actual polymer concrete being used for bridge deck overlays is recommended. Suggested tests include compressive strength, flexural strength, strength sensitivity to temperature, and bonding strength to portland cement concrete. In addition to the testing of laboratory-manufactured specimens, bond strength testing of corings from actual field installations is also recommended. To further verify thermal compatibility with portland cement concrete, modulus of elasticity and thermal expansion characteristics should also be determined.

References

1. Babaei, K., and N. M. Hawkins. 1987. *Evaluation of bridge deck protective strategies*, NCHRP report 297. Washington, D.C.: National Research Council, Transportation Research Board.
2. Brown, D. 1977. Bridge deck deterioration: Some solutions to the problem. *ACI Journal* 74(5): N18-N19.
3. Sohahngpurwala, A. A., and K. C. Clear. 1990. Effectiveness of epoxy coatings in minimizing corrosion of reinforcing steel in concrete. Paper presented at the 69th Annual TRB Meeting. Washington, D.C.: Transportation Research Board.
4. Krauss, P. D. 1985. *New materials and techniques for the rehabilitation of portland cement concrete*, report number FHWA/CA/TL-85/16. Sacramento: California Department of Transportation.
5. Burke, N. D., and J. B. Bushman. 1988. *Corrosion and cathodic protection of steel reinforced concrete bridge decks*, report number FHWA-IP-88-007. McLean, Virginia: Department of Transportation, Federal Highway Administration.
6. Park, S. H. 1984. *Bridge rehabilitation and replacement: Bridge repair practice*. Trenton, N.J.: S. H. Park.
7. Scannell, W. T., and K. C. Clear. 1990. Long term outdoor exposure evaluation of concrete slabs containing epoxy coated reinforcing steel. Paper presented at the 69th Annual TRB Meeting. Washington, D.C.: Transportation Research Board.
8. Crawford, W. C., Jr. 1991. Personal discussion between author and William (Bill) Crawford, Assistant Bridge Engineer, NDOT. May 1991.
9. Clear, K. C., and B. H. Chollar. 1978. *Styrene-butadiene latex modifiers for bridge deck overlay concrete*, report number FHWA-RD-78-35. Washington, D.C.: Department of Transportation, Federal Highway Administration.
10. Kuhlmann, L. A. 1981. Performance history of latex-modified concrete overlays. In *Applications of polymer concrete*, publication SP-69, 123-144. Detroit: American Concrete Institute.
11. Kuhlmann, L. A. 1987. Application of styrene/butadiene latex modified concrete. *Concrete International* 9(12): 48-53.
12. AASHTO Subcommittee on New Highway Materials. 1989. *AASHTO-AGC-ARTBA guide specifications: Manual for design and construction of concrete overlays for bridge decks*. Draft copy.

13. Nevada Department of Transportation. 1982. Special provisions for project SPI-080-1(9) (contract 1937), section 496.
14. Smoak, W. G. 1975. *Polymer impregnation of new concrete bridge deck surfaces: Interim user's manual of procedures and specifications*, report number FHWA-RD-75-72. Washington, D.C.: Department of Transportation, Federal Highway Administration.
15. ACI Committee 548. 1986. Guide for the use of polymers in concrete. *ACI Journal* 86(5): 798-829.
16. Fontana, J. J., and J. Bartholomew. 1982. *Polymer concrete patching manual*, report number FHWA-IP-82-10. Washington, D.C.: Department of Transportation, Federal Highway Administration.
17. ACI Committee 548. 1991. *Guide for polymer concrete overlays*. Draft report.
18. Lee, W. 1991. Telephone conversation between author and William (Bill) Lee, Transpo Industries. July 1991.
19. Oleesky, S. S., and J. G. Mohr. 1964. *Handbook of reinforced plastics of the Society of the Plastics Industry*. New York: Reinhold Publishing.
20. Microsoft Corporation. 1990. *Microsoft Excel for Windows, Version 3.0*. Redmond, Washington.
21. Federal Highway Administration. 1988. *Recording and coding guide for the structure inventory and appraisal of the nation's bridges*, report number FHWA-ED-89-044. Washington, D.C.: Department of Transportation.
22. Nevada Department of Transportation. 1988. *Nevada structure index*. Carson City: State of Nevada.
23. Rudin, A. 1982. *The elements of polymer science and engineering: An introductory text for engineers and chemists*. New York: Academic Press.
24. Kosmatka, S. H., and W. C. Panarese. 1988. *Design and control of concrete mixtures*, 13th ed. Skokie, Ill.: Portland Cement Association.
25. ACI Committee 116. 1978. *Cement and concrete terminology*, publication SP-19(78). Detroit: American Concrete Institute.
26. O'Connor, D. N. 1988. Mix design and testing of portland cement concrete. Unpublished student course work.
27. Nevada Department of Transportation. 1990. Special provisions for project SPI-080-2(3) (contract 2393), section 496.

28. Kobayashi, K., and T. Ito. 1976. Several physical properties of resin concrete. In *Polymers in concrete: Proceedings of the first international congress on polymer concrete*, 236-240. London: The Concrete Society/Construction Press Ltd.
29. Valore, R. C., and D. J. Naus. 1976. Resin bound aggregate material systems. In *Polymers in concrete: Proceedings of the first international congress on polymer concrete*, 216-222. London: The Concrete Society/Construction Press Ltd.
30. Vipulanandan, C., and E. Paul. 1990. Performance of epoxy and polyester polymer concrete. *ACI Materials Journal* 87(3): 241-251.
31. Jerzak, H. 1990. *Rapid set materials for repairs to portland cement concrete pavement and structures*. Sacramento: California Department of Transportation.
32. Herubin, C. A., and T. W. Marotta. 1987. *Basic construction materials: Methods and testing*, 3d ed. Englewood Cliffs, N.J.: Prentice-Hall (Reston).
33. ACI Committee 318. 1989. *Building code requirements for reinforced concrete (ACI 318-89) and commentary-ACI 318R-89*. Detroit: American Concrete Institute.
34. Wang, C., and C. G. Salmon. 1985. *Reinforced concrete design*, 4th ed. New York: Harper & Row.
35. Zoldners, N. G. 1971. Thermal properties of concrete under sustained elevated temperatures. In *Temperature and concrete*, publication SP-25, 1-31. Detroit: American Concrete Institute.
36. Abrams, M. S. 1971. Compressive strength of concrete at temperatures to 1600°F. In *Temperature and concrete*, publication SP-25, 33-58. Detroit: American Concrete Institute.
37. Okada, K., W. Koyanagi, and T. Yonezawa. 1976. Thermo-dependent properties of polyester resin concrete. In *Polymers in concrete: Proceedings of the first international congress on polymer concrete*, 210-215. London: The Concrete Society/Construction Press Ltd.
38. Browne, R. D., M. Adams, and E. L. French. 1976. Experience in the use of polymer concrete in the building and construction industry. In *Polymers in concrete: Proceedings of the first international congress on polymer concrete*, 433-447. London: The Concrete Society/Construction Press Ltd.
39. Dharmarajan, N., and C. D. Armeniades. 1987. Creep studies of polyester concrete under flexural loading. In *Polymer modified concrete*, publication SP-99, ed. D. W. Fowler, 17-30. Detroit: American Concrete Institute.

40. Reynolds, J. C., and J. H. Emanuel. 1974. Thermal stresses and movements in bridges. *Journal of the Structural Division, Proceedings of the American Society of Civil Engineers*, 100(ST1): 63-78.
41. AASHTO Subcommittee on Bridges and Structures. 1989. *Standard specifications for highway bridges*, 14th ed. Washington, D.C.: American Association of State Highway and Transportation Officials.
42. Elbadry, M. M., and A. Ghali. 1983. Temperature variations in concrete bridges. *ASCE Journal of Structural Engineering*, 109(10): 2355-2374.
43. AASHTO Subcommittee on Bridges and Structures. 1989. *AASHTO guide specifications: Thermal effects in concrete bridge superstructures*. Washington, D.C.: American Association of State Highway and Transportation Officials.
44. Celestial Software. 1985. *Images 3D*. Berkeley, California.

Appendix A

Symbols and Abbreviations

a	Depth of equivalent rectangular stress block as defined in ACI-318, Sec. 10.2.7.1, in.
AASHTO	American Association of State Highway and Transportation Officials. When used in the context of design guidelines, refers to the AASHTO document <i>Standard specifications for highway bridges</i> . (Ref. 41).
ACI	American Concrete Institute.
ACI-318	Refers to the ACI document <i>Building code requirements for reinforced concrete (ACI 318-89) and commentary—ACI 318R-89</i> . (Ref. 33)
A_g	Gross section area, in ² .
A_s	Area of non-prestressed tension reinforcement, in ² .
A'_s	Area of compression reinforcement, in ² .
b	Width of compression face of member, in.
c	Distance from extreme compression fiber to neutral axis, in.
D	Dead loads or related internal moments and forces.
d	Distance from extreme compression fiber to centroid of tension reinforcement, in.
d'	Distance from extreme compression fiber to centroid of compression reinforcement, in.
d''	Distance from centroid of compression reinforcement to centroid of tension reinforcement, in.
E	Modulus of elasticity, psi.
E_c	Modulus of elasticity of concrete, psi.
EI	Flexural stiffness of compression member, lb-in ² .
E_s	Modulus of elasticity of reinforcing steel, psi.
f	Stress, psi.
f'_c	Specified compressive strength of concrete, psi.

f_c	Compressive stress, psi.
f_{ct}	Average splitting tensile strength of concrete, psi.
f_D	Bending stress caused by dead load, psi.
f_L	Bending stress caused by live load, psi.
f_r	Modulus of rupture, psi.
f_{sh}	Shear stress at interface, psi.
f_t	Tensile stress, psi.
f_y	Specified yield strength of reinforcing steel, psi.
h	Overall thickness of member, in.
HMWM	High molecular weight methacrylate.
I	Moment of inertia, in ⁴ .
l	Span length of beam, ft or in.
L	Live loads or related internal moments and forces.
LMC	Latex-modified concrete.
LSDC	Low-slump dense concrete.
M	Moment, lb-ft or lb-in.
M_b	Nominal moment capacity at balanced strain condition, lb-ft or lb-in.
M_D	Dead load moment, lb-ft or lb-in.
MEKP	Methyl ethyl ketone peroxide.
M_L	Live load moment, lb-ft or lb-in.
MMA	Methyl methacrylate.
M_n	Nominal moment capacity of flexural section, lb-ft or lb-in.
M_o	Nominal moment capacity in pure bending, lb-ft or lb-in.
M_u	Ultimate moment capacity of flexural section, lb-ft or lb-in.

NBI	National Bridge Inventory.
NDOT	Nevada Department of Transportation.
P	Axial or point load, lb.
P_{20}	Load on one rear wheel of standard HS20 truck ($P_{20} = 16,000$ lb).
P_b	Nominal axial load capacity at balanced strain, lb.
PC	Polymer concrete.
PCC	Portland cement concrete.
PIC	Polymer impregnated concrete.
P_n	Nominal axial load capacity at given eccentricity, lb.
P_o	Nominal axial load capacity at zero eccentricity, lb.
P_u	Ultimate axial load capacity at given eccentricity, lb.
r	Radius of gyration of compression cross-section, in.
T	Temperature loads or related internal moments and forces.
T_c	Compressive temperature loads or related internal moments and forces.
T_o	Reference temperature, °F.
T_t	Tensile temperature loads or related internal moments and forces.
$T(y)$	Temperature at point y , °F.
U	Required strength to resist factored loads or related moments and forces.
w	Unit weight, lb/ft ³ .
w_c	Unit weight of concrete, lb/ft ³ .
w_d	Dead (self) weight of bridge deck, lb/ft ² .
α	Coefficient of thermal expansion, in/in-°F.
β_1	Factor defined in ACI-318, Sec. 10.2.7.3:

$$\beta_1 = 0.85 - 0.05 \left(\frac{4000 - f'_c}{1000} \right) \text{ where } 0.65 \leq \beta_1 \leq 0.85.$$

ΔT Temperature differential across bridge deck, °F.

ϕ Strength reduction factor.

ρ Reinforcement ratio, A_s/bd .

ν Poisson's ratio.

Appendix B

Glossary of Polymer Concrete Terms

Accelerator—See promoter.

Aggregate—Granular material, such as sand, gravel, crushed stone, and iron blast-furnace slag, used with a cementing medium to form a concrete or mortar.¹

Alcohol—Any of various compounds that are hydroxyl derivatives of hydrocarbons.² An alcohol, such as ethylene glycol, HOCH₂CH₂OH, is combined with an organic acid or anhydride to produce an ester in the manufacture of polyester resins.

Binder—A cementing material, such as portland cement, asphalt, resin, or other material, forming the matrix of concretes, mortars, and sanded grouts.¹

Bleeding—The autogenous flow of mixing water within, or its emergence from newly placed concrete or mortar, caused by the settlement of the solid materials within the mass.¹

Catalyst—A substance that initiates a chemical reaction and enables it to proceed under milder conditions (such as lower temperature) than otherwise required and which does not, itself, alter or enter into the reaction.¹

Coefficient of thermal expansion—Change in linear dimension per unit length or change in volume per unit volume per degree of temperature change.¹

Compressive strength, f'_c —The measured maximum resistance of a concrete or mortar specimen to axial loading, expressed as force per unit cross-sectional area; or the specified resistance used in design calculations.¹

Concrete—A composite material which consists essentially of a binding medium within which are embedded particles or fragments of aggregate.¹

Copolymers—Polymers that contain more than one type of repeating unit in the polymer chain, e.g. methyl methacrylate/trimethylolpropane trimethacrylate systems.³

Cobalt naphthenate—A liquid metallic compound widely used as a room-temperature-cure promoter for methyl ethyl ketone peroxide or cyclohexanone peroxide initiated systems.⁴ The cobalt metal present provides the true reaction with the initiator to release free radicals.

Cross-linking agent—A monomer, with functionality greater than two, added to a polymer system which allows the growth of side chains that link the main chains together in a three-dimensional net-like fashion.³

Cure time—Time elapsed between resin initiation and the time peak temperature of the resin is reached during polymerization.⁴

Curing—See polymerization.

Degree of polymerization—Indicates the number of times the repeating unit occurs within the polymer molecule.³

Emulsion—A system consisting of a liquid dispersed with or without an emulsifier (surface-active agent) in an immiscible liquid, usually in droplets of larger than colloidal size.⁵

Endothermic—A reaction characterized by or formed with the absorption of heat.⁶

Epoxy—A thermosetting resin typically based on diglycidyl ether of bisphenol A (DGEBA) and containing epoxide groups on the ends of the molecules.³ Epoxies have excellent resistance to attack by moisture and corrosive chemicals, and provide extraordinarily high strength.⁴

Exotherm curve—A plot of resin temperature versus time following initiation which provides a graphic representation of the physical and chemical changes occurring in resin during polymerization.⁴ Various points and features of the curve may be compared to the Society of the Plastics Industry (SPI) standard 180°F exotherm curve to determine relative performance.

Exothermic—A reaction characterized by or formed with the evolution of heat.⁶

Filler—Finely divided inert material such as pulverized limestone, silica, or colloidal substances sometimes added to resin to reduce shrinkage, improve workability, or act as an extender.¹

Flexural Strength—see modulus of rupture.

Flushing—The emergence of resin at the surface of newly placed polymer concrete or mortar, caused by settlement of the solid materials in the mass.

Free radical—A reactive, electrically neutral molecule with an unpaired electron.³ A free radical forms the "seed" which starts the growth of a polymer chain.

Functionality—The number of sites at which a monomer molecule can link with other monomer molecules to form a long chain.³

γ -methacryloxypropyltrimethoxysilane—A silicon-based chemical added to polymer concrete to increase the bond strength between the organic polymer and the inorganic aggregate. See silane coupling agent.

Gel time—Time elapsed between resin initiation and the time the resin ceases to be a viscous liquid and becomes a soft, elastic, rubbery solid.⁴

Hardener—The chemical component added to epoxy resins that cause the resin to harden or cure (polymerize)⁵. See also initiator.

Heat of hydration—Heat evolved by chemical reactions with water, such as that evolved during the setting and hardening of portland cement.¹

High molecular weight methacrylate (HMWM)—A low viscosity substituted methacrylate monomer which is characterized by low volatility.⁷

Hydration—Formation of a compound by the combining of water with some other substance. In portland cement concrete, the chemical reaction between hydraulic cement and water.¹

Impregnation—The process to cause the void and pore space in hardened concrete to be filled, permeated, or saturated with monomer.⁵

Inhibitor—Free-radical scavengers added to monomers to react with and deactivate the free-radicals in growing polymer chains and to act as antioxidants to prevent polymerization by oxidation product reaction during monomer storage.⁵ Typically added to monomers to increase shelf life.

Initiator—A chemical agent which initiates growth of polymer chains by decomposing into hydrocarbon free-radicals that start the chain's growth.⁵ Often incorrectly called a catalyst.

Isophthalic—Polyester resin in which isophthalic acid, $C_6H_4(COOH)_2$, is used in place of phthalic acid in the esterification process.⁴ Isophthalic resin exhibits a higher light stability, higher adhesion to siliceous matter, higher crazing resistance, and improved creep characteristics and flexural strength at elevated temperature, but lower impact strength than resin made with phthalic acid.⁴

Kick-off temperature—The inflection point on the exotherm curve which marks the beginning of the rapid rise to peak temperature brought on by the full result of the chemical action of polymerization.⁴ The kick-off temperature is a reference point for comparing the relative activity of polyester initiators, inhibitors, and promoters.

Latex—A water emulsion of a synthetic rubber or plastic obtained by polymerization.¹ See also styrene-butadiene rubber.

Latex modified concrete (LMC)—Portland cement concrete in which a portion of the mixing water is replaced with a latex emulsion.

Matrix—The cement paste, resin, or mortar in which concrete aggregate particles are embedded.¹

Methyl ethyl ketone peroxide (MEKP)—An organic peroxide, $(\text{CH}_3\text{COO}_2\text{HC}_2\text{H}_5)_2$, used, in conjunction with cobalt naphthenate, for room-temperature curing of styrene and methacrylate monomers.⁴

Methyl methacrylate (MMA)—An extremely volatile and flammable acrylic monomer,⁴ $\text{CH}_2=\text{C}(\text{CH}_3)\text{COOCH}_3$, widely used in industry to make clear acrylic sheeting (e.g. Plexiglas® and Lucite®) and used in polymer concrete and polymer impregnated concrete. Polymerized methyl methacrylate is often abbreviated PMA.

Modulus of elasticity, E —The ratio of normal stress to corresponding strain for tensile or compressive stresses below the proportional limit of the material.¹ Often referred to as elastic modulus or Young's modulus.

Modulus of rupture, f_r —A measure of the ultimate load-carrying capacity of a beam, calculated for apparent tensile stress in the extreme fiber of a transverse test specimen under the flexural load which produces rupture.¹ Also called flexural strength or rupture strength.

Monomer—An organic liquid, of relatively low molecular weight, that creates a solid polymer by reacting with itself or other compounds of low molecular weight or both.¹

Overlay—A layer of concrete or mortar placed on and usually bonded onto the worn or cracked surface of a concrete slab to either restore or improve the function of the previous surface.¹

Polyester—One of a large group of synthetic resins, mainly produced by polycondensation of the ester products resulting from the reaction of di- or polybasic acids with dihydroxyl alcohols, commonly prepared for application by thinning with a vinyl-group monomer.^{1,4} Polyester resins are widely used in the manufacture of glass-fiber reinforced products, such as boat hulls and bath tubs.

Polymer—A compound formed by the reaction of simple molecules having functional groups that permit their combination to proceed to high molecular weights under suitable conditions.⁸ Polymers may be formed by polymerization (addition polymer) or polycondensation (condensation polymer). When two or more monomers are involved, the product is a copolymer.

Polymer concrete (PC)—Concrete in which an organic polymer serves as the binder.¹

Polymer impregnated concrete (PIC)—A hydrated portland cement concrete which has been impregnated with a monomer that is subsequently polymerized in place.⁵

Polymerization—The chemical reaction in which two or more molecules of the same substance (monomer) or similar substance (a copolymer or cross-linking agent) combine to form a compound containing the same elements, and in the same proportions, but of high molecular weight, from which the original substance can be regenerated, in some cases only with extreme difficulty.¹ Also called curing or hardening.

Prepolymer—A low polymeric structure intermediate between that of the monomer or monomers and the final polymer or resin.⁸

Promoter—A chemical agent which greatly increases the rate of chemical decomposition of an initiator and used to increase the rate of polymerization and/or allow polymerization to occur at room temperature. Also called an accelerator.

Resin—A natural or synthetic, solid or semisolid organic material of indefinite and often high molecular weight, having a tendency to flow under stress. It usually has a softening or melting range and usually fractures conchoidally.¹

Silane coupling agent—Silicon compounds having the general formula $(\text{HO})_3\text{SiR}$ where R is an organic group compatible with thermoplastic or thermosetting resins.⁵ Silanes are used to enhance the chemical bond of organic polymers to inorganic materials such as sand, rock, glass, and metals.

Styrene—A fragrant, mobile liquid unsaturated hydrocarbon monomer, $\text{C}_6\text{H}_5\text{CH}=\text{CH}_2$, obtained by the distillation of storax or the decomposition of cinnamic acid or

more often from ethylbenzene either by catalytic dehydrogenation or by oxidation to acetophenone followed by partial reduction and dehydration, that polymerizes in the presence of an organic peroxide initiator to yield polystyrene.⁶ Styrene is often used as a thinner and cross-linking agent for polyester resin.

Thermoplastic—Capable of softening or fusing when heated and of hardening and becoming rigid again when cooled.⁶

Thermosetting—Capable of becoming permanently hard and rigid when heated or cured.⁶

Trimethylolpropane trimethacrylate (TMPTMA)—An acrylic monomer typically added to methyl methacrylate as a cross-linking agent.

Unsaturated—A molecular compound capable of forming additional products or bonds.⁶

Glossary References

1. ACI Committee 116. 1978. *Cement and concrete terminology*, publication SP-19(78). Detroit: American Concrete Institute.
2. Mish, F. C., Ed. 1983. *Webster's ninth new collegiate dictionary*. Springfield, Mass.: Merriam-Webster.
3. Moore, G. R., and D. E. Kline. 1984. *Properties and processing of polymers for engineers*. Englewood Cliffs, N.J.: Prentice-Hall.
4. Oleesky, S. S., and J. G. Mohr. 1964. *Handbook of reinforced plastics of the Society of the Plastics Industry*. New York: Reinhold Publishing.
5. ACI Committee 548. 1986. Guide for the use of polymers in concrete. *ACI Journal* 86(5): 798-829.
6. Gove, P. B., Ed. 1965. *Webster's third new international dictionary of the English language, unabridged*. Springfield, Mass.: G & C Merriam.
7. ACI Committee 548. 1991. *Guide for polymer concrete overlays*. Draft Report.
8. Simonds, H. R., and J. M. Church. 1963. *A concise guide to plastics*, 2d ed. New York: Reinhold Publishing.

Appendix C

List of CCEER Publications

Report No.	Publication
CCEER-84-1	Saiidi, M., and R. A. Lawver. <i>User's manual for LZAK-C64, a computer program to implement the Q-model on Commodore 64</i> , report number CCEER-84-1. Civil Engineering Department, University of Nevada, Reno. January 1984.
CCEER-84-2	Douglas, B. M., and T. Iwasaki. <i>Proceedings of the first USA-Japan bridge engineering workshop</i> , held at the Public Works Research Institute, Tsukuba, Japan, report number CCEER-84-2. Civil Engineering Department, University of Nevada, Reno. April 1984.
CCEER-84-3	Saiidi, M., J. D. Hart, and B. M. Douglas. <i>Inelastic static and dynamic analysis of short R/C bridges subjected to lateral loads</i> , report number CCEER-84-3. Civil Engineering Department, University of Nevada, Reno. July 1984.
CCEER-84-4	Douglas, B. <i>A proposed plan for a national bridge engineering laboratory</i> , report number CCEER-84-4. Civil Engineering Department, University of Nevada, Reno. December 1984.
CCEER-85-1	Norris, G. M., and P. Abdollaholiae. <i>Laterally loaded pile response: Studies with the strain wedge model</i> , report number CCEER-85-1. Civil Engineering Department, University of Nevada, Reno. April 1985.
CCEER-86-1	Ghusn, G. E., and M. Saiidi. <i>A simple hysteretic element for biaxial bending of R/C columns and implementation in NEABS-86</i> , report number CCEER-86-1. Civil Engineering Department, University of Nevada, Reno. July 1986.
CCEER-86-2	Saiidi, M., R. A. Lawver, and J. D. Hart. <i>User's manual of ISADAB and SIBA, computer programs for nonlinear transverse analysis of highway bridges subjected to static and dynamic lateral loads</i> , report number CCEER-86-2. Civil Engineering Department, University of Nevada, Reno. September 1986.
CCEER-87-1	Siddharthan, R. <i>Dynamic effective stress response of surface and embedded footings in sand</i> , report number CCEER-87-1. Civil Engineering Department, University of Nevada, Reno. June 1987.
CCEER-87-2	Norris, G., and R. Sack. <i>Lateral and rotational stiffness of pile groups for seismic analysis of highway bridges</i> , report number CCEER-87-2. Civil Engineering Department, University of Nevada, Reno. June 1987.

- CCEER-88-1 Orié, J., and M. Saiidi. *A preliminary study of one-way reinforced concrete pier hinges subjected to shear and flexure*, report number CCEER-88-1. Civil Engineering Department, University of Nevada, Reno. January 1988.
- CCEER-88-2 Orié, D., M. Saiidi, and B. Douglas. *A micro-CAD system for seismic design of regular highway bridges*, report number CCEER-88-2. Civil Engineering Department, University of Nevada, Reno. June 1988.
- CCEER-88-3 Orié, D., and M. Saiidi. *User's manual for Micro-SARB, a microcomputer program for seismic analysis of regular highway bridges*, report number CCEER-88-3. Civil Engineering Department, University of Nevada, Reno. October 1988.
- CCEER-89-1 Douglas, B., M. Saiidi, R. Hayes, and G. Holcomb. *A comprehensive study of the loads and pressures exerted on wall forms by the placement of concrete*, report number CCEER-89-1. Civil Engineering Department, University of Nevada, Reno. February 1989.
- CCEER-89-2a Richardson, J., and B. Douglas. *Dynamic response analysis of the Dominion Road Bridge test data*, report number CCEER-89-2. Civil Engineering Department, University of Nevada, Reno. March 1989.
- CCEER-89-2b Vrontinos, S., M. Saiidi, and B. Douglas. *A simple model to predict the ultimate response of R/C beams with concrete overlays*, report number CCEER-89-2. Civil Engineering Department, University of Nevada, Reno. June 1989.
- CCEER-89-3 Ebrahimpour, A., and P. Jagadish. *Statistical modeling of bridge traffic loads: A case study*, report number CCEER-89-3. Civil Engineering Department, University of Nevada, Reno. December 1989.
- CCEER-89-4 Shields, J., and M. Saiidi. *Direct field measurement of prestress losses in box girder bridges*, report number CCEER-89-4. Civil Engineering Department, University of Nevada, Reno. December 1989.
- CCEER-90-1 Saiidi, M., E. Maragakis, G. Ghosn, Jr., Y. Jiang, and D. Schwartz. *Survey and evaluation of Nevada's transportation infrastructure, task 7.2—highway bridges, final report*, report number CCEER-90-1. Civil Engineering Department, University of Nevada, Reno. October 1990.
- CCEER-90-2 Abdel-Ghaffar, S., E. Maragakis, and M. Saiidi. *Analysis of the response of reinforced concrete structures during the Whittier earthquake of 1987*, report number CCEER-90-2. Civil Engineering Department, University of Nevada, Reno. October 1990.

- CCEER-91-1 Saiidi, M., E. Hwang, E. Maragakis, and B. Douglas. *Dynamic testing and analysis of the Flamingo Road Interchange*, report number CCEER-91-1. Civil Engineering Department, University of Nevada, Reno. February 1991.
- CCEER-91-2 Norris, G., R. Siddharthan, Z. Zafir, S. Abdel-Ghaffar, and P. Gowda. *Soil-foundation-structure behavior at the Oakland Outer Harbor Wharf*, report number CCEER-91-2. Civil Engineering Department, University of Nevada, Reno. July 1991.
- CCEER-91-3 Norris, G. M. *Seismic lateral and rotational pile foundation stiffness at Cypress*, report number CCEER-91-3. Civil Engineering Department, University of Nevada, Reno. August 1991.
- CCEER-91-4 O'Connor, D. N., and M. Saiidi. *A study of protective overlays for highway bridge decks in Nevada, with emphasis on polyester-styrene polymer concrete*, report number CCEER-91-4. Civil Engineering Department, University of Nevada, Reno. October 1991.

